MODELLING OF A CALCIUM LOOPING FLUIDIZED BED REACTOR SYSTEM FOR CARBON DIOXIDE REMOVAL FROM FLUE GAS

Maparanyanga Tsitsi

In fulfilment of the requirements for the degree of

Master of Science Engineering at the school of

Chemical Engineering, University of KwaZulu Natal

Supervisor Dr David Lokhat

June 2018

Dedication

To my parents, brothers and sisters

As the candidate's supervisor, I agree to the submission of this thesis:

Dr. D. Lokhat

Declaration

I, Maparanyanga Tsitsi, declare that

1. The research reported in this thesis, except where otherwise indicated, is my original research.

2. This thesis has not been submitted for any degree or examination at any other university.

3. This thesis does not contain other persons' data, pictures, graphs or other information, unless specifically acknowledged as being sourced from other persons.

4. This thesis does not contain other persons' writing, unless specifically acknowledged as being sourced from other researchers. Where other written sources have been quoted, then:
a. Their words have been re-written but the general information attributed to them has been referenced
b. Where their exact words have been used, then their writing has been placed in italics and inside quotation marks, and referenced.

5. This thesis does not contain text, graphics or tables copied and pasted from the Internet, unless specifically acknowledged, and the source being detailed in the thesis and in the References sections.

Signed

……

Date

20/08/2018

……

Acknowledgements

This research project would have been unsuccessful without the contribution of many talented people at the university and home. Special mention goes to the following:

1. Dr David Lokhat for providing guidance and intellectual direction throughout the design project
2. My parents, brothers and sisters for moral support
3. Mostly I would like to thank the Almighty God for pulling me this far.

Abstract

Due to its greater cost advantage compared to conventional amine scrubbing technologies, calcium looping has become the most promising way for carbon dioxide capture in plants. The basic concept in calcium looping is reacting carbon dioxide from flue gas with calcium oxide at approximately 650°C to form calcium carbonate. This reaction takes place in a carbonator. The calcium carbonate from the carbonator is then decomposed in a calciner by subjecting it to higher temperatures (850-950°C). Sulphation (reaction of calcium oxide or calcium carbonate with sulphur dioxide and oxygen to form calcium sulphate) also occurs. Sulphur not only reacts with calcium oxide active for the carbonation reaction, but also can form calcium sulphate with the non-active calcium oxide. Calcium sulphate has a greater molar volume than calcium oxide, resulting in a sulphated layer forming on the outside of the particle, which prevents the uptake of carbon dioxide by the calcium oxide further inside the particle. Calcium sulphate dissociates to calcium oxide and sulphur dioxide at a relatively high temperature, precluding sulphation's reversibility at the conditions present in calcium looping. It is important to quantify this effect and determine the fraction of non-active calcium oxide that reacts with sulphur to form calcium sulphate for not being excessively conservative when considering sulphur.

In this study, the calcium looping process was simulated by solution of the one-dimensional (1D) mass and energy balance equations for both interconnected fluidized bed reactors. Kinetics for the carbonator and calciner were derived from literature sources and were revised to include the effects of sulphation. The degree of apparent carbonation was compared to the actual level of carbon dioxide removal through a series of sensitivity analyses. The calcium looping system is dynamic and a number of carbonation-calcination cycles was used to investigate how the system behaves as time changes.

It has been found that carbonation decreases with an increase in temperature while sulphation increases with an increase in temperature. The optimal temperature for carbonation would be 600°C for it is high enough to drive the carbonation reaction and not too high to accelerate the sulphation reaction. The activity of calcium oxide decreases with an increase in carbonation-calcination cycles. Carbonation rate increases as carbon dioxide concentration in flue gas increase. Increase in sorbent to carbon dioxide flow ratios leads to higher kinetics in the carbonator. Calcination increases with an increase in temperature, and decreases with an increase in carbon dioxide partial fraction. Temperatures above 900 °C should be avoided in the calciner as sintering occurs at an elevated pace at temperatures above 900 °C. The amount of active calcium oxide particles decreases as the number of carbonation-calcination cycles increase. Neglecting the effect of sulphation during the design of the calcium looping system leads to overestimation of active calcium particles that will react with carbon dioxide. The more Sulphur dioxide the flue gas contains, the more the active fraction of calcium oxide will be consumed by the sulphation reaction. In the presented model, it has been shown that for a flue gas containing 0.04% Sulphur dioxide and 21.6 % carbon dioxide (weight basis), sulphation consumes 0.8-4.0% of the active fraction of calcium oxide, depending on the temperature used in the carbonator.

Table of Contents

List of figures

Chapter 2

Chapter 3

Chapter 4

List of Tables

Chapter 2

Chapter 3

Chapter 4

1 Chapter one

1 INTRODUCTION

1.1 Background

The commencement of industrialization saw the marked increase of greenhouse gases in the atmosphere compared to pre-industrialization levels. Carbon dioxide, methane and oxides of nitrogen levels have increased in the atmosphere. Although natural processes like respiration add carbon dioxide into the atmosphere, man's activities are the ones that add a greater fraction of carbon dioxide in the atmosphere. According to the United Nation's Sustainable Development Goal number 13 (United Nations, 2015), all should take urgent action to fight climate change and its impacts which mainly include combating greenhouse gas emissions.

Carbon capture and storage is one of the ways that are used to reduce greenhouse gases emission into the atmosphere. There are various methods of capturing greenhouse gases from the atmosphere, which include separation with sorbents or solvents, separation with membranes and separation by cryogenic distillation.

In this project, the modelling and simulation of a calcium looping system for carbon dioxide removal from flue gases was considered. The calcium-looping method was proposed in 1999 (Shimizu, et al., 1999)and it is a method for carbon dioxide capture from flue gases using two coupled fluidized-bed reactors. A limestone sorbent, calcium oxide, is used for carbon dioxide capture. Carbon dioxide is captured through a chemical reaction resulting in the formation of calcium carbonate. Carbon dioxide capture takes place in the carbonator after which the carbonate is passed to the calciner for regenerating the sorbent and carbon dioxide separation. The separated carbon dioxide is then compressed and stored.

Most of the studies on calcium looping reactor modelling has concentrated on the carbonator, which is the most innovative component. Different models of the carbonator have been proposed in literature with the

first models being the bubbling fluidised bed reactors. The carbonator models that have been suggested by researchers considered the carbonator as a circulating fluidized-bed, which has two compartments, the bottom dense zone and the lean zone. The majority of the models proposed in literature have concluded that the calcium particles that react in the fast regime influence carbonator efficiency. The percentage of the calcium particles that react in the fast regime is defined by the amount of fresh sorbent being introduced into the system and the solid circulation between the calciner and carbonator. It has been proposed in literature to design a model that considers the actual activity of the calcium particles in the system according to their carrying capacity, regardless of their preceding history of partial or full carbonation-calcination cycles. True results would be obtained about the carbonator and general plant performance. It is also important to measure the effect of sulphation and the amount of non-active calcium particles that react with sulphur dioxide in the calcium looping system.

1.2 Aim and Objectives

Aim

To model, simulate and find an optimal range of operating conditions for the calcium looping system for carbon dioxide removal from flue gas.

Objectives

- To carry out a comprehensive literature review on removal of carbon dioxide gas from flue gas using the calcium looping method
- To construct an accurate model of the calcium looping system in terms of the governing material and energy balances and implement the model in MATLAB
- To investigate the effect of sulphation on carbonation kinetics
- To carry out a sensitivity analysis on the model based on variations in the operating conditions.
- To analyze the sensitivity analysis data and determine the best conditions for the carbon dioxide removal

1.3 Dissertation overview

The dissertation is broken down into five chapter and the information to be expected in each chapter is given below.

Chapter 2 gives a general literature review of the calcium looping process. Other methods carbon capture and storage are discussed and a detailed process description of calcium looping as one of the methods for carbon capture is given. General reactions governing the calcium looping system are also given.

Chapter 3 describes the model development. The kinetics for calcium looping process is given. Mass and energy balances for the system are also given out.

Chapter 4 gives the results of the simulation done using mass and energy balance equations as well as reaction kinetics. The results will also be analyzed. The heat exchanger design for the system is also included in the chapter.

The conclusions and recommendations will be given out in Chapter 5.

2

Chapter two

2. LITERATURE REVIEW

High pressure is being put on industries that emit flue gases during their processing so that they reduce carbon dioxide emissions to the atmosphere in order to reduce the greenhouse effect. This pressure has led researchers to suggest capturing the carbon dioxide from the flue gases and discharge it as a separate concentrated stream that can be cleaned easily than the dilute flue gas stream.

Carbon capture and storage is one of the best ways to reduce carbon dioxide emissions from combustion processes and reduce carbon dioxide concentration in the atmosphere in the future (IPCC, 2007). Intensive research and development measures have been carried out worldwide by universities to develop technologies that limit the efficiency penalty and reduce capital costs that affect industries equipped with carbon dioxide capture processes.

Carbon capture and storage is a method used for separating, transporting and storing carbon dioxide from a fuel conversion process.

2.1 Carbon capture and storage methods

Carbon dioxide can be captured from flue gas using pre-combustion, post combustion or oxy-fuel combustion methods.

2.1.1 Post combustion capture

Post-combustion carbon dioxide capture is a method used to capture carbon dioxide after burning the fuel. Post-combustion methods include the use of chemicals in amine solutions to capture the carbon dioxide from flue gases and storing carbon dioxide by making use of chemical reactions to permanently bind the carbon to minerals that are abundant in nature.

The fuel is first burnt with air before carbon capture and storage. Flue gas is passed through a carbon dioxide capturing reactor as shown in Figure 2-1, below;

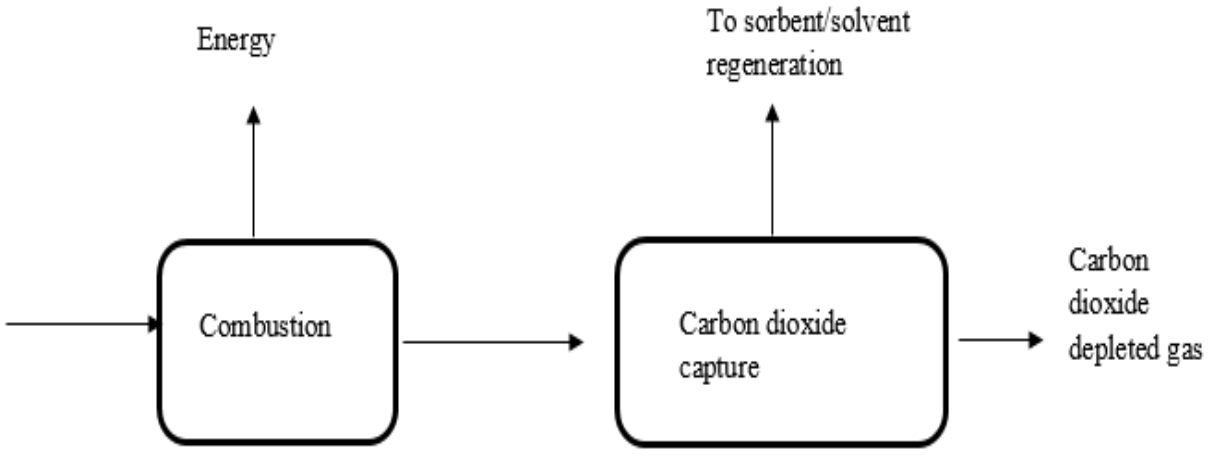

Figure 2- 1:Post-Combustion capture overview, based on (Global CCS Institute, 2014)

Carbon dioxide react with a sorbent or solvent in the separation unit after which it will be treated in another unit to release the carbon dioxide and recover the sorbent or solvent (Global CCS Institute, 2014). Sorbents such as monoethanolamine, ammonia and lime can be used for carbon dioxide capture.

The advantage of employing a post combustion carbon dioxide capture system is that this technology can be added to existing plants without demanding modifications in the operating plant because it is fitted at the exiting flue gas stream (Fransson & Detert, 2014). There are various methods used for post-combustion carbon dioxide capture as well such as absorption, adsorption, cryogenic distillation and membrane separation.

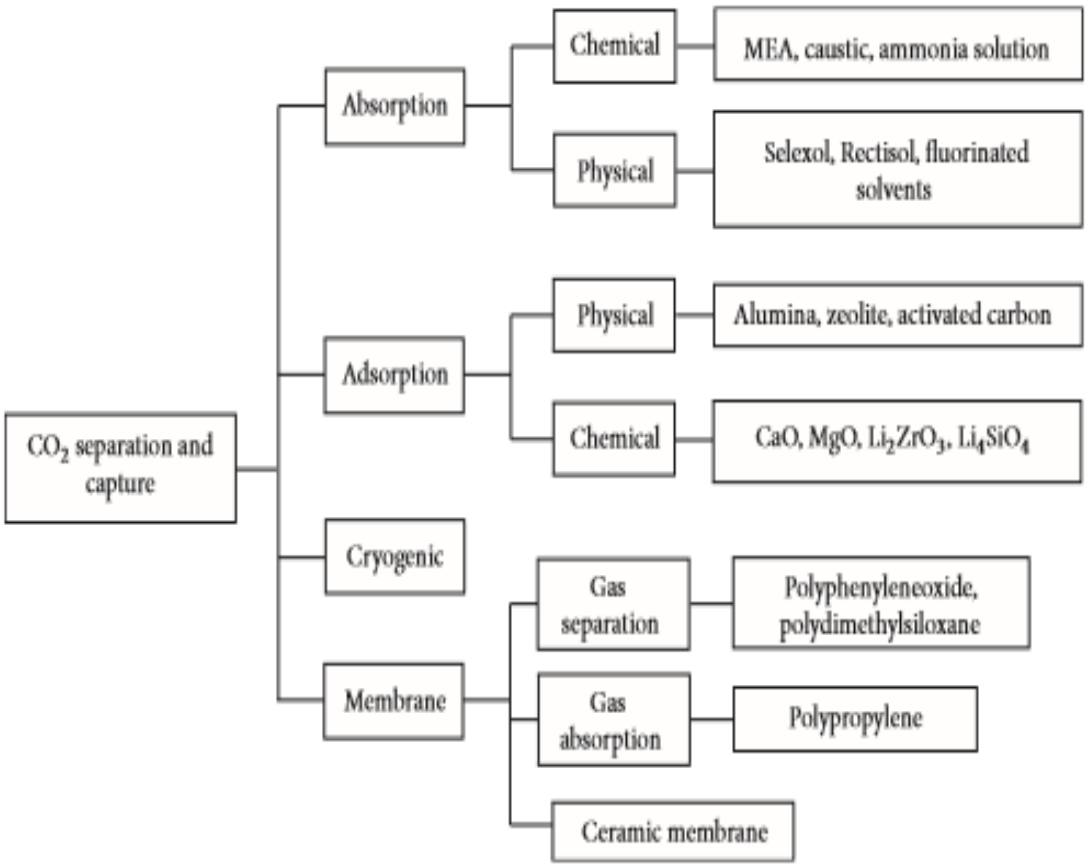

Figure 2- 2:Different methods for carbon dioxide capture (Thiruvenkatachari, et al., 2009)

2.1.1.1 Absorption or solvent based processes

The absorption technology is a well-known method of separating carbon dioxide and has been practiced for a long time in petroleum industries. This method uses a solvent to selectively absorb the carbon dioxide. A variety of solvents is now available to absorb carbon dioxide from flue gases. A stripping column may also be inserted to recover or regenerate the solvent.

2.1.1.1a Monoethanolamine (MEA) solvent

Monoethanolamine is the most common and traditional solvent that is used for carbon dioxide absorption (Sivalingam, 2013).

The flue gas from a power plant is passed through an absorption tower in which MEA solvent selectively absorb carbon dioxide. The carbon dioxide rich solution will be sent to the stripping column where the carbon dioxide is released by thermal regeneration. Absorption is enhanced by high pressure and low temperature while stripping is accelerated by low pressure and high temperature. Temperature

manipulation to release the carbon dioxide and regenerate the MEA makes up 70-80% of the operating cost in MEA process.

The disadvantages of using MEA for capturing carbon dioxide from flue gas include;

- The equipment will be corroded because of the presence of oxygen and impurities
- The solvent is degraded due to reaction with oxygenated impurities
- Environment pollution if solvent is emitted to the environment
- MEA absorption suffers from inherent regeneration costs and inefficiency (Martunus, et al., 2012)

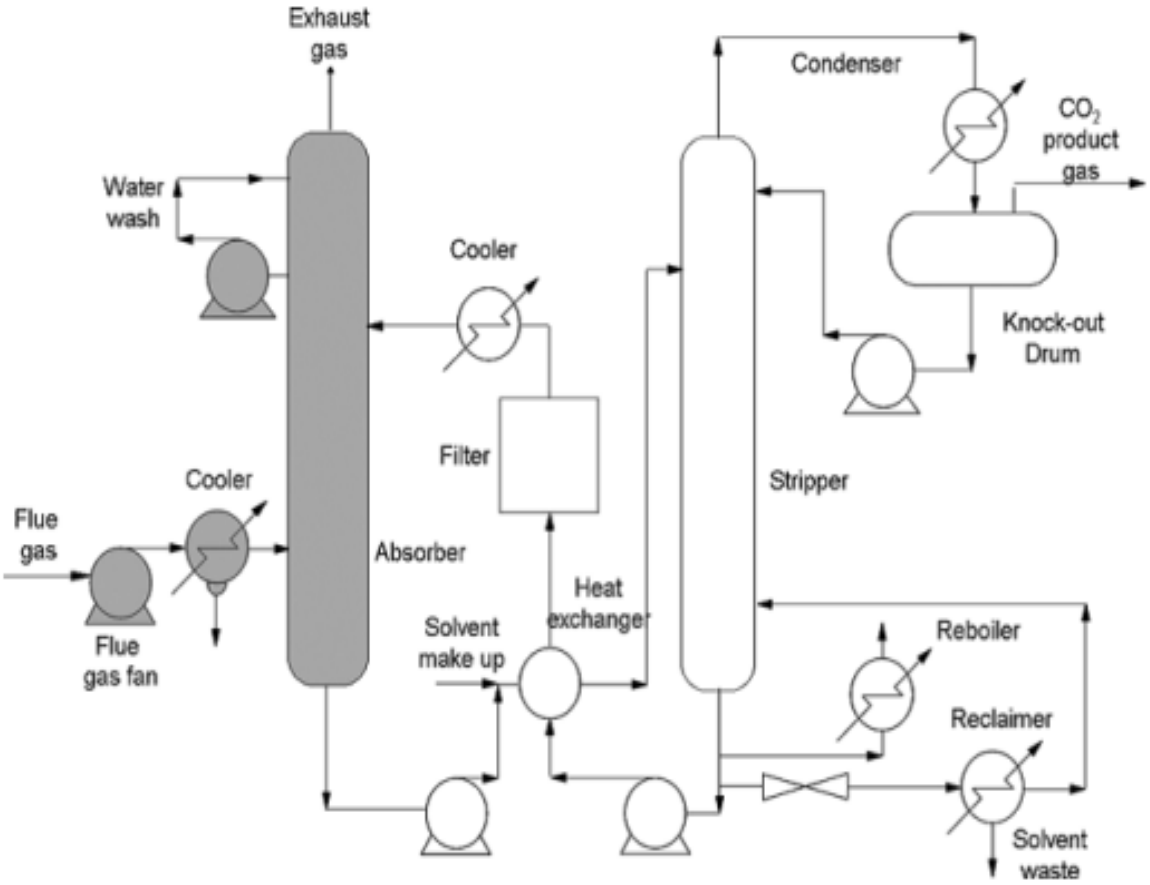

Figure 2- 3:MEA Scheme for CO2 Separation (Spliethoff, 2010)

2.1.1.1. b Other solvents

Mitsubish Heavy Industries developed KS-1™, KS-2™ and KS-3™ solvents that have higher carbon dioxide loading per unit solvent, low regeneration conditions and little corrosion, degradation or amine loss (Sivalingam, 2013).

2.1.1.2 Adsorption

Adsorption reduces the energy cost of capturing or separating carbon dioxide in post-combustion capture. It is required to select adsorbents with suitable properties. A good adsorbent should have high selectivity for the material. It should also have a high adsorption capacity and should stay stable after a number of adsorption-desorption cycles. A good adsorbent possesses good thermal and mechanical stability. There are two main categories for carbon dioxide adsorbents, chemical and physical adsorbents.

2.1.1.2. a Chemical Adsorption (Chemisorption)

This adsorption is driven by a chemical reaction occurring at an exposed surface. Various metals have been studied for carbon dioxide adsorption including (Martunus, et al., 2012);

- Metal oxides for example calcium oxide and magnesium oxide
- Metal salts from alkali metals for example lithium silicate and lithium zinconate
- Hydrotalcites and double salts

Much attention has been given to calcium oxide as the adsorbent because of its high carbon dioxide capture capacity and there is a high availability of raw materials at low cost. Calcium looping is one of the good prospects for post-combustion because of the possibility of the technology to be implemented in existing plants. In addition, the raw material, limestone, is widely available at low price and is harmless towards the environment (Ortiz, et al., 2015). Lithium salts have a good performance in carbon dioxide adsorption but they have not been used by many researchers because they have a high production cost.

2.1.1.2. b Physical Adsorption (Physisorption)

Physical adsorption is a process whereby the electronic structure of an atom or molecule is barely disturbed upon adsorption. Activated carbon and inorganic porous materials like zeolites are the major physical adsorbents for carbon dioxide. Coal is also being suggested as an adsorbent for carbon dioxide separation. Activated carbon is preferred as an adsorbent because it has low cost, high hydrophobicity, high adsorption capacity, and low energy requirement for regeneration. The main disadvantage of activated carbon is that it has a relatively low selectivity for CO_2/N_2. Zeolites offer CO_2/N_2 selectivity, which is more than 5 times greater than that of carbonaceous materials (Sevilla & Fuertes, 2012).

The selectivity and adsorption capacity of zeolites is affected by their charge density, pore diameter, size, and chemical composition of cations in their pores.

2.1.1.3 Cryogenic distillation

In cryogenic distillation, gas components are separated by a series of compression, cooling and expansion steps. This allows production of liquid carbon dioxide that can be stored at high pressure through liquid pumping.

2.1.1.4 Membrane separation

This is a simple, continuous, and clean process for carbon capturing that saves energy. It is a pressure driven process. Flue gases have a low pressure, which makes membrane separation process not a good method for carbon dioxide capture as it offers high separation performance when carbon dioxide concentration in the feed stream increases.

The energy requirement for membrane separation processes depend on target purity of exit gas, composition of flue gas and membrane selectivity for carbon dioxide. Membrane separation requires a lot of energy for post combustion carbon dioxide capture. Another disadvantage is the low selectivity of the membrane for CO_2, SO_x and NO_x.

2.1.2 Pre-combustion capture

Pre-combustion capture refines a hydrocarbon into a low carbon gaseous fuel before combustion. In pre-combustion capture, carbon dioxide is captured after gasification. An example of a pre-combustion method is Integrated Gasification Combined Cycle (IGCC) refining solid fuel for gas turbine use (Thiruvenkatachari, et al., 2009).

In pre-combustion, carbon dioxide is captured after gasification before the syngas is burnt. The first step is to make a syngas (mixture of hydrogen, carbon dioxide, carbon monoxide and other hydrocarbons) through the gasification step depending on the nature of fuel used. The amount of hydrogen is increased by a water gas shift reaction, where carbon monoxide is converted to carbon dioxide. The increase in amount of hydrogen is done in order to get a final gas, which is rich in hydrogen that produces water when burnt. In this way, carbon is removed in the form of carbon dioxide.

It is difficult to apply the pre-combustion capture technology in existing power plants because the fuel combustion steps involved in pre-combustion are more complex compared to the processes that are involved in post-combustion.

2.1.3 Oxy-fuel combustion

In this method, pure oxygen is used as an oxidant and carbon dioxide is captured during combustion. The products for oxy-fuel combustion consists mainly carbon dioxide and water, which can be easily separated. This method uses an atmosphere of oxygen separated from air and re-circulated flue gas to burn fossil fuels creating a flue gas with rich in carbon dioxide and appropriate for transportation and storage.

2.2 Transport, storage and reuse of carbon dioxide

After capture, carbon dioxide will have to be compressed and transported to storage points. Pipelines are useful in transporting the compressed gas to storage points (Global CCS Institute, 2012).

Another option is carbon dioxide capture and reuse. The captured carbon dioxide is useful in the production of methanol, acetic acid, electricity and hydrogen.

2.3 Calcium looping

Calcium looping is a method that can be used for carbon dioxide capture in pre-combustion and post-combustion. Calcium looping involves carbon dioxide capture in a reactor, carbonator, in a process called carbonation where carbon dioxide react with calcium oxide to form calcium carbonate. The calcium carbonate is passed into the second reactor, calciner, where the calcination process takes place. Calcination is an endothermic reaction where calcium carbonate is decomposed to carbon dioxide and calcium oxide. The main advantage of calcium looping technology is that the calcium looping reactors have already been established commercially in large scale (Alonso, et al., 2010).

Shimizu et al (Shimizu, et al., 1999) first proposed calcium looping. It involves the carbon dioxide separation from flue gas making use of the reversible reaction of calcium oxide and carbon dioxide and the calcination of calcium carbonate to regenerate calcium oxide.

Important steps have been taken in the past to demonstrate the viability of the calcium looping technology. Experimental testwork to test the viability of using calcium oxide as carbon dioxide absorber in a calcium looping system have been carried out. Carbon dioxide capture efficiencies ranging from 70-97% have been achieved in different test facilities at lab-scale from 10-30KWth (Charitos, et al., 2011) (Alonso, et al., 2010) (Abanades, et al., 2004).

Several approaches have been made towards the development of carbonator reactor models integrated into a calcium looping system. Shimizu et al. (Shimizu, et al., 1999) and Abanades et al (Abanades, et al., 2004) used the bubbling bed model proposed by Kunii and Levenspiel (Levenspiel, 1999) to predict the carbon dioxide captured in a bubbling-bed absorber that consisted of calcium oxide particles. Circulating fluidised bed carbonators are the most common choice for large-scale systems when high volumes of flue gases are expected to enter the carbonator on condition that it operates at atmospheric pressure. The first approach to modelling of a CFB reactor acting as carbonator was proposed by Hawthorne et al (Hawthorne, et al., 2008) and Alonso et al (Alonso, et al., 2009). The models projected that capture efficiencies above 80 % can be achieved under reasonable conditions.

Advantages of calcium sorbents and calcium looping process

- The sorption capacity of calcium oxide is high compared to other processes. At best conditions, the sorption capabilities of silica gel, monoethanolamine and activated carbon are 13.2, 60 and 88 grams of carbon dioxide for every kilogram of sorbent respectively. In contrast, that of calcium

oxide is 393 grams of carbon dioxide for every kilogram of sorbent, assuming that calcium oxide is converted to 50% after many carbonation-calcination cycles.

- The abundance of calcium carbonate in nature as limestone and dolomite and its low cost allows the technology to be used by even developing countries.
- Calcination energy can be recovered effectively in the carbonator since both calcination and carbonation happen at high temperature (above 600 ^{o}C).

2.3.1 Process description

The main components in the calcium looping technology are the carbonator and regenerator (calciner). Flue gas is fed into the carbonator, which operates between 600^{o}C and 700^{o}C where carbon dioxide reacts with calcium oxide to form calcium carbonate. Lime is carbonated and passes through the cyclone where the stream is separated into a carbon dioxide depleted gas stream and a stream of solids that are passed to the calciner for regeneration of the sorbent (Alonso, et al., 2010). Limestone releases the carbon dioxide at high temperature in the calciner. The products from the calciner passes through a cyclone, where carbon dioxide is separated from solids.

Solids from carbonator are fed into the calciner where calcium carbonate is calcined to form calcium oxide, which is recirculated back to the carbonator. The sorbent (usually limestone) is injected into the bed of the regenerator at a temperature around 850^{o}C to 950^{o}C where the limestone is calcined. Combustion, heat transfer or electrical heating can supply heat. After calcination, a fluidizing gas carries the lime is carried out of the calciner to the cyclone for separation from the gas thereafter it is lead to the carbonator. Since a high concentration of carbon dioxide is targeted at the exit of the regenerator, the equilibrium of carbon dioxide on calcium oxide (approximately 900^{o}C for pure carbon dioxide at atmospheric pressure) requires that calcination take place at elevated temperatures. Calcination uses a great amount of energy, almost 50% of energy used in the calcium looping system, because there is need of heating up the solids from carbonator and calcination is an endothermic reaction (I.Martinez, et al., 2013).

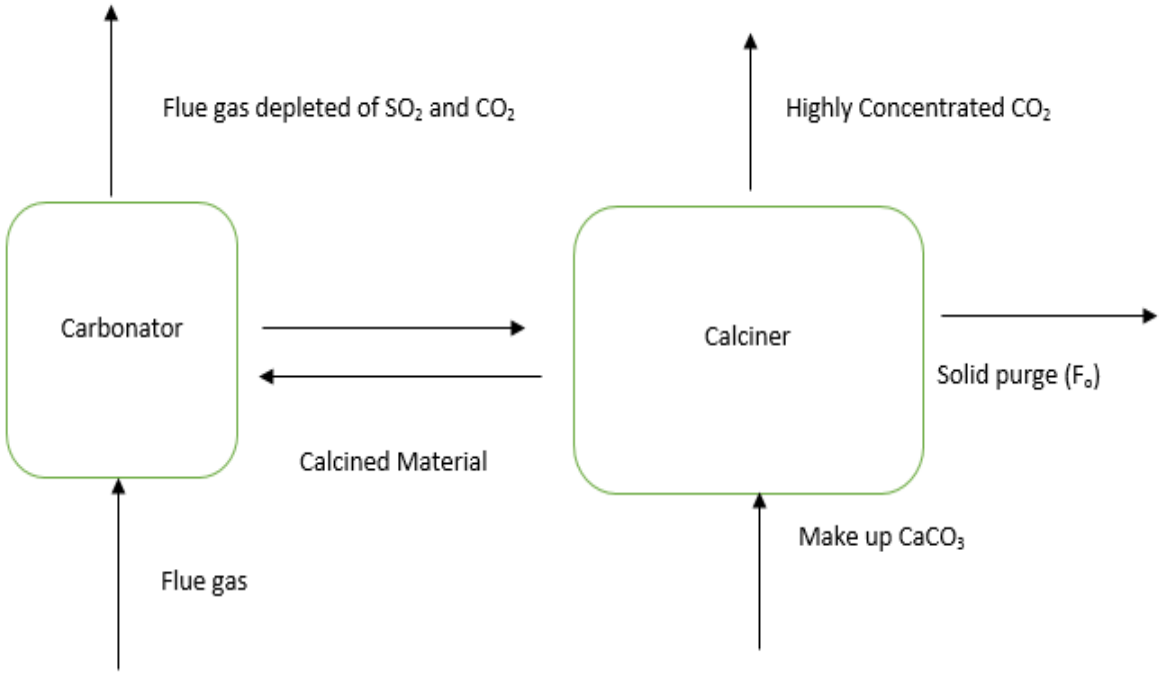

Figure 2- 4:Calcium looping system

Side reactions such as sulphation and sintering result in the sorbent being inactive. Fresh sorbent will have to be added to compensate for the loss.

2.3.1.1. Carbonator

Calcium oxide is transferred to the carbonator, where calcium oxide reacts with carbon dioxide as given below:

$$CaO + CO_2 \leftrightarrow CaCO_3 \qquad \Delta H = -178KJ/mol \qquad \text{(Eq. 2-1)}$$

Calcium oxide also react with sulphur dioxide in flue gas. Calcination and sulphation reactions can limit the carbonator temperature to a maximum of 700ºC, above which sulphation rate increases and the calcium carbonate decomposes releasing carbon dioxide (Dean, et al., 2011).

There are two stages of carbonation:

- Fast carbonation stage

In this stage, the carbon dioxide is bound on the surface of the calcium oxide.

- Slow carbonation stage

Diffusion occurs and carbon dioxide is bound in the calcium oxide particle.

The carbonation reaction may be represented by the following empirical correlation:

$$r_{carb} = m_s S_{ave}(W_{max} - W)k_{carb}(C_{CO_2} - C_{CO_{2e}}) \quad \text{(Eq. 2-2)}$$

Where: m_s is mass of solid

S_{ave} is the reaction surface area

$W_{max} - W$ represent the active fraction of the solid material

k_{carb} represents the kinetic constant for the carbonation reaction

C_{CO_2} is carbon dioxide concentration in the flue gas

The optimum carbonation temperature is 650ºC above which the reaction improves but also the equilibrium carbon dioxide partial pressure increases resulting in the carbonation reaction slowing or reversing.

2.3.1.2 Calciner/regenerator

In the regenerator, limestone is calcined releasing carbon dioxide

$$CaCO_3 \leftrightarrow CaO + CO_2 \qquad \Delta H = 178KJ/mol \quad \text{(Eq.2-3)}$$

Because calcination reaction is endothermic, heat has to be supplied. Calcination is carried out at higher temperature than carbonation. Due to sintering and sulphation reactions, and the sorbent deactivation caused by these reactions, the maximum recommended temperature for calcination is 900ºC (Dean, et al., 2011). Calcination process normally takes 0 to 15 minutes to complete. If the sorbent is exposed to high temperatures for a longer period, it will end up deviating from the required process (calcination) and is sintered.

Calcination is mainly affected by surrounding temperature and carbon dioxide partial pressure at the calcium oxide/calcium/carbonate/carbon dioxide interface. Calcination rate depends on the properties of the limestone used and the relation of carbon dioxide partial pressure, P_{CO_2} to equilibrium partial pressure (Stanmore & Gilot, 2005)

$$r_{calc} = m_s W S_{ave} \frac{M_{CaCO_3}}{\rho_{CaCO_3}} k_{calc} \left(1 - \frac{P_{CO_2}}{P_{CO_{2e}}}\right) \quad \text{(Eq.2-4)}$$

Where: S_{ave} represents the reaction surface area

ρ_{CaCO_3} represents the density of calcium carbonate

M_{CaCO_3} represents the molar mass of calcium carbonate

k_{calc} represents the kinetic parameter for the calcination reaction of the selected limestone

The evaluation of the kinetics of calcination can be complicated by:

- The concentration of carbon dioxide which hinder the reaction
- Particle size which may cause mass transfer limitations
- Catalysis or inhibition by impurities. Vanadium pentoxide and fly ash are commonly known to inhibit calcination while lithium carbonate accelerates it.

2.3.2 Sorbent deactivation

2.3.2.1 Sulphation

When a fuel with a sulphur content burn, sulphur dioxide is formed which competes with carbon dioxide on reaction with calcium oxide. Sulphur dioxide reacts with calcium oxide in two possible ways:

$$CaO + SO_2 + \frac{1}{2}O_2 \rightarrow CaSO_4 \quad \Delta H = -502KJ/mol \qquad \text{(Eq. 2-5)}$$

$$CaCO_3 + SO_2 + \frac{1}{2}O_2 \rightarrow CaSO_4 + CO_2 \quad \Delta H = -324KJ/mol \qquad \text{(Eq. 2-6)}$$

These reactions take over the formation of calcium carbonate due to the differences in heat of reaction. The significance of their influence depends on the Sulphur dioxide content of the flue gas. Sulphation reaction can also take place in the calciner if heat is supplied using oxy-fuel combustion.

As the sorbent is used, the pores become blocked with a layer of solid product. In normal case, the solid would be calcium carbonate. However, in the case of Sulphur dioxide, calcium sulphate will block the layer of the solid product. The critical aspects of calcium sulphate formation are that calcium sulphate has a higher density than calcium carbonate, which results in the pores closing faster and all together regenerating the calcium oxide from the calcium sulphate is impractical as it is only possible at high temperatures (Dean, et al., 2011).

In addition to the formation of calcium sulphate, loses in sorbent capacity also occur due to high temperature. High temperature results in sintering and reduction in surface area of the particles resulting in less carbon dioxide being captured per cycle.

There basic patterns for sulphation are;

i) The unreacted core/core-shell pattern

The core-shell pattern dominates direct sulphation. This is characterized by the blockage of the external pore of the surface, which is caused by the molar volume differences of calcium sulphate and calcium oxide. Pore blocking prevents further sulphation of the innermost core of the particle, hence hindering the

conversion of calcium oxide to calcium sulphate. Only the external surface of the sorbent is sulphated and the inner part remains unsulphated or slightly sulphated since the sorbents have very small pores that have no fractures (Cordero & Alonso, 2015).

ii) The network pattern

This is composed of particles with a connected network of very small fractures, which allow sulphur dioxide to penetrate inside and thereby reacting and forming calcium sulphate. The fractures divide the particles into blocks with each block acting like an unreacted core as only the external surfaces achieve high levels of sulphation.

iii) Homogeneous/uniform pattern

This is where there are small porous particles with connected fractures. There is uniform sulphation as sulphur dioxide can reach all surfaces. High conversion rates are achieved in this pattern.

In post-combustion, number of carbonation-calcination cycles can alter the sulphation pattern since it modifies the original porous structure of the particles.

Sulphation is affected by temperature. Pore blockage is likely to occur at elevated temperatures since at such temperatures the diffusional resistance of the reactant in the pores is increased (Cordero & Alonso, 2015). Large particle sizes cause core sulphation to occur.

For low number of carbonation-calcination cycles, unreacted core sulphations are more like to occur while for highly cycled particles in the carbonator, the uniform patterns are more likely to occur. The random pore model (RPM) is therefore a suitable model for fitting the kinetic parameters and for developing the mathematical expressions to predict the experimental conversion curves of calcium oxide to calcium sulphate.

Assumptions of RPM are;

- The particles are isotherm
- Negligible diffusional effects in the pores
- Sulphation is first order with respect to sulphur dioxide concentration

Bhatia and Perlmutter (Bhatia & Perlmutter, 1981) proposed the expression below for the random pore model;

$$\frac{dX_{CaO}}{dt} = \frac{k_s S C_s (1-X_{CaO})\sqrt{1-\varphi \ln(1-X_{CaO})}}{(1-\varepsilon)\left[1+\frac{\beta Z}{\varphi}\sqrt{1-\varphi \ln(1-X_{CaO})}-1\right]} \qquad \text{(Eqn.2-7)}$$

Where; φ represents the internal structure parameter that accounts for the internal structure of the particle.

Equation 2-7 fits for both the kinetic and diffusional control of reactants through the product layer.

$$\varphi = \frac{4\pi L(1-\varepsilon)}{S^2} \quad \text{(Eq.2-8)}$$

$$\beta = \frac{2k_s a\rho(1-\varepsilon)}{bM_{CaO}D_p S} \quad \text{(Eq.2-9)}$$

Two cases for simplifying equation 2-7 are;

i) Under fast kinetic regime (i.e. $\beta = 0$)

$$\frac{dX_{CaO}}{dt} = \frac{k_s S C_s (1-X_{CaO})\sqrt{1-\varphi \ln(1-X_{CaO})}}{(1-\varepsilon)} \quad \text{(Eq.2-10)}$$

Equation 2-10 can be integrated to find an expression of kinetic regime:

$$\frac{1}{\varphi}\left[\sqrt{1-\varphi \ln(1-X_{CaO})}-1\right] = \frac{k_s S C_s t}{2(1-\varepsilon)} \quad \text{(Eq.2-11)}$$

ii) Under diffusion through the product layer regime

$$\left|1+\frac{\beta Z}{\varphi}\sqrt{1-\varphi \ln(1-X_{CaO})}-1\right| \gg 1 \quad \text{(Eq.2-12)}$$

Which allows equation 2-7 to be integrated to give:

$$\frac{1}{\varphi}\left[\sqrt{1-\varphi \ln(1-X_{CaO)}}-1\right] = \frac{S}{(1-\varepsilon)}\sqrt{\frac{D_p M_{Cao} C_s t}{2\rho_{CaO} Z}} \quad \text{(Eq.2-13)}$$

Where: C_s is concentration of sulphur dioxide (kmolm^3)

D_p is effective product layer diffusivity (m^2/s)

ρ is density

ε is porosity

β is modified Biot modulus

k_s is the rate constant for surface reaction (m^4/mol s)

The reaction parameters k_s and D_p can be obtained by fitting equations 2-11 and 2-13 to the experimental data for each regime.

2.3.2.2 Sintering

Heating solid particles at high temperatures but below their melting point will cause them to start to merge. Porous materials like calcium oxide will shrink and the pores close as al the grains that initially formed the sorbent will fuse together to form larger grains. This is known as sintering and is more evident at high temperatures and long periods of reaction. It will cause a drop in the reactivity of the sorbent.

If temperatures become too high (above 900°C for calcium oxide), sintering occurs at a high rate. This means the make-up flow will have to be increased too. Conditions in fluidized bed allow for sintering to occur. Sintering reduces the porosity and surface area of the sorbent. Sintering is accelerated by presence of carbon dioxide and water (Grasa, et al., 2008).

2.3.3 Vertical density profile of solids in the reactor

The solid phase consist of two solid materials, calcium oxide and calcium carbonate. The vertical density profile is modelled using a correlation proposed by Ylatalo (J.Ylatalo, et al., 2012);

$$\rho_s(h) = (\rho_b - \rho_e e^{KH_e})e^{-ah} + \rho_e e^{K(H_e-h)} \quad \text{(Eq.2-14)}$$

Where: K is the transport zone solid decay constant

h is local height coordinate

a is the splash zone decay constant

a describes the formation of solid clusters over the dense area as shown in equation 2-15, below.

a and K are calculated as follows;

$$a = 4\frac{U_t}{U_g} \quad \text{(Eq.2-15)}$$

K defines the entrainment of the solids at the exit as shown in equation 2-16, below.

$$K = \frac{0.23}{U_g - U_t} \quad \text{(Eq.2-16)}$$

U_t is the particle terminal velocity at the upper part of the riser

U_g is the velocity of the gas mixture at the grid and H_e is the height to the exit channel.

Terminal velocity can be calculated from;

$$U_t = \left[\frac{4gd_p}{3C_d}\left(\frac{\rho_s}{\rho_g} - 1\right)\right]^{0.5} \quad \text{(Eq.2-17)}$$

d_p is the particle diameter

C_d is particle drag coefficient

ρ_g is the density of the gas phase

ρ_s is the apparent density of the solid phase

The solid exit density;

$$\rho_e = \rho_{s,pt} \frac{U-U_t}{U_{pt}-U_t} \quad \text{(Eq.2-18)}$$

Where: U is gas mixture velocity of the particles

U_t is the gas mixture velocity which corresponds pneumatic transport condition

$\rho_{s,pt}$ represents the solid density at pneumatic transport condition

The solid bed density,ρ_b, at h=0 is found by integrating the equation for $\rho_s(h)$ above.

2.3.4 Calcium looping reactors

A great effort has been made in the past to design the calcium-looping reactor with much emphasis being put on the carbonator (Romano, et al., 2013). Different types of reactors have been proposed in literature for use in calcium looping carbonator and calciner. Some researchers have proposed the use of the bubbling fluidised-bed reactor (Abanades, et al., 2004) (Shimizu, et al., 1999) (Romano, 2009) while others have used the circulating fluidized reactor (Alonso, et al., 2010) (Hawthorne, et al., 2011) (Romano, 2012). Table 1-1 below shows a comparison of various reactor types which can be used for carbonation;

Table 2- 1:Comparisons of reactors based on (Kunii & Levenspiel, 1991)

Reactor	**Gas-Solid Reaction**	**Temperature Distribution in the bed**
Fixed bed	Not suited for continuous operations. Bath operations yield non-uniform product	If much heat is involved, there will be a large temperature gradient
Moving bed	Can be used for larger scale operations. Ideal for uniform sized feed with little or no fines	Temperature gradient is controlled by proper gas flow or can be reduced by large solids circulation
Bubbling and turbulent fluidized bed	A wide range of solids with many fines can be used. It can be used for large-scale operations at uniform temperature. It is excellent for uniform operations. It yields a uniform product	Constant temperature throughout. Temperature is controlled by heat exchange or by proper feeding or removal of solids
Fast fluidized bed and co-current pneumatic transport	Ideal for fast reactions. Recirculation of fines is crucial	Sufficient circulation of solid can minimize temperature gradients in the direction of solid flow.
Rotary kiln	Suitable for solids which may sinter or agglomerate	Severe temperature gradients, which are difficult to control.
Flat hearth	Suitable for solids that are likely to sinter or melt.	Temperature gradients are severe and difficult to control

In fluidized and fast-fluidized beds, smooth and steady state recirculation of solids through the dipleg or other solid trapping device is essential for good operation. Theses beds are called circulating fluidized beds.

3

Chapter three

3 MODEL DEVELOPMENT

3.1 Kinetics

The progressive –conversion model and the shrinking core models are the simple, idealized models used for non-catalytic reactions with surrounding fluid. These models are used in assessing how the calcium looping reaction proceeds.

3.1.1 Progressive-Conversion Model (PCM)

The PCM visualizes the reactant gas entering and reacting throughout the particle at all times, mostly at different rates and at different locations within the particle (Levenspiel, 1999)as shown below.

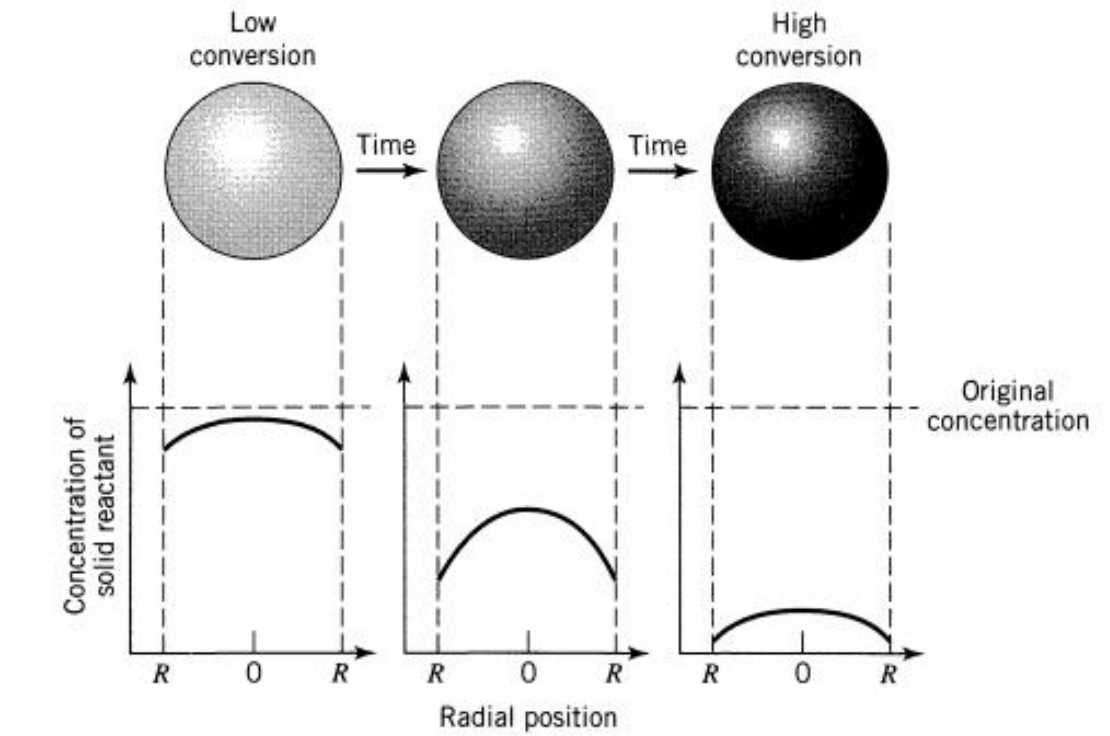

Figure 3- 1:Progressive Conversion Modell (Levenspiel, 1999)

3.1.2 Shrinking-Core Model

For the shrinking-core model, reaction occur at the surface layer of the particle first then the reaction zone proceeds into the core leaving behind a wholly converted solid and inert solid, ash, therefore at any time there will be an unreacted core of solid which reduces in size during reaction.

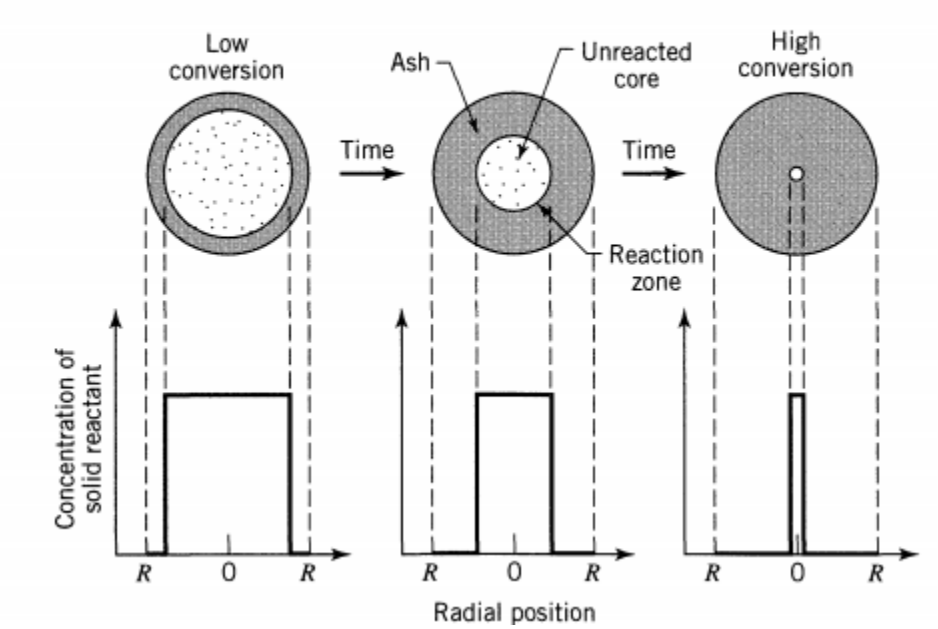

Figure 3- 2:Shrinking Core Model (Levenspiel, 1999)

The shrinking core model gives a better approximation of real particles than the progressive conversion model. The shrinking-core model can be applied for particles of unchanging size.

The reaction mechanism consists of:

- The reactant diffusing through the boundary film surrounding the particle.
- Reactant penetrating and diffusing the layer of solid product until reaching the surface of unreacted core
- Reaction at the core surface

3.1.3 Carbonation kinetics

Kinetic data on the carbonation reaction, below, revealed that the reaction is rapid initially and chemically controlled but undergoes a sudden transition to a slower diffusion controlled regime.

$$CaO + CO_2 \leftrightarrow CaCO_3 \qquad \Delta H = -170 KJ/mol \qquad \text{(Eqn. 3-1)}$$

The reaction can be expressed by combining the mass transfer and intrinsic chemical reaction resistances.

$$\frac{-dr_c}{dr} = \frac{bC_a/\rho}{r_c^2/R^2k_g + \frac{(R-r_c)r_c}{RD} + 1/k_c} \quad \text{(Eqn. 3-2)}$$

The reaction conversion can be expressed in terms of the unreacted core radius as;

$$X = 1 - (\frac{r_c}{R})^3 \quad \text{(Eqn. 3-3)}$$

$$\frac{dX}{dt} = \frac{P_1(1-X)^{2/3}}{(1-X)^{2/3} + P_2(1-X)^{\frac{1}{3}}\left(1-(1-X)^{\frac{1}{3}}\right) + P_3} \quad \text{(Eqn. 3-4)}$$

Where: $P_1 = 3k_g bc_a/R\rho$

$P_2 = k_g/D$

$P_3 = k_g/k_c$

Where: r_c is radius of unreacted core

c_a is concentration

ρ is density

R is radius of particle

k_g is mass transfer coefficient of the gas film

D is the effective diffusion coefficient in porous structures

k_c is the first order reaction rate constant for surface reaction

X is reaction conversion

According to Rodriguez et al (N.Rodriguez, et al., 2011) the carbonator efficiency can be expressed by the equation below;

$$E_{carb} = \frac{CO_2 \text{ reacting with } CaO \text{ in the bed}}{CO_2 \text{ entering the bed in the flue gas}} \quad \text{(Eqn.3-5)}$$

Calcined particles are fed to the carbonator where they react with carbon dioxide to form calcium carbonate. Carbon dioxide balance can be expressed as;

$$CO_2\ reacting\ with\ CaO\ in\ the\ bed = CaCO_3 formed\ in\ the\ circulating\ stream\ of\ CaO = CO_2\ removed\ from\ the\ gas\ phase \quad \text{(Eqn.3-6)}$$

For a constant carbonation conversion and solid circulation rate;

$$F_{CaO}(X_{carb} - X_{calc}) = F_{CO_2}E_{carb} \quad \text{(Eqn.3-7)}$$

Where: F_{CaO} is calcium oxide circulation rate (kmol/m^{2}s)

X_{carb} is average conversion in the carbonator

X_{calc} is the carbonate content of the solids coming from the calciner

In addition, in a stationary state period equation 3-5 can be reduced to;

$$F_{CO_2}E_{carb} = \frac{W_{CaO}}{PM_{CaO}}\frac{dX_{carb}}{dt} \quad \text{(Eqn.3-8)}$$

Where: W_{CaO} is the total inventory of solids in the carbonator (kg/m^2)

PM_{CaO} is the average molar weight of the solids inventory in the carbonator (kg/mol)

$\frac{dX_{carb}}{dt}$ is the average reaction rate of the solids in the reactor (s^{-1}) at the average temperature carbon dioxide carbon dioxide concentration in the carbonator.

The bed contains active calcium oxide particles that react in the fast regime (X_{active}), inactive calcium oxide from preceding carbonation-calcination cycles, calcium carbonate resulting from carbonate conversion (X_{carb}).

If a first order carbonation reaction rate is assumed, the expression given below is obtained (N.Rodriguez, et al., 2011);

$$\frac{dX}{dt_{reactor}} = \varphi_e k_{rea-max} X_{active}(v_{CO_2} - v_{CO_{2,eq}})_{reactor} \quad \text{(Eqn.3-9)}$$

Where: $k_{rea-max}$ is the reaction rate constant of active calcium oxide

X_{active} is the active fraction of the calcium oxide in the carbonator reactor

v_{CO_2} is average volume fraction of carbon dioxide in the reactor

$v_{CO_{2,eq}}$ is the equilibrium volume fraction of carbon dioxide in the reactor

The overall carbonator efficiency is;

$$\varphi_e = \frac{E_{carb} F_{CO_2}}{W_{CaO}/PM_{CaO} k_{reac-max} X_{active} (\bar{v}_{CO_2} - v_{CO_{2,eq}})_{reactor}} \quad \text{(Eq.3-10)}$$

Where: $\bar{v}_{CO_2}$ is the average volume fraction of carbon dioxide in the carbonator

φ_e equals to one during stationary state .When φ_e is equal to one, equation 3-9 will be the same as the that modelled by Ylatalo et al (J.Ylatalo, et al., 2012)

$$r_{carb} = m_s (W_{max} - W) k_{carb} (C_{CO_2} - C_{CO_{2e}}) \quad \text{(Eq.3-11)}$$

Where: m_s is mass of solid

$W_{max} - W$ is the active fraction of the solid material

k_{carb} Is the kinetic constant for the carbonation reaction

The active fraction of solid material;

$$W_{max} - W = f_a = 1 - e_{\tau}^{-t^*} \quad \text{(Eq.3-12)}$$

Where: $t^*$is the characteristic time at which the reaction rate becomes zero

τ is average residence time in the carbonator

$$\tau = \frac{N_{ca}}{F_r} = \frac{W_{ca}}{F_r}$$

The characteristic time at which the reaction rate becomes zero can be evaluated based on graph below;

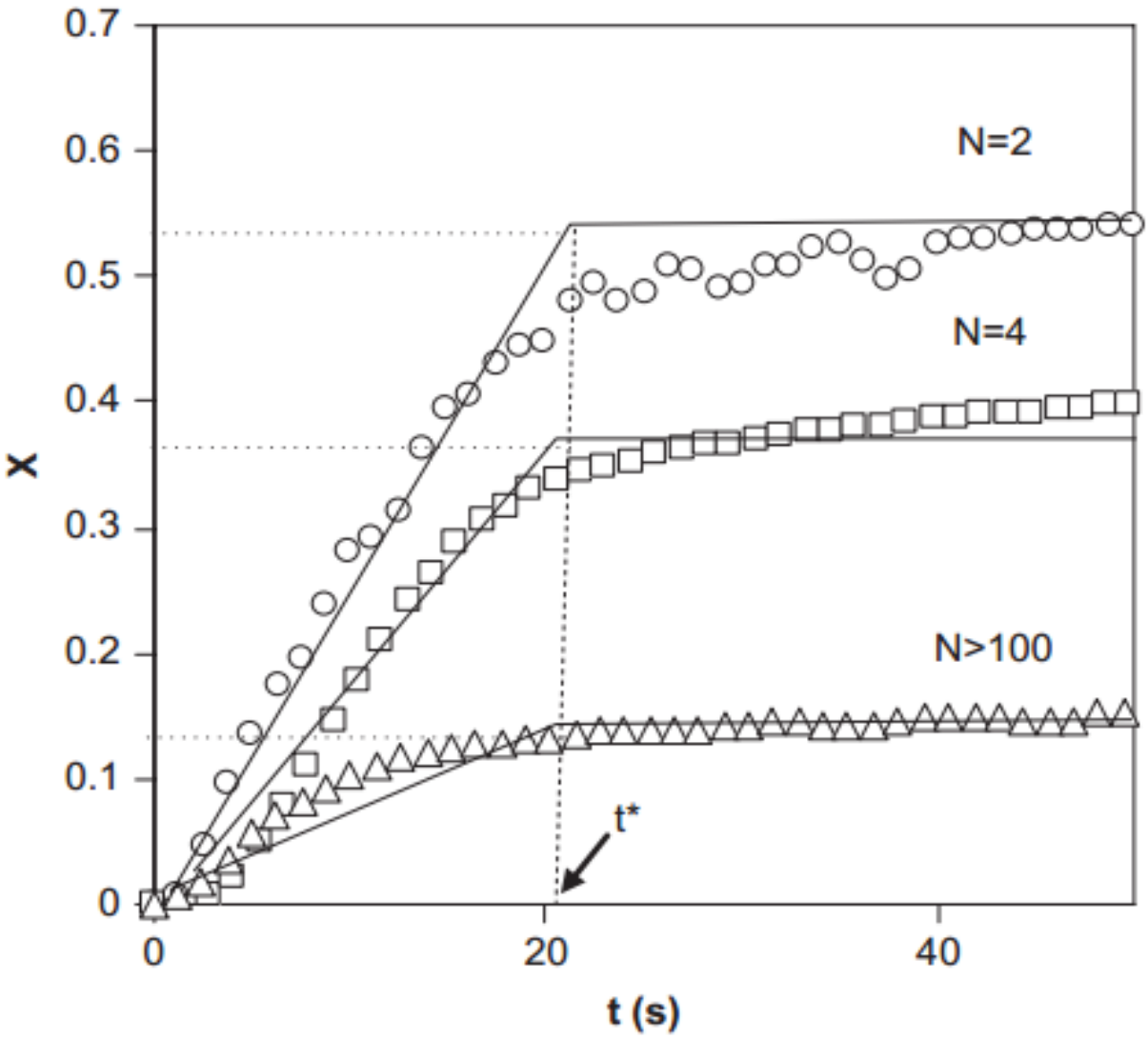

Figure 3- 3:Scheme of the kinetic model adopted to describe the progress of the carbonation reaction with time for different cycle number (Alonso, et al., 2009)

Alonso (Alonso, et al., 2009) includes the average reaction surface area S_{ave} in the equation for rate of carbonation. Thus, the rate of carbonation is given by Equation 3-13.

$$r_{carb} = m_s f_a \, S_{ave} k_{carb} (C_{CO_2} - C_{CO_{2e}}) \qquad \text{(Eq.3-13)}$$

$$S_{ave} = \frac{X_{ave} \frac{\rho_{CaO}}{PM_{Cao}}}{e_{max} \frac{\rho_{CaCO_3}}{PM_{CaCO_3}}} \qquad \text{(Eq.3-14)}$$

Where: ρ_{CaO} and ρ_{CaCO_3} are densities of calcium oxide and calcium carbonate

X_{ave} is the average conversion of solids

PM_{Cao} and PM_{CaCO_3} are molecular weights of calcium oxide and calcium carbonate

e_{max} is maximum thickness of the layer of calcium carbonate on the pore wall

The average value of the carbonation rate constant was calculated by Bhatia and Permutter for temperatures ranging from 550 °C to 725 °C (Bhatia & Permutter, 1983) as 5.95×10^{-10} $m^4(mol\ s)^{-1}$.

3.1.4 Calcination kinetics

Calciner efficiency E_{calc} is defined as the fraction of calcium carbonate calcined in the reactor (I.Martinez, et al., 2013);

$$E_{calc} = \frac{Moles\ of\ CaCO_3\ calcined}{Moles\ of\ CaCO_3\ entering\ the\ calciner} = \frac{X_{carb}-X_{calc}}{X_{carb}} \quad \text{(Eq.3-15)}$$

A typical carbon dioxide concentration in the calciner is between 70% and 75% assuming instantaneous and complete combustion of the fuel at the entrance of the calciner.

The shrinking-core model considers calcium carbonate breakdown at a calcium oxide-calcium carbonate interface around the particles and the diffusion of carbon dioxide released through the porous calcium oxide to particle surface (Garcia-Labiano, et al., 2002). The sorbent is assumed to be isothermal and spherical.

Calcination is governed by the equation below:

$$\frac{dR_c}{dt} = -k_c V_{MCao} f(P_{CO_2}) \quad \text{(Eq.3-16)}$$

With R_c=R_o at t=0

Where: V_{MCao} is molar volume of calcium oxide (m^3/mol)

R_c is radius of shrinking core of calcium carbonate within the particle (m)

P_{CO_2} is carbon dioxide partial pressure

R_o is particle radius

The equation which governs the diffusion of carbon dioxide through the pores of calcium oxide is:

$$\frac{\partial^2 P_{CO_2}}{\partial R^2} + \left(\frac{2}{R} + \frac{1}{D_e}\frac{\partial D_e}{\partial R}\right)\frac{\partial P_{CO_2}}{\partial R} = \frac{1}{D_e}\frac{\partial P_{CO_2}}{\partial t} \quad \text{(Eq.3-17)}$$

Where: D_e is effective diffusivity within the particle (m^2/s)

With the two boundary conditions:

$$-D_e\frac{dP_{CO_2}}{dR} = k_g\left(P_{CO_2} - P_{bulk}\right) \text{ at } R=R_o \quad \text{(Eq.3-18)}$$

$$-\frac{D_e}{R_g T}\frac{dP_{CO_2}}{dR} = k_c f\left(P_{CO_2}\right) \text{ at } R=R_c \quad \text{(Eq.3-19)}$$

Where: k_g is external mass transfer coefficient (m/s)

k_c is chemical reaction rate constant (mol/m^{2}s)

P_{CO_2} is carbon dioxide partial pressure (Pa)

P_{bulk} is carbon dioxide partial pressure (Pa)

Applying the pseudo-steady state approximation for gas-solid reactions, and considering D_e as constant with time, equation 3-17 can be simplified to:-

$$\frac{\partial^2 P_{CO_2}}{\partial R^2} + \frac{2}{R}\frac{\partial P_{CO_2}}{\partial R} = 0 \quad \text{(Eq.3-20)}$$

Using the Langmuir-Hinshelwood mechanistic model to describe the chemical reaction accounting for the sorption of carbon dioxide on the calcium carbonate surface, chemical decomposition of calcium carbonate to give calcium oxide and adsorbed carbon dioxide:-

$$CaCO_3 + nL \rightleftharpoons CaO + nL(CO_2), K_1 = k_1/k_2 \quad \text{(Eq.3-21)}$$

Where: $nL(CO_2)$ accounts for one carbon dioxide molecule chermisobed on n active sites L

k_1 is forward reaction kinetic constant for the chemical decomposition (mol/m^{2}sPa)

k_2 is backward reaction kinetic constant for the chemical decomposition (mol/m^{2}sPa)

K_1 is equilibrium constant for the chemical decomposition, dimensionless

Garcia-Labiano et al (Garcia-Labiano, et al., 2002) gives an expression for Equation 3-21 when chemical decomposition is controlling:

$$r_c = k_c S_e (1-\theta)\left(1 - \frac{P_{CO_2}}{P_{eq}}\right) \quad \text{(Eq.3-22)}$$

Where: θ is the fraction of active sites that is occupied

r_c is reaction rate of calcination (molm^3/s)

Equation 3-22 agrees with that given by Ylatalo (J.Ylatalo, et al., 2012);

$$r_{calc} = m_s W S_{ave}\frac{M_{CaCO_3}}{\rho_{CaCO_3}} k_{calc}\left(1 - \frac{P_{CO_2}}{P_{CO_2 e}}\right) \quad \text{(Eq.3-23)}$$

Where: S_{ave} is the reaction surface area

ρ_{CaCO_3} is the material density of calcium carbonate

M_{CaCO_3} is the molar mass of calcium carbonate

k_{calc} is the kinetic parameter for the calcination reaction of the selected limestone

r_{calc} is reaction rate of calcination (molm^3/s)

W is mass based conversion of limestone

The kinetic parameter for calcination was modelled by Silcox et al (Silcox, et al., 1989) as given below;

$k_{calc} = 1.22\exp(-4026/T)$ (mol.m^{-2}.s^{-1}.atm^{-1}) (Eq.3-24)

3.1.5 Sulphation kinetics

The sulphation reaction rate as presented by Ylatalo (Ylatalo, 2013) is given below:

$r_{sulf} = m_s k_{sulf} X_{CaO} x_{SO_2} x_{O_2}$ (Eq.3-25)

Where: k_{sulf} is the kinetic constant for sulphation

X_{CaO} is calcium oxide mass fraction in the soilds

x_{SO_2} and x_{O_2} are mass fraction of sulphur dioxide and oxygen in the flue gas

The kinetic constant for sulphation as given by De-Souza Santos (De-Souza Santos, 2010) is;

$k_{sulf} = 4.9 \times 10^3(-3.843T + 5640)e^{\frac{-8810}{T}}$ (s^{-1}) (Eq.3-26)

3.2 Material balance

The material balance will include solid and gaseous material balance. The solids that are considered are calcium oxide, calcium carbonate (the major solids) and calcium sulphate. The gaseous stream will comprise of oxygen, nitrogen, sulphur dioxide and carbon dioxide. Air will be assumed to be the inlet gas for the calciner. Figure 3-4 shows the reactor boundary conditions. The flue gas enters from the bottom (first) control volume and the carbon dioxide depleted gas leaves from the last control volume.

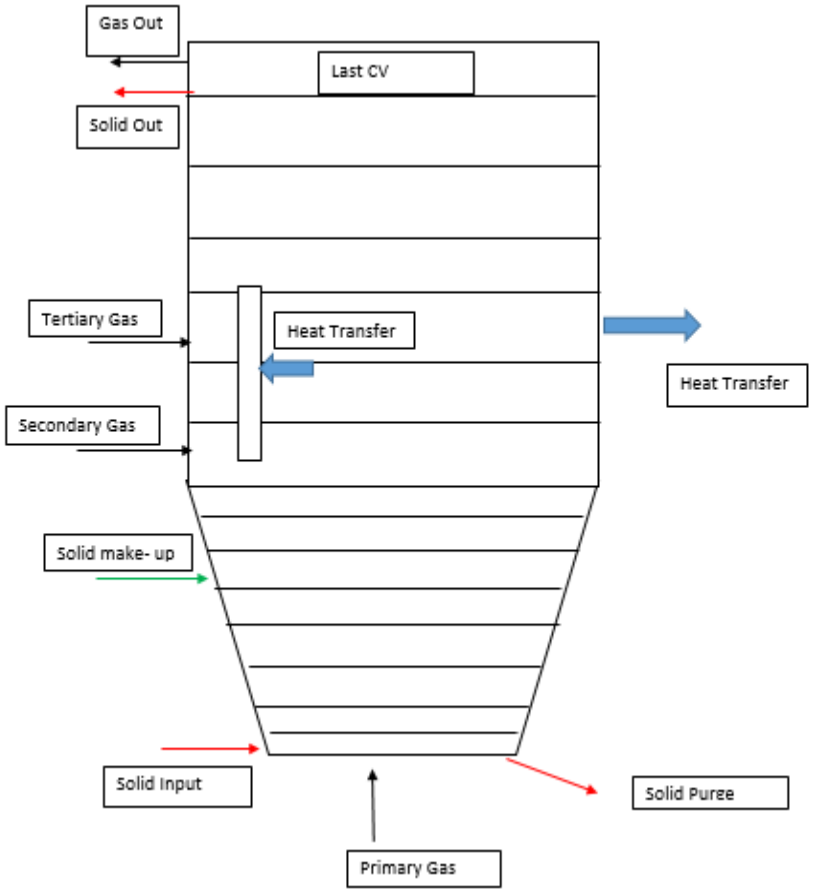

Figure 3- 4:Reactor model boundary conditions based on (Ylatalo, 2013)

3.2.1 Solids material balance

Two solids, calcium oxide and calcium carbonate, form the most part of carbonator and calciner. The required lime mass flow rate is calculated depending on the carbon dioxide mass flow rate and the absorption efficiency.

Change in mass =total mass flows in-total mass flows out + amount of material regenerated

$$\frac{dm_s}{dt} = \sum \dot{m}_{s,in} - \sum \dot{m}_{s,out} + \sum r_s \qquad \text{(Eqn.3-27)}$$

Where: m_s is the total mass in the reactor (kg)

$\dot{m}_{s,in}$ is mass of solids entering the reactor (kg/s)

$\dot{m}_{s,out}$ is mass of solids exiting the reactor (kg/s)

r_s represents solid mass change due to chemical reaction (kg/s)

Incoming solids can be from make-up flow or from another reactor. Figure 3-5, below, shows the solids flow through an element, resulting from core-wall layer interactions (shown by the slanted line), element heterogeneous reactions, and the local solid density change.

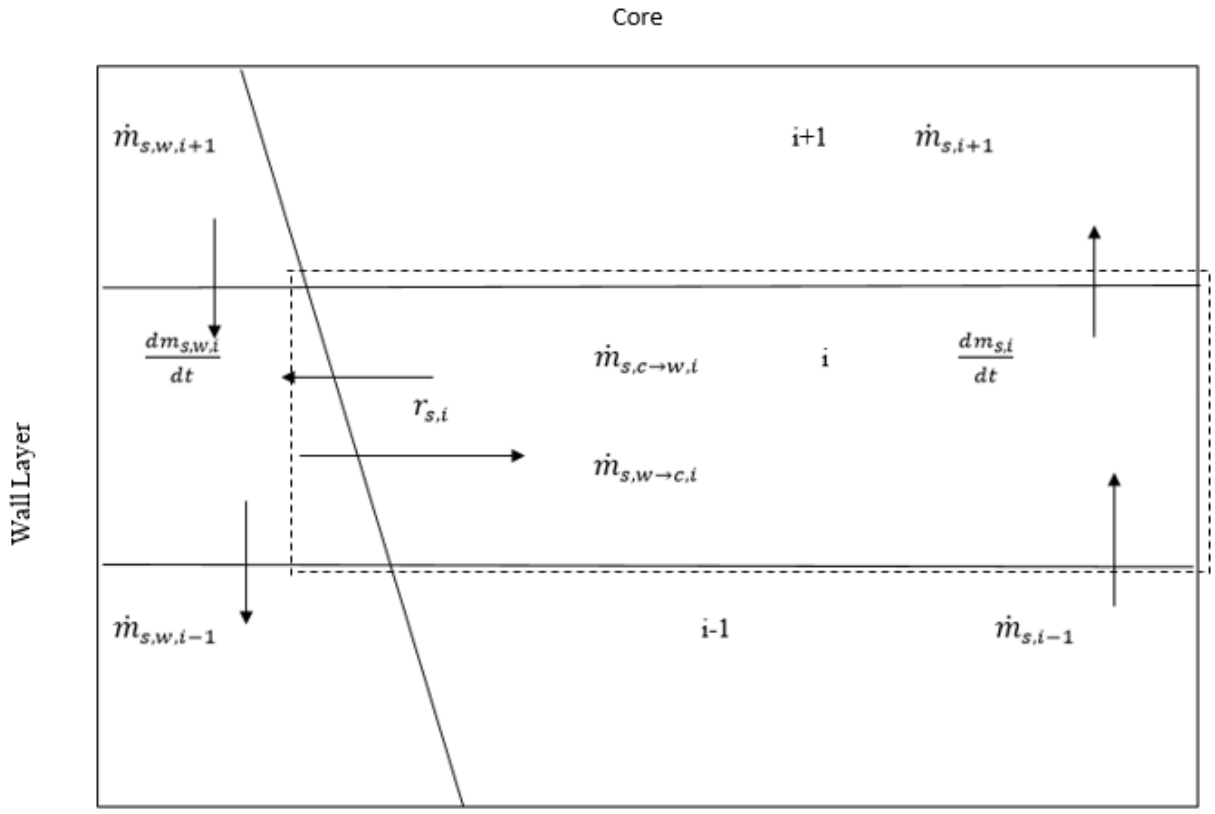

Figure 3- 5:Solids mass flow for a single control volume based on(Ylatalo, 2013)

For a single control volume,

$$\frac{dm_{s,i}}{dt} = \sum \dot{m}_{s,in,i} - \sum \dot{m}_{s,out,i} + r_{s,i} \qquad \text{(Eqn.3-28)}$$

Where: $m_{s,i}$ is control volume mass

$\dot{m}_{s,in,i}$ represents total solids mass flow entering the element

$\dot{m}_{s,out,i}$ represents the total solids mass flow exiting the element

$r_{s,i}$ represents mass change in solids from chemical reactions in a single control volume

Total solid mass exiting an element is;

$$\sum \dot{m}_{s,out,i} = \dot{m}_{s,i+1} + \dot{m}_{s,c\rightarrow w,i} \quad \text{(Eqn.3-29)}$$

Where: $\dot{m}_{s,c\rightarrow w,i}$ represents the mass flows from core to wall layer (kg/s)

Solid mass entering the element is given by;

$$\sum \dot{m}_{s,in,i} = \dot{m}_{s,i-1} + \dot{m}_{s,w\rightarrow c,i} \quad \text{(Eqn3-30)}$$

Re-writing equation 3-28:

$$\dot{m}_{s,i+1} = \dot{m}_{s,i-1} + \dot{m}_{s,w\rightarrow c,i} + r_{s,i} - \dot{m}_{s,c\rightarrow w,i} - \frac{d\rho_{s,i}}{dt}V_i \quad \text{(Eqn.3-31)}$$

The mass balance is not applicable to the first and the last control volumes. In the first control volume there is no flow from preceding element while in the last control volume there is no flow to the next element.

3.2.2 Gas mass balance

The gas mass balance is shown in figure 3-6. The gas mass derivative is much smaller than the solid mass derivative and for this reason, the mass of the gas in the domain can be assumed constant and therefore the change in gas mass to the element is neglected.

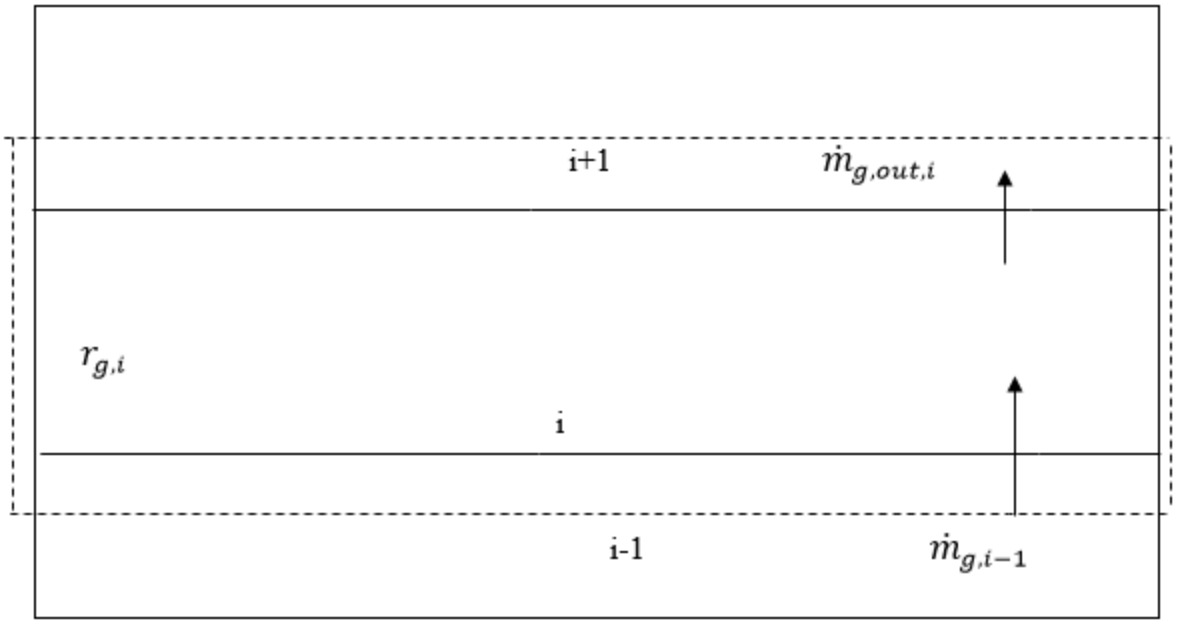

Figure 3- 6:Control volume mass balance

$$\frac{dm_{g,i}}{dt} = \sum \dot{m}_{g,in,i} - \dot{m}_{g,out,j} + r_{g,i} \quad \text{(Eqn.3-32)}$$

There is no gas deposition into the control volume;

$$\dot{m}_{g,out,i} = \sum \dot{m}_{g,in,i} + r_{g,i} \quad \text{(Eqn.3-33)}$$

$$\sum \dot{m}_{g,in,i} = \dot{m}_{g,i-1} \quad \text{(Eqn.3-34)}$$

Where: $m_{g,i}$ is the total gas mass in the domain

$\dot{m}_{g,in,i}$ is gas flow into the element

$\dot{m}_{g,out,j}$ is gas flows out of the element

$r_{g,i}$ is the combined effect of chemical reactions such as calcination, carbonation, sulphation, combustion of char and volatiles

The exiting gas either enter the succeeding control volume or leaves the reactor if the control volume was located at the exit of the reactor. The 1-dimensional gas balance for a single gas component, *a* is given by;

$$\frac{dm_{a,i}}{dt} = \sum \dot{m}_{a,in,i} - \dot{m}_{a,out,i} + \sum r_{a,i} = \sum \dot{m}_{a,in,i} - w_{a,i}\dot{m}_{a,out,i} + \sum r_{a,i} \quad \text{(Eqn.3-35)}$$

Where: $m_{a,i}$ is the mass of the gas component (kg/s)

$\dot{m}_{a,in,i}$ represents gas component entering a control volume (kg/s)

$\dot{m}_{a,out}$ represents the gas component exiting the control volume (kg/s)

$r_{a,i}$is the term for chemical reaction term for the gas component(kg/s)

$$\frac{dw_i}{dt} = \frac{1}{m_{gi}}(\dot{m}_{i,in} - \dot{m}_{i,out} + r_i) \quad \text{(Eq.3-36)}$$

3.3 Energy balance

The energy present in a control volume equals is associated with total convective flows in solids and gases and total energy by dispersion, total heat transfer and chemical reactions.

$$\frac{dE_i}{dt} = \sum q_{conv,s} + \sum q_{conv,g} + \sum q_{disp} + \sum q_{ht} + \sum q_{chem} \quad \text{(Eqn.3-37)}$$

Where: E_i is energy present in the control volume (J)

$q_{conv,s}$ is energy associated with convective flows in solids (J/s)

$q_{conv,g}$ is energy associated with convective flows in gases (J/s)

q_{disp} is energy associated with dispersion between elements (J/s)

q_{ht} is heat transfer (J/s)

q_{chem} is energy associated with chemical reactions (J/s)

The left hand side of equation 3-37 can be further expanded as follows;

$$\frac{dE_i}{dt} = \frac{dU_{s,i}}{dt} + \frac{dU_{g,i}}{dt} = \frac{d(m_{s,i}u_{s,i})}{dt} + \frac{d(m_{g,i}u_{g,i})}{dt} = \frac{d(m_{s,i}(h_{s,i}-p_iv_i))}{dt} + \frac{d(m_{g,i}(h_{g,i}-p_iv_i))}{dt} = \frac{d(m_{s,i}c_{p,s}T_i)}{dt} + \frac{(m_{g,i}h_{g,i})}{dt} = \frac{dm_{s,i}}{dt}c_{p,s}T_i + \frac{dT_i}{dt}m_{s,i}c_{p,s} + \frac{dm_{g,i}}{dt}h_{g,i} + \frac{dh_{g,i}}{dt}m_{g,i} \quad \text{(Eqn.3-38)}$$

Assuming that gas mass is very small,

$$\frac{dm_{g,i}}{dt}h_{g,i} = 0$$

Where: $U_{s,i}$ is the internal energy of the solid

$U_{g,i}$ is the internal energy of the gas

$u_{s,i}$ is specific internal energy of solid phase

$u_{g,i}$ is the specific internal solid and gas phase enthalpies energy of gas phase

$h_{s,i}$ and $h_{g,i}$ are solid and gas phase enthalpies

p_iv_i is work done by phase

$c_{p,s}$ is specific heat capacity of the solids

Solving the temperature derivative from equation 3-38 results in:

$$\frac{dT_i}{dt} = \frac{\sum q_{conv,s+g}+\sum q_{disp}+\sum q_{ht}+\sum q_{chem}-\frac{dm_{s,i}}{dt}c_{p,s}T_i-\frac{dh_{g,i}}{dt}m_{g,i}}{m_{s,i}c_{p,s}} \quad \text{(Eqn.3-39)}$$

3.3.1 Solid phase convective flows

From the mass balance, the convective flow of solids can be written as;

$$\sum q_{conv,s} = \sum q_{conv,s,in} - \sum q_{conv,s,out} = \sum \dot{m}_{s,in,i}c_{p,s}(T_{s,in} - T_{NTP}) - \sum \dot{m}_{s,out}c_{p,s}(T_i - T_{NTP}) \quad \text{(Eqn.3-40)}$$

Where: $q_{conv,s,in}$ represents the convective flows of energy in control volume

$q_{conv,s,out}$ represents the convective flows of energy out of the control volume

$T_{s,in}$ represents temperature of the incoming mass flows

T_{NTP} is reference temperature of the system

Substituting equation 3-39 into equation 3-40 gives;

$$\sum q_{conv,s} - \frac{dm_{s,i}}{dt} c_{p,s} T_i = c_{p,s} \left(\sum \dot{m}_{s,in,i} T_{s,in} - \sum \dot{m}_{s,out,i} T_i - \frac{dm_{s,i}}{dt} T_i \right) \quad \text{(Eqn.3-41)}$$

For solids with different heat capacities, equation 3-41 can be written as;

$$\sum q_{conv,s} - \frac{dm_{s,i}}{dt} c_{p,s} T_i = \sum c_{p,s} \dot{m}_{s,in,i} \left(T_{s,in} - T_{NTP} \right) - \sum c_{p,s} \dot{m}_{s,in,i} \left(T_i - T_{NTP} \right) \quad \text{(Eqn.3.42)}$$

3.3.2 The gas phase convective flows

The convective flows of the gas can be written as shown below;

$$\sum q_{conv,g} = \sum q_{conv,g,in} - \sum q_{conv,g,out} = \sum \dot{m}_{g,in,i} h_{g,in} - \sum \dot{m}_{g,out,i} h_{g,i} \quad \text{(Eqn.3-43)}$$

Where: $q_{conv,g,in}$ is convective of gases into the control volume

$q_{conv,g,out}$ is convective energy flows of gases out of the control volume.

Substituting equation 3-39 to equation 3-43;

$$\sum q_{conv,g} - \frac{dh_{g,i}}{dt} m_{g,i} = \sum \dot{m}_{g,in,i} h_{g,in} - \sum \dot{m}_{g,out,i} h_{g,i} - \frac{dh_{g,i}}{dt} m_{g,i} \quad \text{(Eqn.3-44)}$$

Where: $h_{g,in}$ is the enthalpy of the incoming flows

The enthalpy change in time can be written as;

$$\frac{dh_{g,i}}{dt} m_{g,i} = m_{g,i} \sum \frac{dw_i}{dt} h_{a,i} \quad \text{(Eqn.3-45)}$$

Where: $h_{a,i}$ is the gas component enthalpy

3.3.3 Energy transfer in chemical reactions

Chemical reactions that can be taken into account include evaporation, carbonation, sulphation, and the combustion of char and volatiles.

$$\sum q_{chem} = \sum r_{c,i} Q_i \quad \text{(Eqn.3-46)}$$

Where: $r_{c,i}$ is the rate of reaction

Q_i is the general reaction enthalpy

3.3.4 Energy associated with dispersion

Applying Fick's law of diffusion to the modelling approach, the following equation is obtained (Ylatalo, 2013);

$$\sum q_{disp} = D_s c_{p,s} A_b \rho_{ave}^{-} \frac{dT_i^{-}}{dz} + D_s c_{p,s} A_t \rho_{ave}^{+} \frac{dT_i^{+}}{dz} \quad \text{(Eqn.3-47)}$$

Where: D_s is the dispersion coefficient (m^2/s)

$A_{b/t}$ is the cross section of the bottom/top element boundary (m^2)

$\rho_{ave}^{+/-}$ is the average density between calculation element and siding element (kg/m^3)

3.3.5 Heat transfer

Heat transfer to the surfaces is given by the expression;

$$\sum q_{ht} = \alpha_{tot} A_x (T_i - T_x) \quad \text{(Eq.3-48)}$$

Where: α_{tot} is the total heat transfer coefficient

$$\alpha_{tot} = 5.0 \rho_s^{0.391} T_i^{0.408} \quad \text{(Eq.3-49)}$$

3.3.6 Overall energy balance equation

Substituting equations 3-49, 3-48, 3-47, 3-46, 3-44 and 3-42 into equation 3-39;

$$\frac{dT_i}{dt} m_{s,i} c_{p,s} = \sum c_{p,s} \dot{m}_{s,in,i} \left(T_{s,in} - T_{NTP}\right) - \sum c_{p,s} \dot{m}_{s,in,i} \left(T_i - T_{NTP}\right) + \sum \dot{m}_{g,in,i} h_{g,in} - \sum \dot{m}_{g,out,i} h_{g,i} - m_{g,i} \sum \frac{dw_i}{dt} h_{j,i} + D_s c_{p,s} A_b \rho_{ave}^{-} \frac{dT_i^{-}}{dz} + D_s c_{p,s} A_t \rho_{ave}^{+} \frac{dT_i^{+}}{dz} + 5.0 \rho_s^{0.391} T_i^{0.408} A_x (T_i - T_x) + \sum r_{c,i} Q_i$$

(Eq.3-55)

3.4 Summary of modelling approach

Each reactor was divided into 1-Dimensional control volumes. Time -dependent mass and energy balances were solved numerically using appropriate ODE tools in MATLAB. Figure 3-7, below, shows the calculation procedure for the reactor model.

3.4.1 Design of simulated experiments

The output variables (mass fraction of exit gases, mass of exiting solids and energy adsorbed or released by the system) were extracted from the MATLAB solution of the time-dependent mass and energy balances. These values were then transferred to an excel spreadsheet for plotting and analyzing. Mass flowrate of sorbent, carbon dioxide partial pressure at the calcium oxide-calcium carbonate interface, temperature of incoming solid flows and concentration of carbon dioxide and Sulphur dioxide in the flue gas stream were

varied based on literature data, using values above and below those stipulated by different researchers. While one variable was being varied, all the other variables were being kept constant. The following assumptions were made;

- Instant and complete mixing of solids in both reactors
- Plug-flow of the gas phase in the carbonator
- Calcination goes to completion instantaneously in the calciner

The input conditions for the laboratory simulation are shown in table 3.1 below;

Table 3- 1:Laboratory simulation input variables

Variable	**Value**
Flue gas mass flow (kg/s)	0.403
Flue gas temperature (ºC)	25
CO_2 in flue gas (w-%)	14.4-43.2
O_2 in flue gas (w-%)	5.00
N_2 in flue gas (w-%)	51.76-80.56
SO_2 in flue gas (w-%)	0.04-0.08
Solid mass in reactor (kg)	1.83

Table 3-2, below, shows the input parameters for the different simulations done.

Table 3- 2:Input variables for the different simulations done

Simulation number	**Sorbent flowrate (kg/s)**	**Input sorbent temperature (ºC) (carbonator)**	**Input solid temperature (ºC) (Calciner)**	**Carbon dioxide concentration in flue gas (mol/m^3)**	**Carbon dioxide partial pressure (kPa)**	**Flue gas composition (w-%)**		
						SO_2	**CO_2**	**O_2**
1	100.000	610-690	900-990	1.320-3.961	2.026-9.119	0.04-0.08	10.0-30.0	5.0
2	1.743	610-690	900-990	1.320-3.961	2.026-9.119	0.04-0.08	10.0-30.0	5.0
3	1.743	500-590	900-990	1.320-3.961	2.026-9.119	0.04-0.08	10.0-30.0	5.0
4	0.116	610-690	900-990	1.320-3.961	2.026-9.119	0.04-0.08	10.0-30.0	5.0
5	0.011	610-690	900-990	1.320-3.961	2.026-9.119	0.04-0.08	10.0-30.0	5.0
6	1.743	610-690	900-990	1.320-3.961	2.026-9.119	0	10.0-30.0	5.0

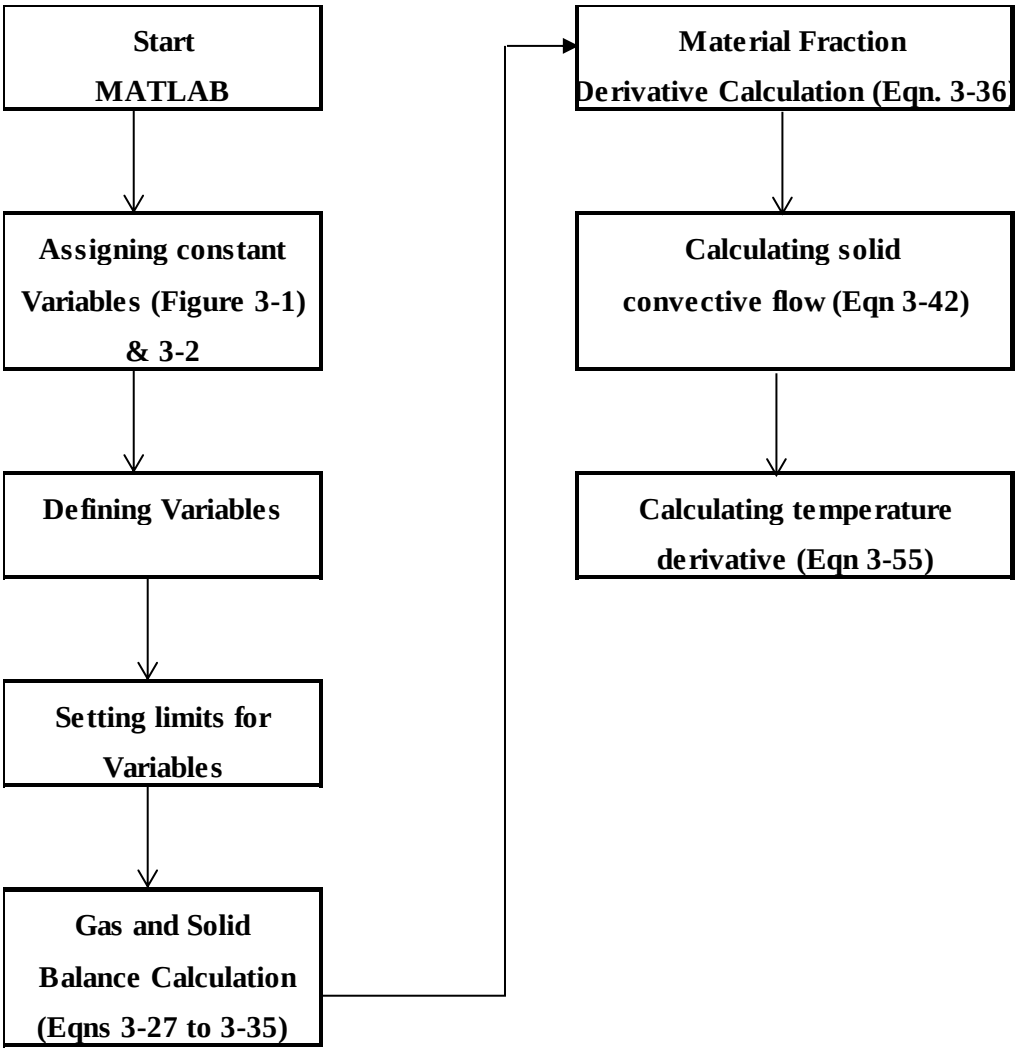

Figure 3- 7:Calculation procedure for reactor model

The following variables were defined using the MATLAB syms command; time, temperature, flow rates of gases and solids and partial pressure of carbon dioxide.

4 Chapter four

4. Introduction

Carrying out a sensitivity analysis on the two reactors, carbonator and calciner, mass flowrate of sorbent, carbon dioxide partial pressure, temperature and concentration of carbon dioxide and sulphur dioxide in the flue gas stream were varied basing on literature data, using values above and below those stipulated by different researchers. While one variable was being varied, all the other variables were being kept constant.

Flue gas carrying carbon dioxide enters the carbonator and carbon dioxide react with the active fraction of calcium oxide (f_a) while the remaining calcium oxide (1-f_a) is considered inactive. Carbonation occurs in two stages, a fast reaction regime followed by a slow reaction regime, which is controlled by carbon dioxide diffusion through the product layer of calcium carbonate formed on the free calcium oxide surfaces. Furthermore, the maximum conversion of calcium oxide, which marks the end of the fast carbonation period, decreases rapidly with an increase in number of carbonation-calcination cycles increases (Curran, et al., 1967). To model these key sorbent features, it is assumed that the calcium oxide particles attain the maximum conversion, X_N, at a constant rate, in a characteristic time, t^*, and after that the reaction becomes zero (Alonso, et al., 2009).

$$r_{CaO} = X_N \; if \; t < t^*$$

$$r_{CaO} = 0 \; if \; t > t^*$$

Where r_{CaO} is rate of conversion of calcium oxide.

Alonso et al (Alonso, et al., 2009) experimented on finding the characteristic time for fast carbonation stage and found the time to be at least 20 seconds and for some sorbents extending to about 40 seconds. In this research, more time was allowed for the fast carbonation stage to go to completion and 50 seconds was used.

The solid inventory of both calciner and carbonator was varied from laboratory scale (less than 1kg) to pilot plant simulation (above 100kg). This chapter will dwell much on the laboratory scale results (1.83kg solid loading in each of the reactors) as they show clearer the changes taking place in solid masses and gas compositions. 1.83kg gives the sorbent to carbon dioxide flowrate ratio of 20 for a flue gas stream containing 15 w-% carbon dioxide and having a flow rate of 0.403 kg/s.

4.1 Carbonator

For the carbonator, effect of temperature, carbon dioxide concentration in inlet flue gas and ratio of sorbent to carbon dioxide flow was investigated. The carbonator temperature increases as reaction proceeds. Figure 4-16 shows the heat released as carbonation occurs.

4.1.1 Effect of temperature

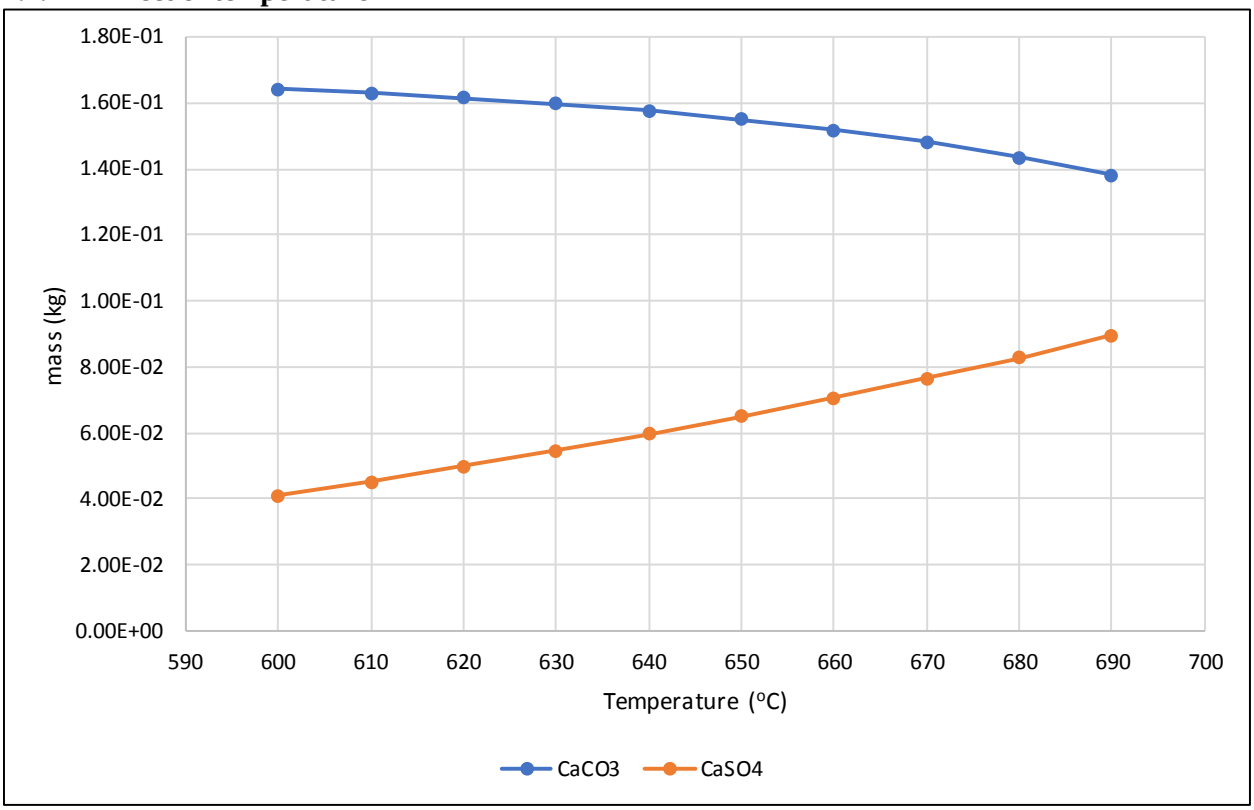

Figure 4- 1:Mass of solid formed versus temperature at constant flue gas composition for first carbonation-calcination cycle

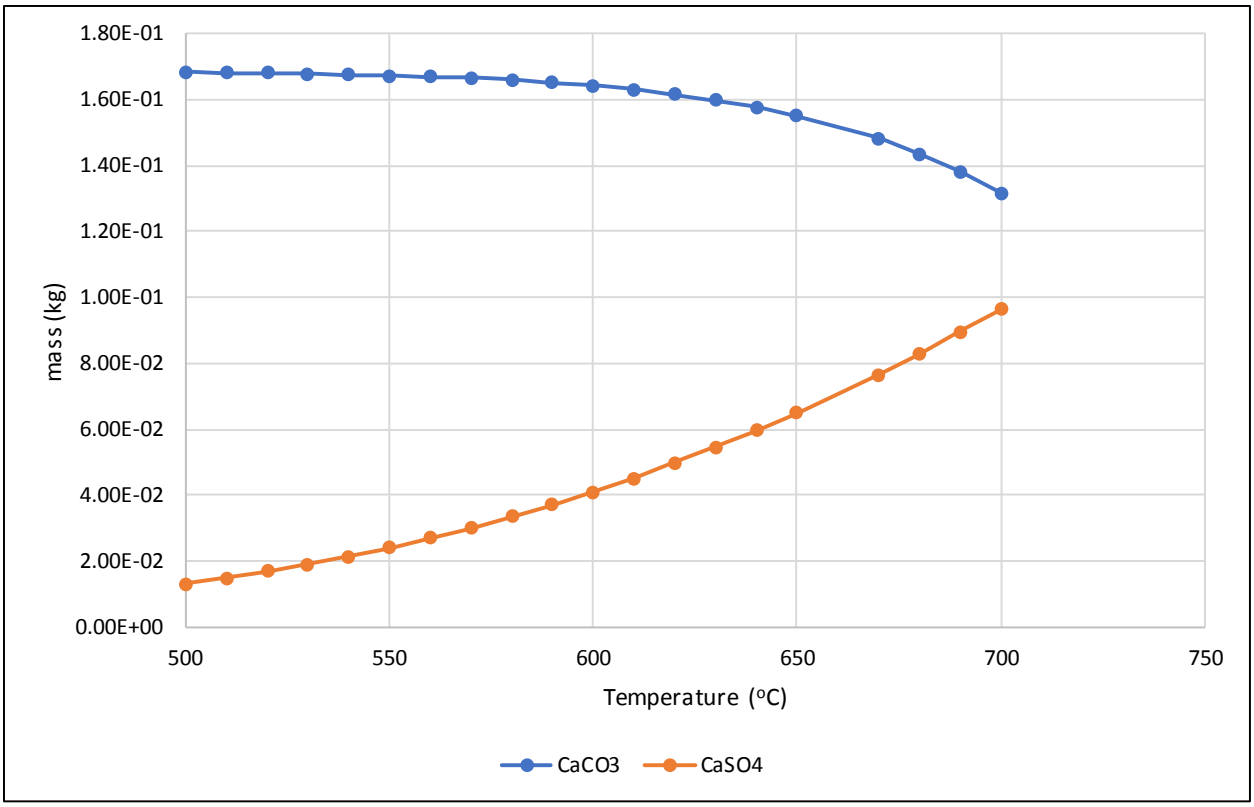

Figure 4- 2:Mass of solid formed versus temperature at constant flue gas composition for first carbonation-calcination cycle

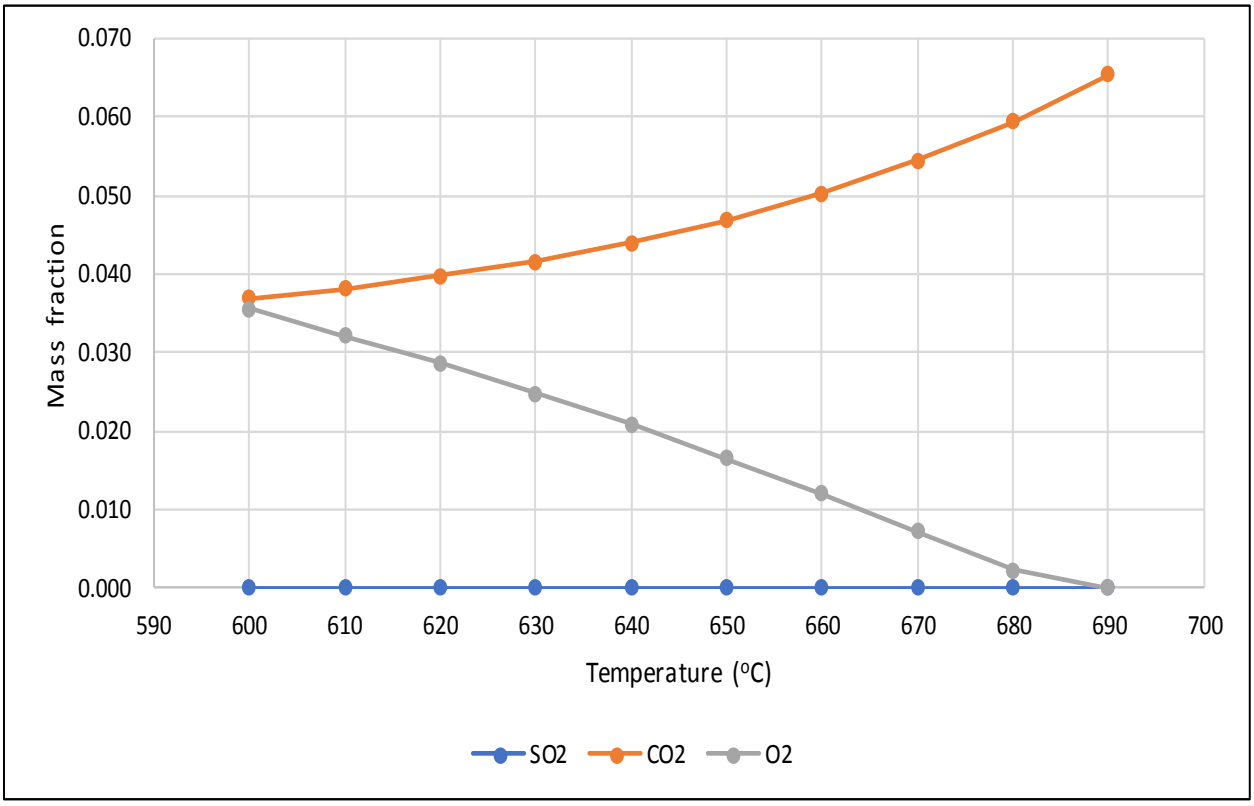

Figure 4- 3: Exit gases mass fraction versus temperature at constant flue gas composition for first carbonation-calcination cycle

As the temperature increases, the mass of carbonate formed or rate of carbonation decreases as shown in figure 4-1. In the exit stream, mass fractions of carbon dioxide increase and mass fraction of sulphur dioxide (defined as the mass of gas element in the exit stream divided by the total amount of gas in the exit stream) decrease as temperature increase (figure 4-3). According to Le Chatelier, if a constraint (such as a change in pressure, temperature or concentration of a reactant) is applied on a system in equilibrium, the equilibrium will move so as to tend to counter the effect of the constraint (Ihde, 1989). Carbonation is an exothermic reaction therefore increasing the temperature will favor the reverse reaction thus lowering the rate of carbonation. According to Lu et al (Lu, et al., 2008) , there is an increase in carbonation as temperature decreases but temperatures below 500^{o}C are too low to drive the carbonation reaction.

The rate of sulphation increases as temperature increases. Unfortunately, increase in temperature accelerates sulphation because of the higher activation energy needed for the sulphation reaction (Manovic & Anthony, 2010). With low amounts of Sulphur dioxide in the flue gas, sulphation goes to completion and no sulphur dioxide will be found in the exit stream.

Figure 4-2 shows the mass of solid formed at different temperatures from 500 ^{o}C. It can be seen that for temperatures below 600 ^{o}C, the decrease in amount of carbonate formed (carbonation) is less than it is after 600 ^{o}C. The optimal temperature for carbonation would be 600^{o}C for it is high enough to drive the carbonation reaction and not too high to accelerate the sulphation reaction

4.1.2 Bed mass versus number of carbonation-calcination cycles

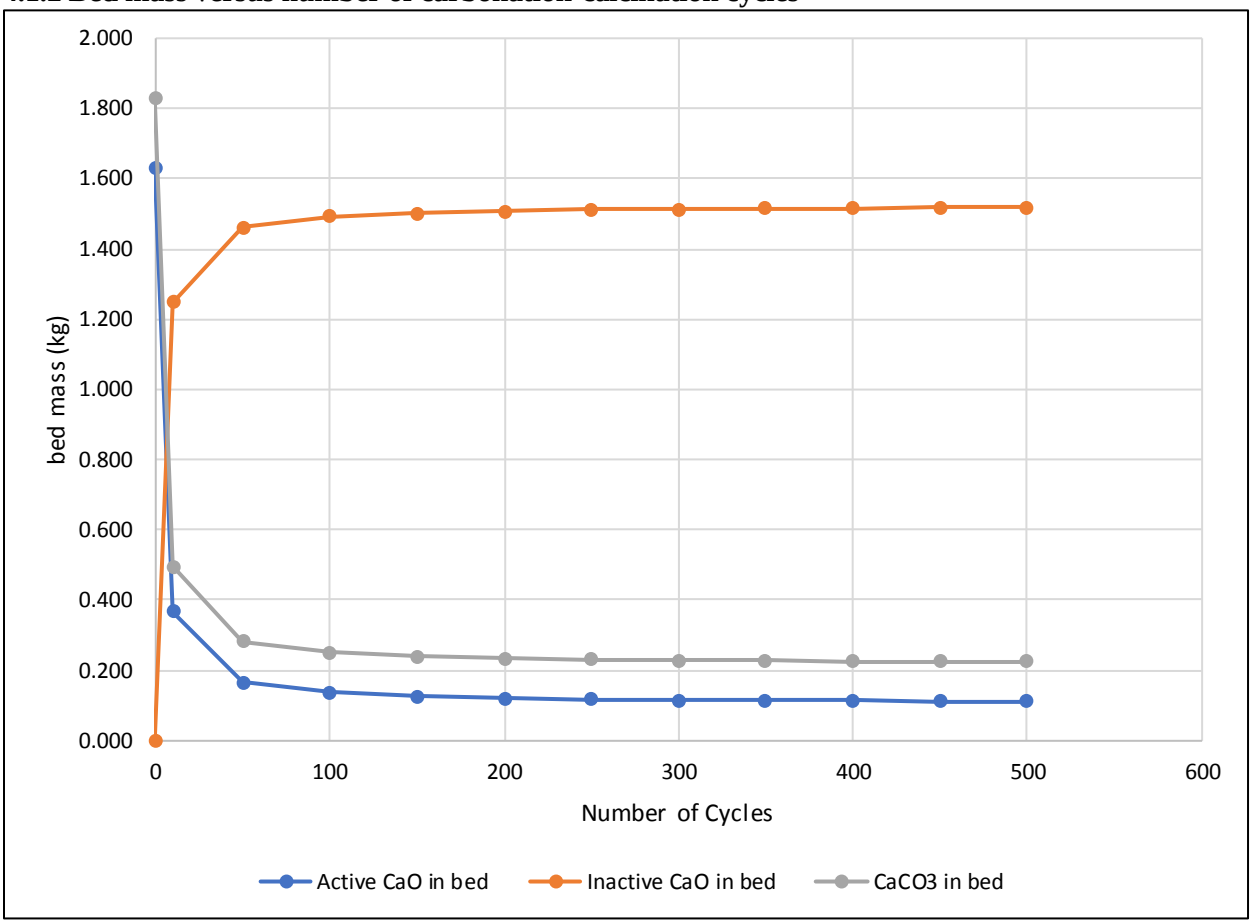

Figure 4- 4:Bed mass versus number of carbonation-calcination cycles at constant temperature (610 ^{o}C) and flue gas composition

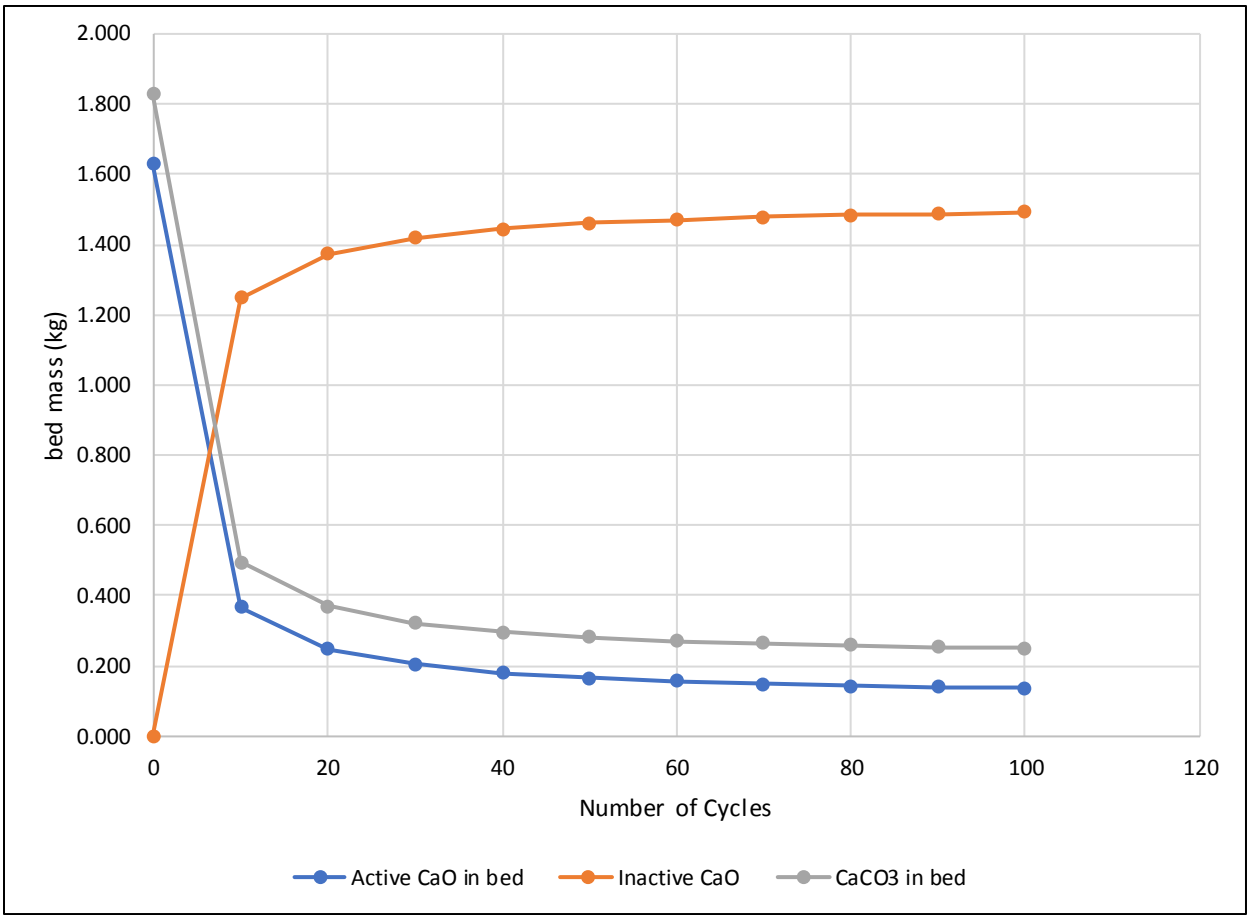

Figure 4- 5:Bed mass versus number of carbonation-calcination cycles at constant temperature (610 ^{o}C) and flue gas composition

From figure 4-4, the amount of active calcium oxide decrease as number of carbonation-calcination cycles increase. Figure 4-5 shows the changes in bed mass composition versus carbonation-calcination cycles, up to 100 cycles. There is a sharp decrease in active calcium oxide in the first 10 cycles and after about 100 cycles, the active calcium particles remain constant. This is caused by the decay in activity of calcium oxide as the number of carbonation-calcination cycles increases (Abanades & Alvarez, 2003).

The amount of calcium oxide not reacted (inactive) increases as number of carbonation-calcination cycles increases because of the decay in activity of calcium oxide with an increase in number of carbonation-calcination cycles. Calcium carbonate recycled into the system also decreases with increasing number of carbonation-calcination cycles.

The optimum number of carbonation-calcination cycles from figure 4-4 and figure 4-5 is less than 20 after which the most part (more than 75 %) of the sorbent will be inactive.

4.1.3 Effect of changing carbon dioxide concentration in the flue gas

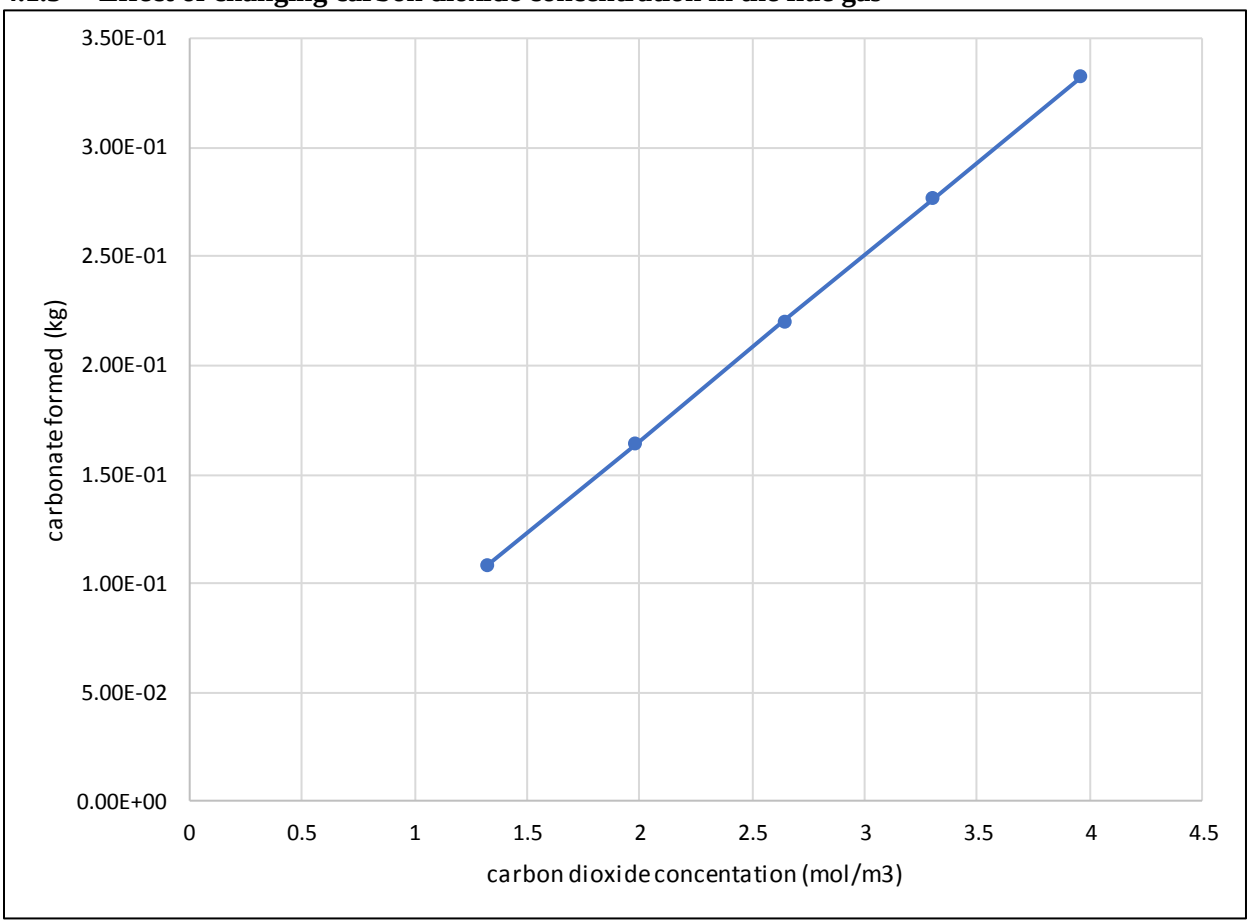

Figure 4- 6:Mass of carbonate formed versus Carbon dioxide concentration in flue gas at constant temperature (600 ° C)

Rate of carbonation, which is directly proportional to rate of formation of calcium carbonate, increases as carbon dioxide concentration in the feed stream increase. The increase in rate of carbonation is due to an increase in reactant available for reaction. There is a linear correlation between carbonation and amount of carbon dioxide in flue gas because the rate of carbonation is directly proportional to carbon dioxide concentration in the flue gas as proposed by Ylatalo (Ylatalo, et al., 2012) in the equation below;

$$r_{carb} = m_s S_{ave}(W_{max} - W)k_{carb}(C_{CO_2} - C_{CO_{2e}})$$

4.1.4 Change in sorbent to carbon dioxide flow ratio

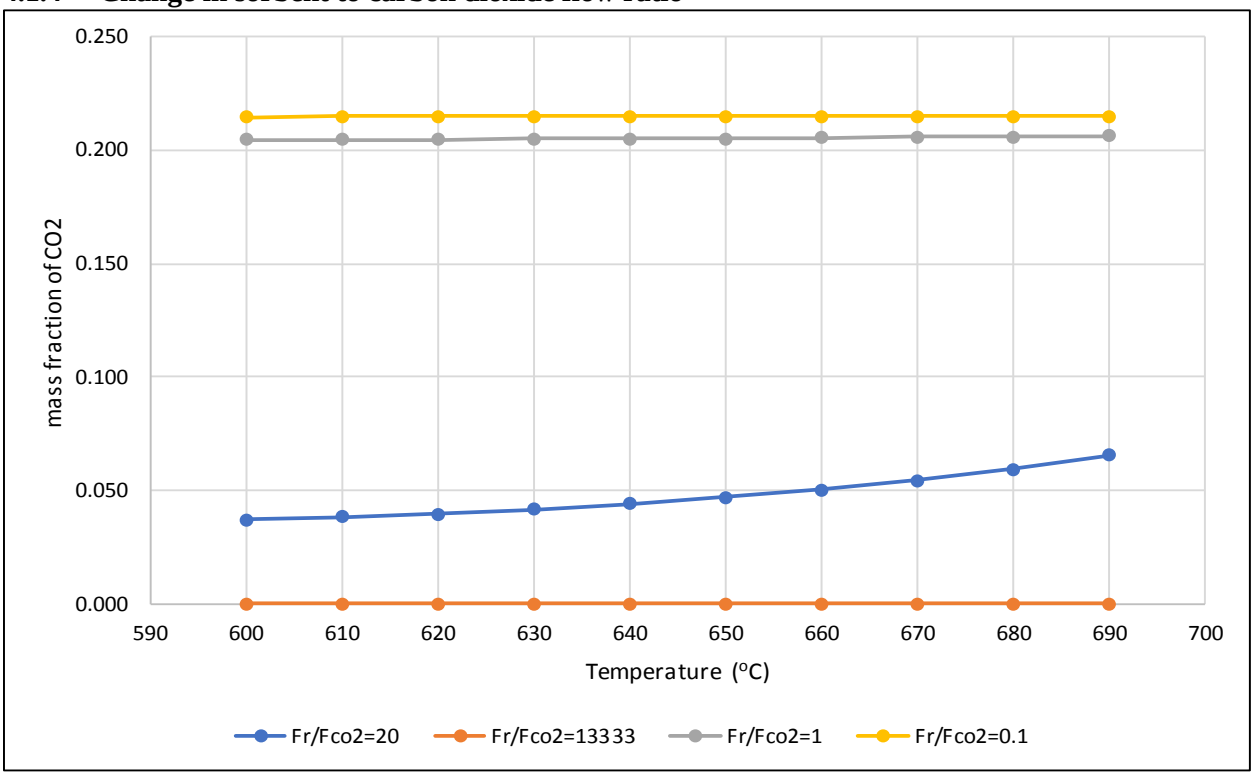

Figure 4- 7:Variation in Carbon dioxide mass fraction in the exit gas as a function of temperature and sorbent to carbon dioxide flow ratio (Fr/Fco2)

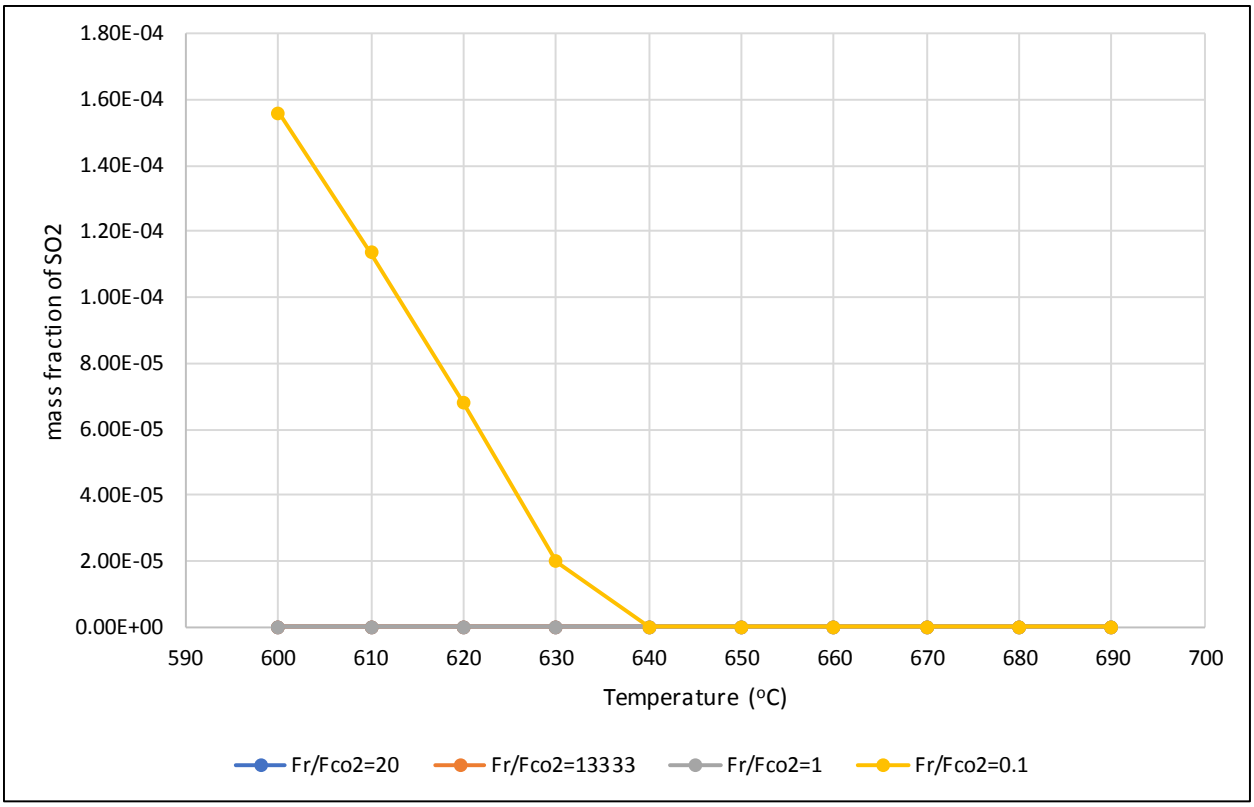

Figure 4- 8:Variation in Sulphur dioxide mass fraction in the exit gas as a function of temperature and sorbent to carbon dioxide flow ratio

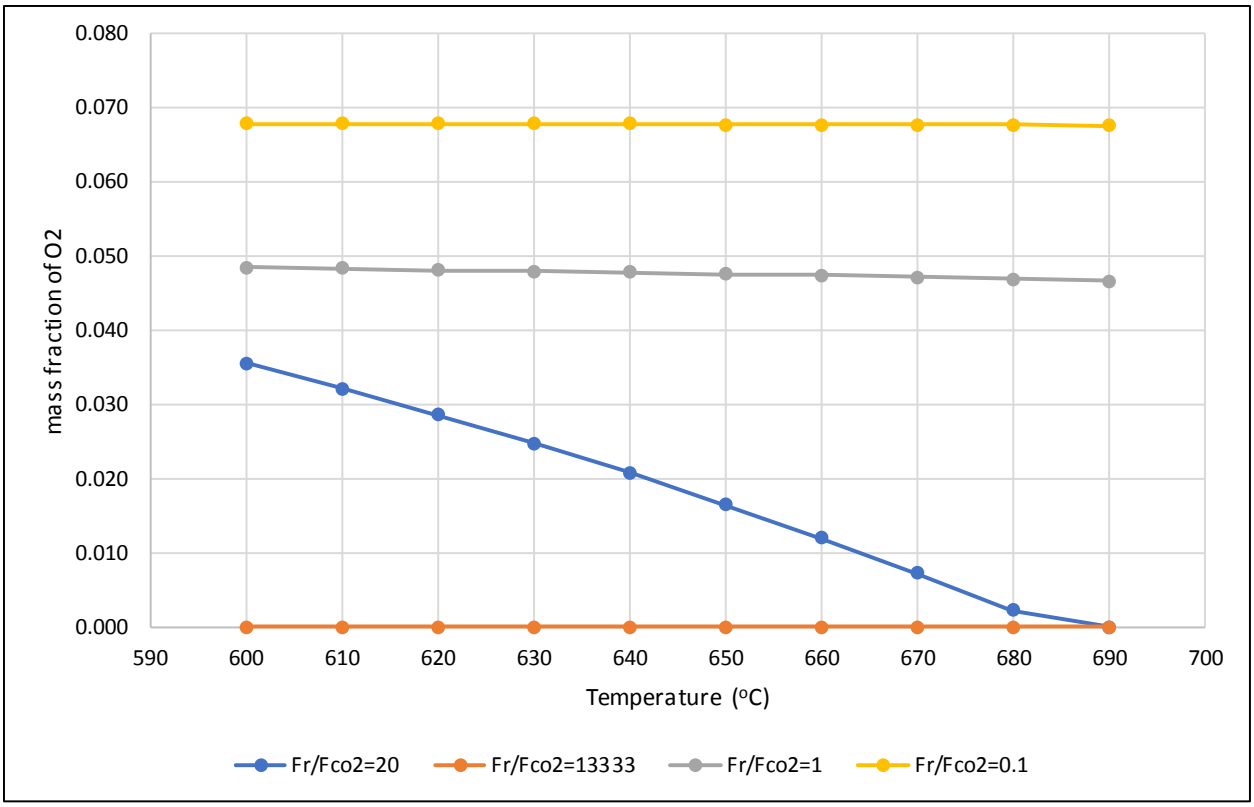

Figure 4- 9:Variation in oxygen mass fraction in the exit gas as a function of temperature and sorbent to carbon dioxide flow ratio

Increase in sorbent to carbon dioxide flow rate ratios leads to higher reaction rate in the carbonator. The sulphation reaction also increases as shown by the decrease in mass fraction of Sulphur dioxide leaving the reactor as sorbent to carbon dioxide flow ratios increase. As the amount of sorbent increases, there will more sorbent available for reaction with the carbon dioxide as well as the Sulphur dioxide hence an increase in rate of reaction. Figure 4-8 shows that Sulphur dioxide is depleted instantly as sorbent to carbon dioxide flow rate ratios increase. This is because Sulphur dioxide will be present in very small quantities in the feed gas and hence will be totally absorbed by the sorbent. As sorbent to carbon dioxide flow rate ratio decrease to below 1, sulphur dioxide depletion becomes slow and only goes up at elevated temperature (above 640^{o}C) because of the higher activation energy needed for the sulphation reaction.

A higher sorbent to carbon dioxide flow rate ratio (Figure 4-7) allows for higher absorption of carbon dioxide and sorbent to carbon dioxide ratios above 20 are optimal. It can clearly be seen that at this ratio, the mass fraction of the gas in the exit goes down rapidly. Lower sorbent to carbon dioxide flow rates (<20) result in high carbon dioxide mass fractions in the exit gas stream. The challenge of higher sorbent to carbon dioxide flow rate ratios is that they also allow for higher adsorption of sulphur dioxide.

4.2 Calciner

4.2.1 Effect of temperature

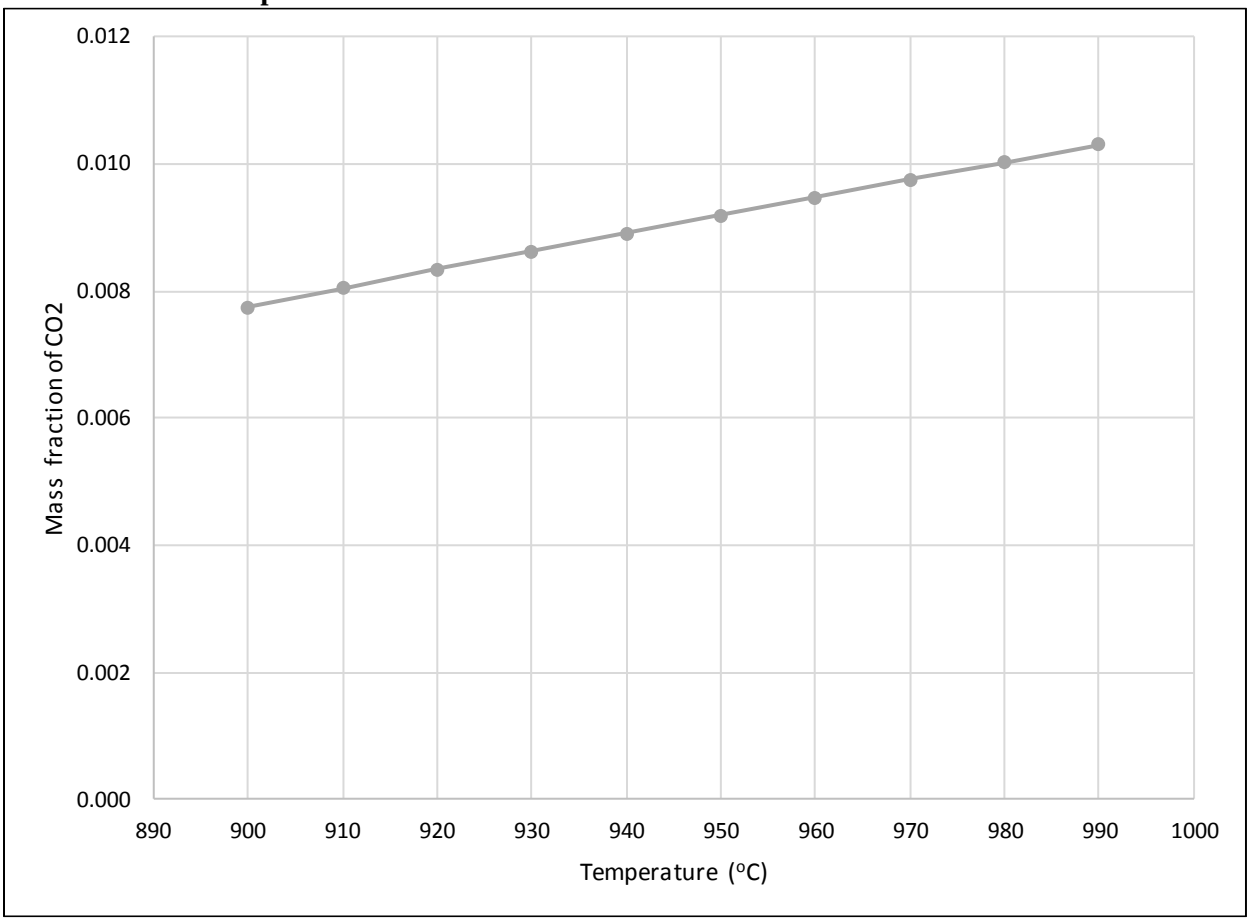

Figure 4- 10:Carbon dioxide mass fraction versus temperature at constant carbon dioxide partial pressure (9119.25 Pa)

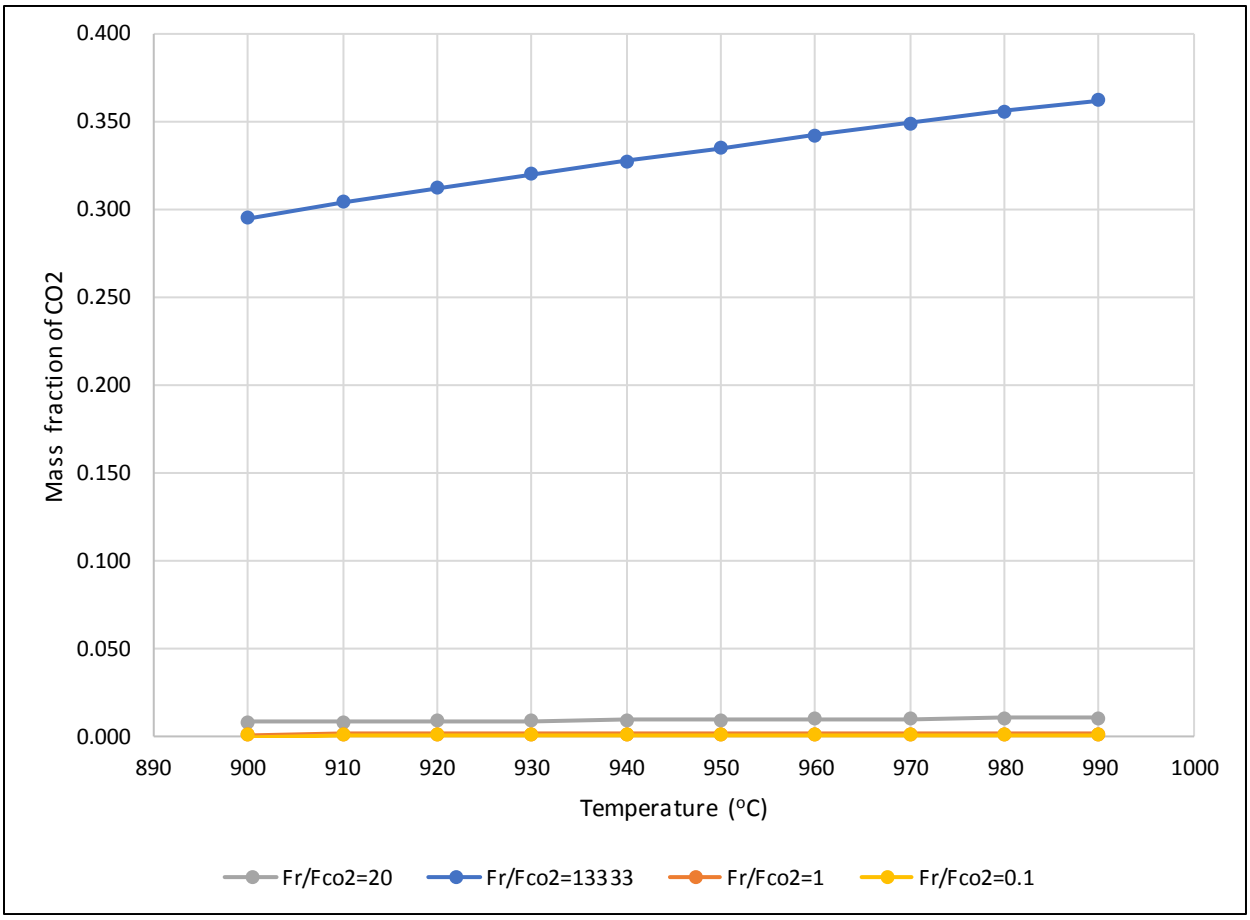

Figure 4- 11:Variation in carbon dioxide mass fraction in the exit gas as a function of temperature and sorbent to carbon dioxide flow ratio

As temperature increases, carbon dioxide mass fraction also increases. This shows that calcination rate will be also increasing thus more carbon dioxide being formed. Calcination is an endothermic reaction therefore increasing the temperature will favor the forward reaction which if formation of products (carbon dioxide and calcium oxide).

It can be seen from Figure 4-11 that as amount of sorbent increases, the calciner exit stream will be containing more carbon dioxide. This is because more carbon dioxide would have been absorbed by the sorbent.

It is therefore recommended to use high sorbent to carbon dioxide flow rates (above 10000) so that a more concentrated stream of carbon dioxide will be produced and collected for storage.

4.2.2 Effect of change in carbon dioxide partial pressure

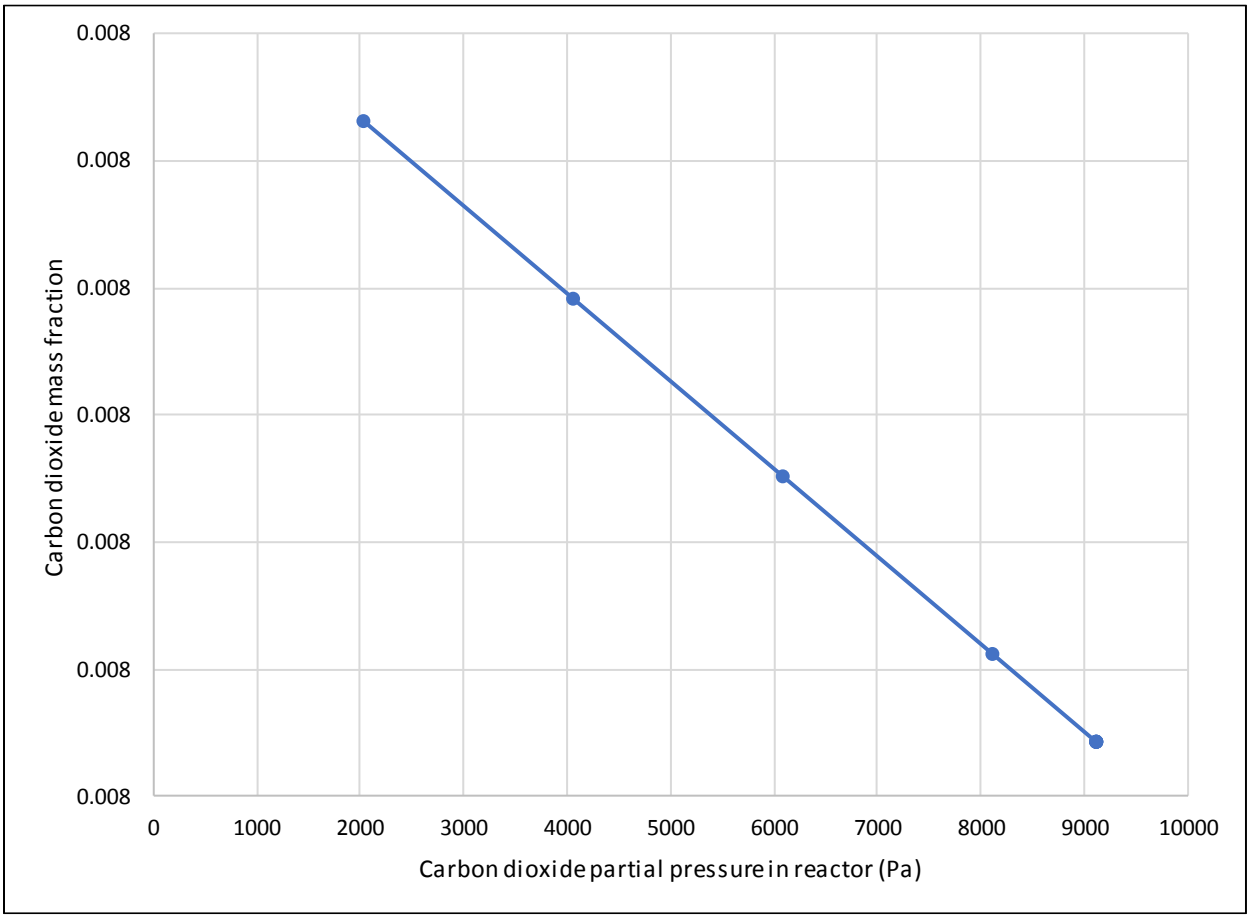

Figure 4- 12:Carbon dioxide mass fraction versus partial pressure at constant temperature (900 ° C)

As carbon dioxide partial pressure (at the calcium oxide-calcium carbonate interface) increases in the calciner, the rate of calcination, which is directly proportional to increase in carbon dioxide mass fraction in the exit gas stream, decreases (Figure 4-12). More calcium carbonate is recycled to carbonator without conversion to calcium oxide. Maybe sorption effects at the calcium oxide/calcium carbonate/carbon dioxide interface are the reason for the decay (Khinast, et al., 1996).

4.3 No sulphation

Simulation was also done for the case in which the effect of sulphation was ignored.

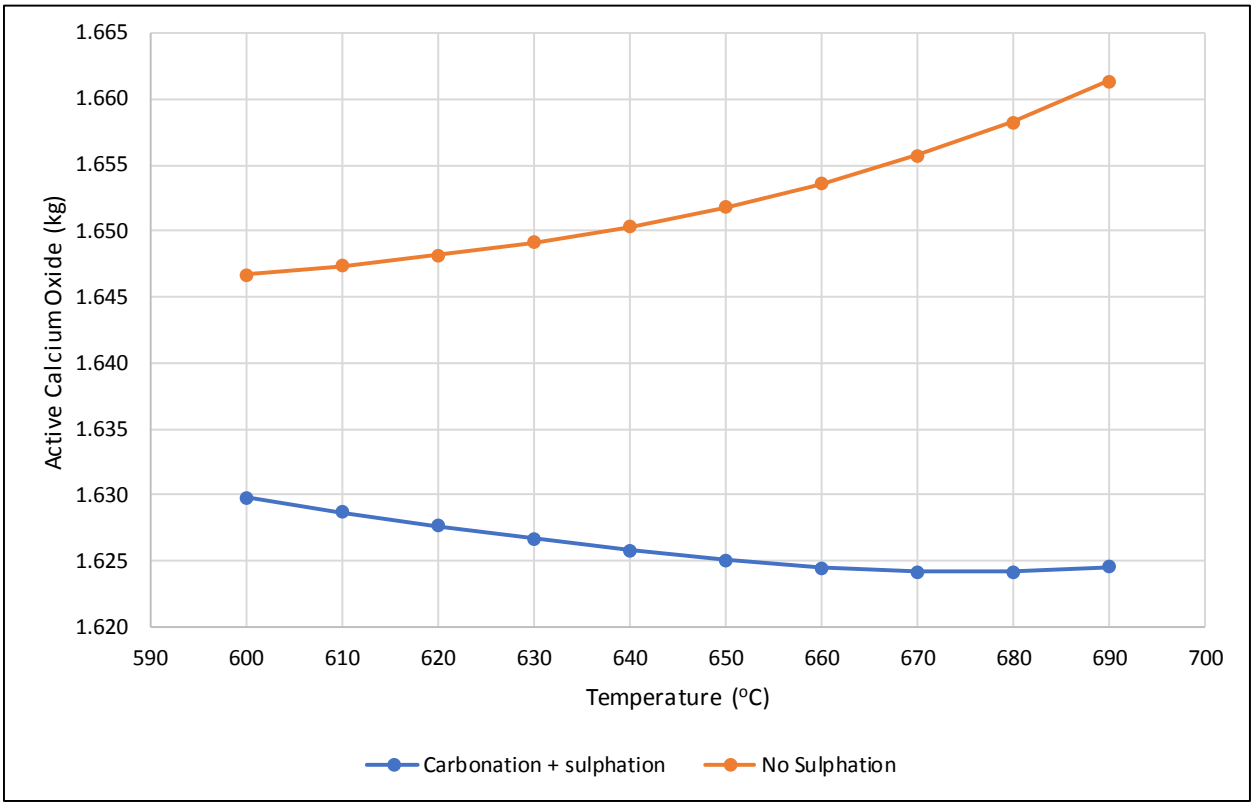

Figure 4- 13: Active calcium oxide in carbonator versus Temperature at constant flue gas composition and sorbent flow rate

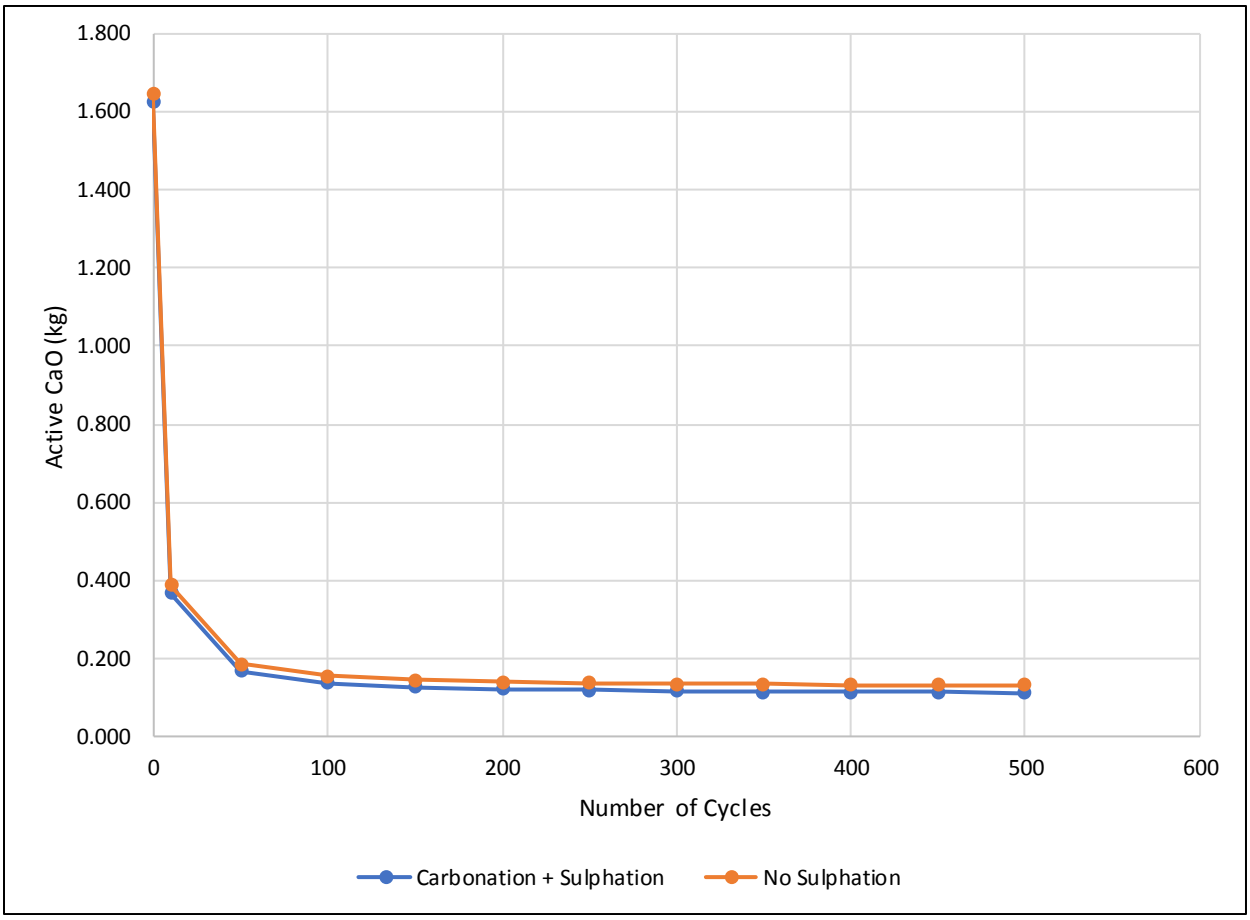

Figure 4- 14: Active Calcium Oxide vs Number of carbonation-calcination cycles at constant temperature (610 ° C) and flue gas composition

When carbonation takes place in the absence of Sulphur dioxide, more calcium oxide will be in the bed and available for reaction with carbon dioxide as shown by Figures 4-13 and 4-14. When Sulphur dioxide is taken into account, more active calcium oxide is consumed by both reactions (carbonation and sulphation) but when sulphation is ignored, one reaction, carbonation, consumes the active calcium oxide thus a bigger amount of calcium oxide will be in the bed.

Neglecting sulphation when designing calcium looping reactors will therefore lead to over estimation of active calcium oxide in the carbonator and therefore lower amount of carbon dioxide absorbed than expected.

In figure 4-14, there is a sharp decrease in active calcium oxide in the first 10 cycles and after about 100 cycles, the active calcium particles remain constant. This is caused by the decay in activity of calcium oxide as the number of carbonation-calcination cycles increases (Abanades & Alvarez, 2003). Figure 4-5 also

shows the same effect. There is no appreciable difference in the curves because Sulphur dioxide concentration in the flue gas is very low compared to that of carbon dioxide making the amount of active calcium oxide used in the sulphation reaction small.

4.4 Energy balance

It has been assumed that the conductivity of the solids is high enough or the particles are small enough so that the temperature of any one particle may be assumed uniform always. Assuming also a constant heat transfer coefficient between fluid and solid, the equation for forced convection continuous exchangers may be applied leading to:

$$Q = hA\frac{(T_{hi}-T_{cout})-(T_{hout}-T_{cin})}{ln\left(\frac{T_{hi}-T_{cout}}{T_{hout}-T_{ci}}\right)} = hA\Delta T_{mean}$$

Where: h is heat transfer coefficient

T_{hi} is hot fluid temperature at the inlet

T_{hout} is hot fluid temperature at the oulet

T_{ci} is cold fluid temperature at the inlet

T_{cout} is cold fluid temperature at the outlet

$$\sum q_{ht} = \alpha_{tot}A_x(T_i - T_x)$$

Where: α_{tot} is the total heat transfer coefficient

$$\alpha_{tot} = 5.0\rho_s^{0.391}T_i^{0.408}$$

Heat transfer is also given by:

$$Q = mc_p\Delta T$$

An assumption was made that both reactors are perfectly insulated therefore no heat transfer to the surroundings. The energy balance equation therefore reduces to:

$$\frac{dT_i}{dt}m_{s,i}c_{p,s} = \sum c_{p,s}\dot{m}_{s,in,i}\left(T_{s,in} - T_{NTP}\right) - \sum c_{p,s}\dot{m}_{s,in,i}\left(T_i - T_{NTP}\right) + \sum \dot{m}_{g,in,i}\,h_{g,in} - \sum \dot{m}_{g,out,i}\,h_{g,i} - m_{g,i}\sum\frac{dw_i}{dt}h_{j,i} + D_s c_{p,s}A_b\rho_{ave}^{-}\frac{dT_i^{-}}{dz} + D_s c_{p,s}A_t\rho_{ave}^{+}\frac{dT_i^{+}}{dz} + \sum r_{c,i}\,Q_i$$

The reference temperature was taken as 298 Degrees Kelvin

Graphs below summarize the energy balances;

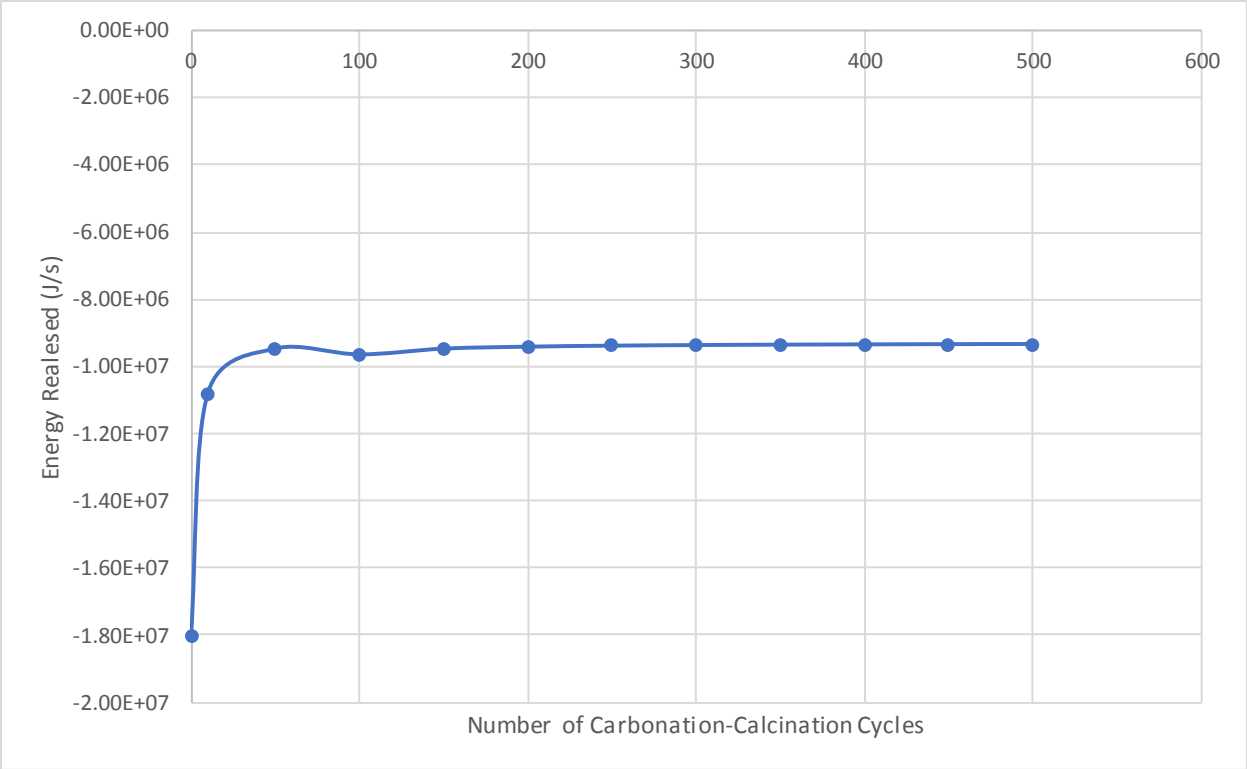

Figure 4- 15: Energy released in carbonator vs number of carbonation-calcination cycles

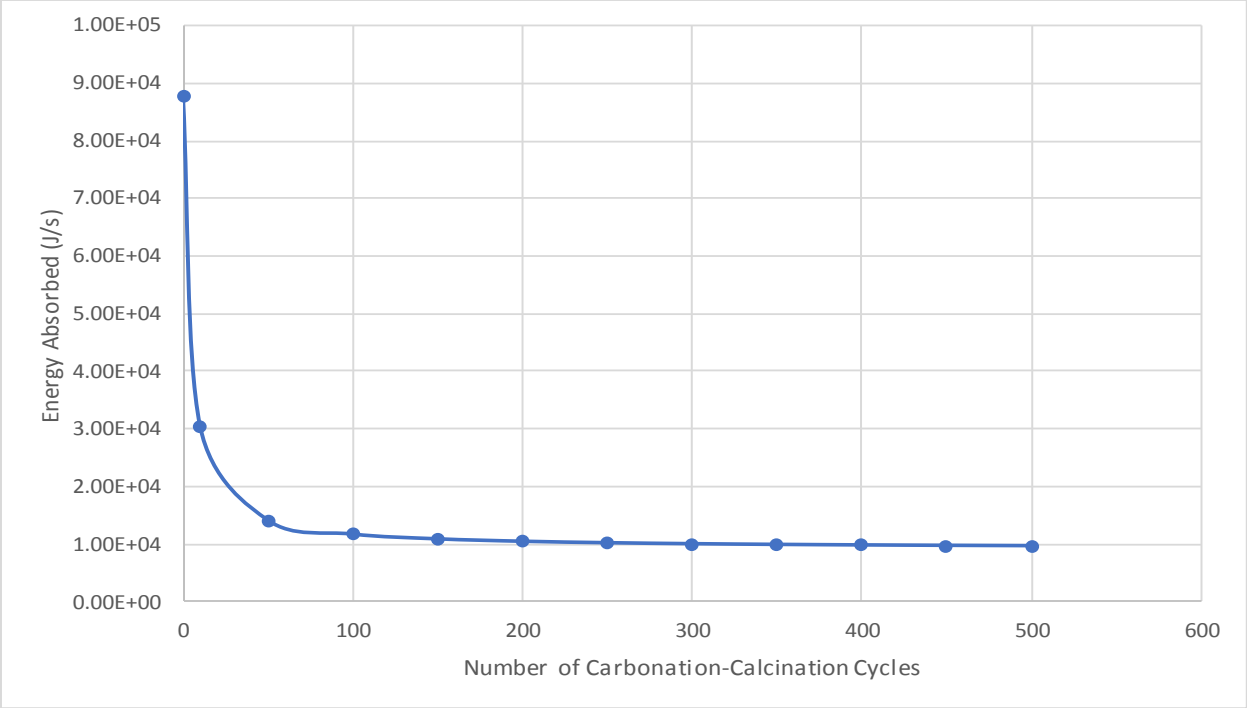

Figure 4- 16:Energy absorbed in the calciner vs number of carbonation-calcination cycles

Figure 4-15 shows the relationship between amount of energy released during carbonation and number of carbonation-calcination cycles. As number of carbonation-calcination cycles increases, the amount of energy released decreases. This is because as the carbonation-calcination cycles increase the rate of carbonation decreases.

As the number of carbonation-calcination cycles increases, the amount of energy absorbed in the calciner decreases (Figure 4-16). The same reason as in carbonator applies; the rate of calcination also decreases with increase in number of carbonation calcination cycles. The decreases in reaction rates is caused by deactivation of the sorbent (calcium oxide) as number of carbonation-calcination cycles increase.

The best way to remove heat from solids from the calciner and to cool solids from carbonation is by an external heat exchanger. Other studies point out that, if a refractory material protects the absorber bed, the heat transfer rate in the bed is insufficient to cool the solids to 650 ^{o}C. In-bed heat transfer tubes can cool the solids quickly however, they can also wear out the tubes. If solids are cooled before being loaded into the carbonator, the heat transfer load to the lower part of the carbonator is eased (Ylatto, et al., 2014) .

4.5 Heat exchanger design

For calcium looping system, a heat exchanger is required to cool solids from regenerator and carbonation reaction.

The major objective in the design of a heat exchanger is to determine the surface area required for the specified duty using the temperature differences available (Perry & Green, 2008). For heat exchange across a typical heat-exchanger tube the relationship between the overall coefficient and the individual coefficients, which are the reciprocals of the individual resistances, is given by:

$$\frac{1}{U_o} = \frac{1}{h_o} + \frac{1}{h_{od}} + \frac{d_o \ln\left(\frac{d_o}{d_i}\right)}{2k_w} + \frac{d_o}{d_i} \times \frac{1}{h_{id}} + \frac{d_o}{d_i} \times \frac{1}{h_i}$$

Where U_o is the overall coefficient based on the outside area of the tube, W/m^2 ^{o}C

h_o is the outside fluid film coefficient, W/m^2 ^{o}C

$h_i$is the inside fluid film coefficient, W/m^2 ^{o}C

h_{od} is the outside dirt coefficient (fouling factor), W/m0^2 ^{o}C

h_{id} is the inside dirt coefficient, W/m^2 ^{o}C

k_w is the thermal conductivity of the tube wall material, W/m ^{o}C

d_i is the tube inside diameter, m,

d_o is the tube outside diameter, m.

Heat exchangers that are mainly used in the chemical processing and allied industries, are:

1. Double-pipe exchanger
2. Plate-fin exchanger
3. Air cooled heat exchangers for example coolers and condensers
4. Fired heaters
5. Direct contact heat exchangers
6. Agitated vessels
7. Spiral heat exchanger
8. Heat exchangers for divided solids: fluidized bed, tubed-shell type

The shell and tube heat exchanger is the mostly used heat-transfer equipment in chemical processing and allied industries. Its advantages are:

1. Good mechanical design
2. Large surface area per unit volume.
3. Wide range of materials for construction of the exchanger
4. It uses well-established fabrication techniques.
5. Well-established design procedures
6. Easy to clean

- Shell and tube heat exchanger

The fixed tube design is the simplest and cheapest type of shell and tube exchanger .Its major disadvantages are that the tubes cannot be removed for cleaning and it is not possible to expand the shell and tubes. Because the shell operate at different temperatures, the shell and tube heat exchanger is restricted to temperature differences below 80 ^{o}C.

- The tubed-shell heat exchanger

The tubed-shell also known as rotating drum dryer is a rotating drum type of heat exchanger for cooling or heating divided solids. The solids will be in the shell in which they will be moved through it continuously

because the drum will be rotating slightly inclined to the horizontal. It features good mixing with the aim of increased heat transfer performance. The tubed-shell is rarely applicable for stick, soft caking, scaling or heat sensitive burdens. They are also not ideal for abrasive materials. Tubed-shell heat exchangers are mainly used for drying but when water or refrigerants are flowing in the tubes, it can also be effective for cooling operations.

The steps given below are used when designing a heat exchanger;

1. Defining the duty

2. Collecting the physical properties of the fluid

3. Deciding on the type of heat exchanger to use

4. Selecting a trial value for the overall coefficient.

5. Calculating the mean temperature difference

6. Calculating the required area

7. Deciding on the heat exchanger layout

8. Calculation of individual coefficients

9. Calculating the overall coefficient and comparing with the trial value. If there is a significant difference between the calculated value and the estimated value, substitute the calculated figure for the estimate and return to step 6

10. Pressure drop calculation; if inacceptable return to steps 7 or 4 or 3.

11. Optimize the design by repeating steps 4 to 10, where necessary, determining the cheapest heat exchanger that will satisfy the duty. The cheapest exchanger is usually the one with the smallest area.

In this research, the heat exchanger design is based on the pilot plant simulation (105 kg).

4.5.1 Shell and tube heat exchanger to cool carbonator exit gases

The carbonator flue gases need to be cooled to room temperature. Assuming the gas has been depleted of carbon dioxide and oxygen and the exit gas contains nitrogen

1. Duty

Nitrogen is being cooled from 923 K to 453 K.

The average temperature is (923+453)/2 =688 K

Heat capacity of nitrogen at this temperature is 30.709J/kg.K. Average heat to be absorbed is given by;

$$Q = \dot{m}C_p\Delta\theta = 0.798 * 0.403 * 30.709 * (923 - 453) = \mathbf{4\,641.6W}$$

Where $\dot{m}$= mass flow rate, kg/s

Using water flowing at same mass flow rate as the outlet gas (0.798*0.403kg/s), heat capacity of water at 298 degrees Kelvin is 4180J/Kg. K

The outlet temperature of water is;

$$Q = \dot{m}C_p\Delta\theta = 0.798 \times 0.403 \times 4180 \times (t_2 - 298) = 4\,641.6W$$

$$t_2 = 301.5\ K = 28.5\ degrees\ Celcious$$

The average temperature of water is (298+301.5)/2= 299.75 K= 26.75 ^oC

The heat capacity of water at 26.75 ^oC is 4179J/kg.K

2. The mean temperature

$$\Delta T_{lm} = \frac{(T_1 - t_2) - (T_2 - t_1)}{\ln\left(\frac{T_1 - t_2}{T_2 - t_1'}\right)} = [(650 - 26.75) - (180 - 25)]/\ln\left(\frac{(650 - 26.75)}{(180 - 25)}\right) = 336.5$$

$$R = \frac{(T_{hin} - T_{hout})}{(t_{cout} - t_{+cin})} = \frac{650 - 180}{28.5 - 25} = 134.3$$

$$P = \frac{(t_{cout} - t_{cin})}{(T_{hin} - t_{cin})} = \frac{28.5 - 25}{650 - 25} = 0.0056$$

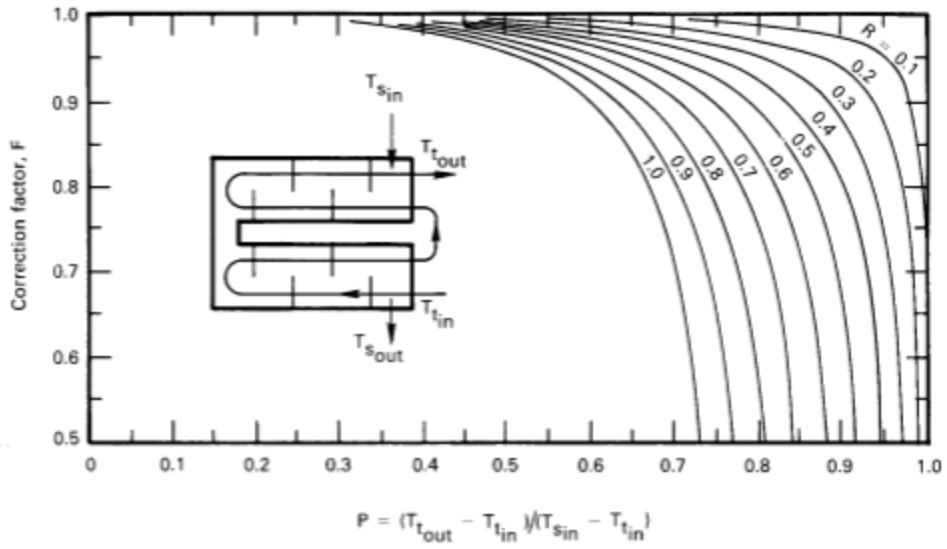

Figure 4- 17:F for a two-shell-pass, four or more tube-pass exchanger (Lienhard & Leinhard, 2006)

Since R>1, P becomes (134.3*0.0056) =0.75 and R=1/134.3=0.007, therefore from Figure 4-17, $F_t = 1$

$\Delta T_m = F_t \Delta T_{lm} = 1 \times 336.5 = 336.5^oC$

From the table 4-1, below assuming the overall coefficient to be 20W/m^2 ^{o}C

Table 4- 1:Typical Overall Coefficients (Coulson & Richardson, 1999)

Shell and tube exchangers		
Hot fluid	Cold fluid	U (W/m^2°C)
Heat exchangers		
Water	Water	800–1500
Organic solvents	Organic solvents	100–300
Light oils	Light oils	100–400
Heavy oils	Heavy oils	50–300
Gases	Gases	10–50
Coolers		
Organic solvents	Water	250–750
Light oils	Water	350–900
Heavy oils	Water	60–300
Gases	Water	20–300
Organic solvents	Brine	150–500
Water	Brine	600–1200
Gases	Brine	15–250
Heaters		
Steam	Water	1500–4000
Steam	Organic solvents	500–1000
Steam	Light oils	300–900
Steam	Heavy oils	60–450
Steam	Gases	30–300
Dowtherm	Heavy oils	50–300
Dowtherm	Gases	20–200
Flue gases	Steam	30–100
Flue	Hydrocarbon vapours	30–100

Therefore,

3. Area of heat transfer

$Q = UA\Delta T_m$=4641.6W

$A = \frac{Q}{U\Delta T_m} = \frac{4641.6}{20\times336.5} = 0.69\text{m}^2$

4. Layout and tube size

Using a 19.05 mm (3/4 inch) outside diameter, 14.83 mm inside diameter, 5 m Long tubes (A popular size) on a triangular 23.81 mm pitch (pitch/diameter=1.25)

5. Number of tubes

Area of one tube=$\pi \times 19.05 \times 10^{-3} \times 5 = 0.299m^2$

Number of tubes = heat transfer area/area of one tube=$\frac{0.69}{0.2992} = 2.3 \cong 2$

For 2 passes, tubes per pass= 1

Tube cross sectional area=$\frac{\pi}{4}(14.83 \times 10^{-3})^2 = 0.0001127m^2$

Area per pass=$1 \times 0.0001127 = 0.0001127m^2$

Volumetric flow=$\frac{0.798\times0.403}{1000} \times \frac{1}{1000} = 3.21 \times 10^{-7}m^3/s$

Tube side velocity=volumetric flow/ area per pass= $\frac{3.21\times10^{-7}}{0.0001127} = 0.0029m/s$

6. Bundle and shell diameter

$$D_b = d_o\left(\frac{N_t}{K_1}\right)^{1/n_1}$$

Where N_t is the number of tubes,

$D_b$is the bundle diameter, mm,

$d_o$is tube outside diameter, mm

Table 4- 2:Constants for tube pitch (Coulson & Richardson, 1999)

Triangular pitch, $p_t = 1.25d_o$					
No. passes	1	2	4	6	8
K_1	0.319	0.249	0.175	0.0743	0.0365
n_1	2.142	2.207	2.285	2.499	2.675
Square pitch, $p_t = 1.25d_o$					
No. passes	1	2	4	6	8
K_1	0.215	0.156	0.158	0.0402	0.0331
n_1	2.207	2.291	2.263	2.617	2.643

Using Table 4-2, for 1 pass, K_1=0.319 and n_1=2.242

$$D_b = 19.05\left(\frac{2}{0.319}\right)^{1/2.242} = 43.2mm$$

For a split-ring floating heat exchanger, the typical shell is 50mm (Figure 4-18, below):

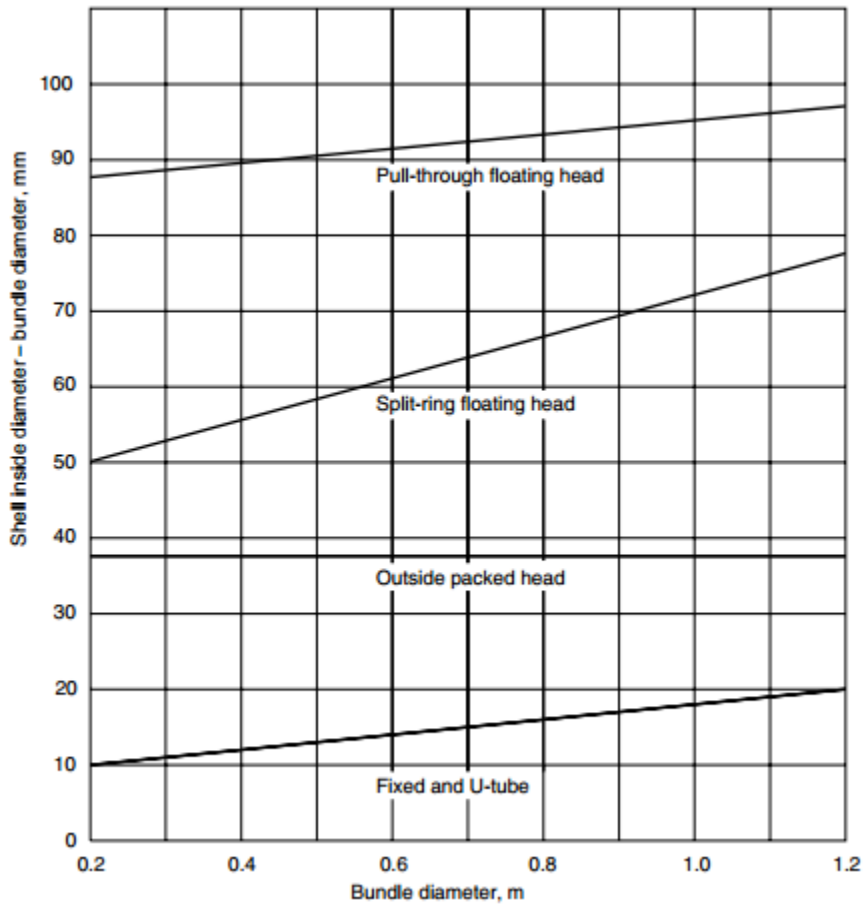

Figure 4- 18:Shell-bundle clearance (Coulson & Richardson, 1999)

Shell inside diameter=43.2mm+ 50mm= 93.2mm

7. Tube side heat transfer coefficient

Re=Reynolds number=$\frac{\rho u_t d_e}{\mu} = \frac{996.3\times0.0029\times14.83\times10^{-3}}{0.891\times10^{-3}} = 48.09$

Pr= Prandtl number=$\frac{C_p\mu}{k_f} = \frac{0.891\times10^{-3}\times4180}{607\times10^{-3}} = 6.14$

$$\frac{L}{d_i} = \frac{5000}{14.85} = 337$$

$h_i = \frac{4180(0.0048T-1)U_t^{0.8}}{d_i^{0.2}} = \frac{4180((0.00488T(298))-1)0.0029^{0.8}}{(14.83\times10^{-3})^{0.2}} = 131.67W/m^2$°C

u_t is the fluid velocity, m/s,

k_f is the fluid thermal conductivity, W/m °C

μ is the fluid viscosity at the bulk fluid temperature, Ns/m^2

μ_w is the fluid viscosity at the wall,

C_p is fluid specific heat, heat capacity, J/kg °C

8. Shell-side heat transfer coefficient

The area for cross-flow A_s for the hypothetical row of tubes at the shell equator, given by:

$$A_s = \frac{(p_t - d_o)D_s I_B}{p_t}$$

Where p_t is the tube pitch,

d_o is the tube outside diameter,

$D_s$is the shell inside diameter, m,

$I_B$is baffle spacing, m.

$$A_s = \frac{(p_t - d_o)D_s I_B}{p_t} = \frac{(23.81 - 19.05)101.53 \times 20}{23.81} = 405.95mm^2$$
$$= 405.95 \times 10^{-6} m^2$$

Buffle spacing:

$$d_e = \frac{1.10(p_t^2 - 0.917d_o^2)}{d_o}$$

Where d_e =equivalent diameter, m.

$$d_e = \frac{1.10(p_t^2 - 0.917d_o^2)}{d_o} = \frac{1.10(23.81^2 - 0.917(19.05)^2)}{19.05} = 13.52mm$$

From the Figure 4-19, below, $j_h = 7 \times 10^{-2}$ at 25% baffle cuts

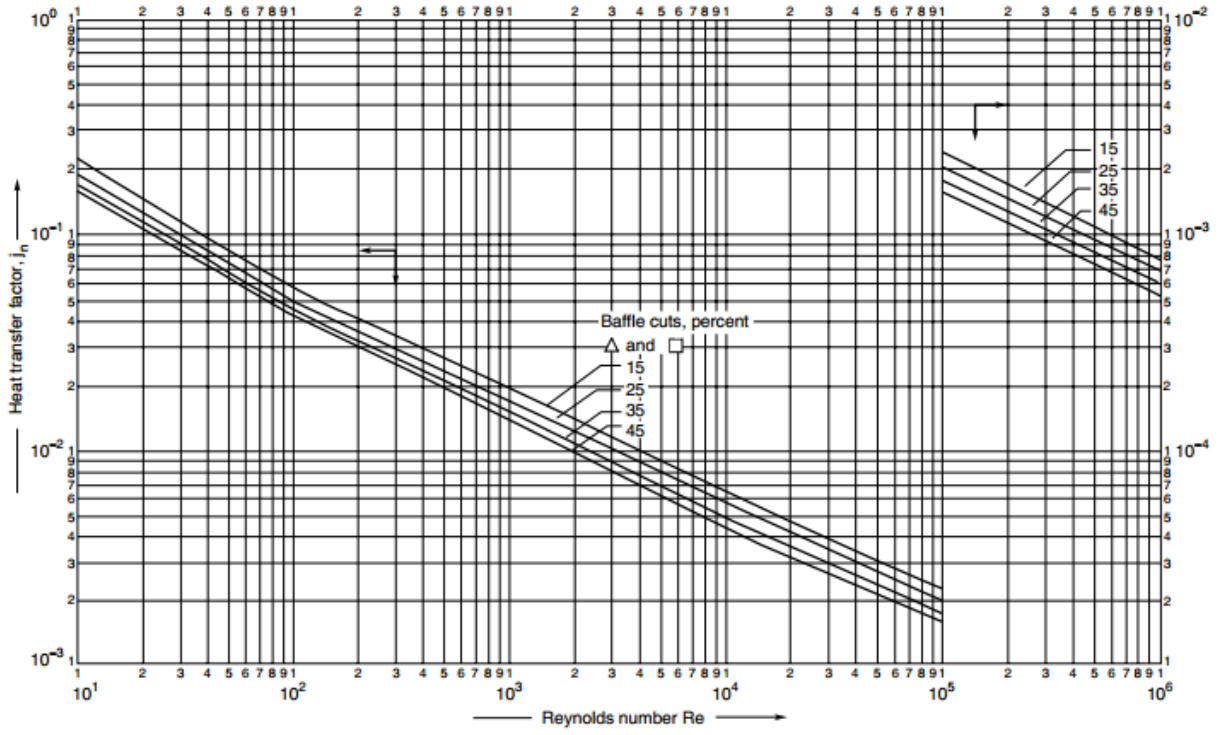

Figure 4- 19:Shell-side heat-transfer factors, segmental baffle: (Coulson & Richardson, 1999)

Therefore, the shell side heat coefficient:

$$h_o = h_s = \frac{k_f j_h Re Pr^{1/3}}{d_e} = \frac{607\times10^{-3}\times48.09\times(6.14)^{1/3}}{13.52\times10^{-3}} = 3\,953.6 \text{W/m}^2\,^{o}\text{C}$$

$$\frac{1}{U_o} = \frac{1}{h_o} + \frac{1}{h_{od}} + \frac{d_o \ln\left(\frac{d_o}{d_i}\right)}{2k_w} + \frac{d_o}{d_i}\times\frac{1}{h_{id}} + \frac{d_o}{d_i}\times\frac{1}{h_i}$$

Where U_o is the overall coefficient based on the outside area of the tube, W/m^2 ^{o}C

h_o is the outside fluid film coefficient, W/m^2 ^{o}C

h_i is the inside fluid film coefficient, W/m^2 ^{o}C

h_{od} is the outside dirt coefficient (fouling factor), W/m^2 ^{o}C

$h_{id}$is inside dirt coefficient, W/m^2 ^{o}C

k_w is the thermal conductivity of the tube wall material, W/m ^{o}C

d_i is tube inside diameter, m,

$d_o$is tube outside diameter, m.

Finding the values for the dirty coefficients from Table 4-3, below:

Table 4- 3: Fouling factors (coefficients), typical values (Coulson & Richardson, 1999)

Fluid	Coefficient (W/m^2°C)	Factor (resistance) (m^2°C/W)
River water	3000–12,000	0.0003–0.0001
Sea water	1000–3000	0.001–0.0003
Cooling water (towers)	3000–6000	0.0003–0.00017
Towns water (soft)	3000–5000	0.0003–0.0002
Towns water (hard)	1000–2000	0.001–0.0005
Steam condensate	1500–5000	0.00067–0.0002
Steam (oil free)	4000–10,000	0.0025–0.0001
Steam (oil traces)	2000–5000	0.0005–0.0002
Refrigerated brine	3000–5000	0.0003–0.0002
Air and industrial gases	5000–10,000	0.0002–0.0001
Flue gases	2000–5000	0.0005–0.0002
Organic vapours	5000	0.0002
Organic liquids	5000	0.0002
Light hydrocarbons	5000	0.0002
Heavy hydrocarbons	2000	0.0005
Boiling organics	2500	0.0004
Condensing organics	5000	0.0002
Heat transfer fluids	5000	0.0002
Aqueous salt solutions	3000–5000	0.0003–0.0002

Therefore

$$\frac{1}{U_o} = \frac{1}{3953.6} + \frac{1}{2000} + \frac{19.05 \times 10^{-3} \ln\left(\frac{19.05}{14.83}\right)}{2(55)} + \frac{19.05}{14.83} \times \frac{1}{3000} + \frac{19.05}{14.83} \times \frac{1}{131.67}$$

$$= 0.0114$$

U_o =87.9W/m^2 ^{o}C

4.5.2 Shell and tube heat exchanger to cool calciner exit gases

The calciner flue gases need to be cooled to room temperature. Assuming carbon dioxide have been separated from the other gases and the exit gas contains nitrogen, carbon dioxide and oxygen at mass fractions of 0.51, 0.34 and 0.15 respectively.

1. Duty

All gases are to be cooled from 1223 K to 453 K.

The average temperature is (1223+453)/2 =838 K

Heat capacities of nitrogen, carbon dioxide and oxygen at this temperature are 31.6J/kg. K, 12.4J/kg. K and 8.2J/kg.K. Average heat captured from calciner exit gases is given by;

For nitrogen,

$$Q = \dot{m}C_p\Delta\theta = 0.51 * 0.075 * 31.6 * (1223 - 453) = \mathbf{930.7}\boldsymbol{W}$$

For carbon dioxide,

$$Q = \dot{m}C_p\Delta\theta = 0.34 * 0.075 * 12.4 * (1223 - 453) = \mathbf{243.5}\boldsymbol{W}$$

For oxygen,

$$Q = \dot{m}C_p\Delta\theta = 0.15 * 0.075 * 8.2 * (1223 - 453) = \mathbf{71.0}\boldsymbol{W}$$

Total heat to be absorbed from the exit gases is 1 245.2 W

Using water flowing at same mass flow rate as the outlet gas (0.075kg/s), heat capacity of water at 298 degrees Kelvin is 4180J/Kg. K

The outlet temperature of water is;

$$Q = \dot{m}C_p\Delta\theta = 0.075 \times 4180 \times (t_2 - 298) = 1245.2W$$

$$t_2 = 302\ K = 29\ degrees\ Celcious$$

The average temperature of water is (298+302)/2= 300 K= 27 ^oC

The heat capacity of water at 27 ^oC is 4179J/kg. K

2. The mean temperature

$$\Delta T_{lm} = \frac{(T_1 - t_2) - (T_2 - t_1)}{\ln\left(\frac{T_1 - t_2}{T_2 - t_1}\right)} = [(950 - 29) - (180 - 25)]/\ln\left(\frac{(950 - 29)}{(180 - 25)}\right) = 429.8$$

$$R = \frac{(T_{hin} - T_{hout})}{(t_{cout} - t_{cin})} = \frac{950 - 180}{29 - 25} = 192.5$$

$$P = \frac{(t_{cout} - t_{cin})}{(T_{hin} - t_{cin})} = \frac{29 - 25}{950 - 25} = 0.004$$

Since R>1, P becomes (192.5*0.004) =0.77 and R=1/192.5=0.005

Using Figure 4-17, F_t =1

$\Delta T_m = F_t\Delta T_{lm} = 1 \times 429.8$=429.8$^oC$

Taking the overall coefficient to be 20W/m^2 ^oC

Therefore,

3. Area of heat transfer

$Q = UA\Delta T_m$=1245.2W

$A = \frac{Q}{U\Delta T_m} = \frac{1245.2}{20\times429.8} = 0.15$m^2

4. Layout and tube size

Using a 16.00 mm outside diameter, 14.00 mm inside diameter, 1.83 m Long tubes

(A popular size) on a triangular 20.00 mm pitch (pitch/diameter=1.25)

5. Number of tubes

Area of one tube=$\pi \times 16.00 \times 10^{-3} \times 1.83 = 0.092m^2$

Number of tubes = heat transfer area/area of one tube=$\frac{0.15}{0.092} = 1.6 \cong 2$

For 2 passes, tubes per pass= 1

Tube cross sectional area=$\frac{\pi}{4}(14.00 \times 10^{-3})^2 = 0.000154m^2$

Area per pass=$1 \times 0.000154 = 0.000154m^2$

Volumetric flow=$\frac{0.075}{1000} \times \frac{1}{1000} = 7.5 \times 10^{-8} m^3/s$

Tube side velocity=volumetric flow/ area per pass= $\frac{7.5 \times 10^{-8}}{0.000154} = 0.00049m/s$

6. Bundle and shell diameter

$$D_b = d_o \left(\frac{N_t}{K_1}\right)^{1/n_1}$$

From Table 4-2, for 1 pass, K_1=0.319 and n_1=2.242

$$D_b = 16.00 \left(\frac{2}{0.319}\right)^{1/2.242} = 36.3mm$$

For a split-ring floating heat exchanger, the typical shell is 50mm (Figure 4-18):

Shell inside diameter=36.3mm+ 50mm= 86.3mm

7. Tube side heat transfer coefficient

Re=Reynolds number=$\frac{\rho u_t d_e}{\mu} = \frac{996 \times 0.00049 \times 14.00 \times 10^{-3}}{0.798 \times 10^{-3}} = 8.56$

Pr= Prandtl number=$\frac{C_p \mu}{k_f} = \frac{0.798 \times 10^{-3} \times 4178}{615 \times 10^{-3}} = 5.42$

$$\frac{L}{d_i} = \frac{1860}{14.00} = 132.9$$

$h_i = \frac{4178(0.00488t - 1)U_t^{0.8}}{d_i^{0.2}} = \frac{4178(0.00488(298) - 1)0.00049^{0.8}}{(14.00 \times 10^{-3})^{0.2}} = 10.03 W/m^{2o}\text{C}$

8. Shell-side heat transfer coefficient

The area for cross-flow A_s for the hypothetical row of tubes at the shell equator, given by:

$$A_s = \frac{(p_t - d_o)D_s I_B}{p_t}$$

$$A_s = \frac{(p_t - d_o)D_s I_B}{p_t} = \frac{(20.00 - 16.00)36.3 \times 20}{20.00} = 145.2mm^2 = 145.2 \times 10^{-6} m^2$$

Buffle spacing:

$$d_e = \frac{1.10(p_t^2 - 0.917d_o^2)}{d_o}$$

Where d_e =equivalent diameter, m.

$$d_e = \frac{1.10(p_t^2 - 0.917d_o^2)}{d_o} = \frac{1.10(20.00^2 - 0.917(16.00)^2)}{16.00} = 11.36mm$$

From the figure, j_h=1.9 at 25% baffle cuts

Therefore, the shell side heat coefficient:

$$h_o = h_s = \frac{k_f j_h Re Pr^{1/3}}{d_e} = \frac{615\times10^{-3}\times8.56\times(5.42)^{1/3}}{11.36\times10^{-3}} = 814.0 \text{W/m}^2\,^{o}\text{C}$$

$$\frac{1}{U_o} = \frac{1}{h_o} + \frac{1}{h_{od}} + \frac{d_o \ln\left(\frac{d_o}{d_i}\right)}{2k_w} + \frac{d_o}{d_i} \times \frac{1}{h_{id}} + \frac{d_o}{d_i} \times \frac{1}{h_i}$$

Finding the values for the dirty coefficients from the Table 4-3:

Therefore

$$\frac{1}{U_o} = \frac{1}{814} + \frac{1}{2000} + \frac{16.00 \times 10^{-3} \ln\left(\frac{16.00}{14.00}\right)}{2(55)} + \frac{16.00}{14.00} \times \frac{1}{3000} + \frac{16.00}{14.00} \times \frac{1}{10.03} = 0.1161$$

U_o =8.62W/m^2 ^{o}C

4.5.3 Tubed-shell heat exchanger to cool solids from calciner and carbonation reaction

1. Duty

Calcium oxide is being cooled from 1223 K to 923 K.

The average temperature is (1223+923)/2 =1073 K

Heat capacity of calcium oxide at 1073 K is 63.389J/kg.K. Average heat released by carbonation is given by;

$$Q = \dot{m}C_p\Delta\theta = \mathbf{22\ 000\ 000}\boldsymbol{W}$$

Where $\dot{m}$ is the mass flow rate, kg/s

Using water in the tube flowing at 100kg/s. Heat capacity of water at 298 degrees Kelvin is 4180J/Kg. K

The outlet temperature of water is;

$$Q = \dot{m}C_p\Delta\theta = 100 \times 4180 \times (t_2 - 298) = 22\ 000\ 000W$$

$$t_2 = 350.6\ K = 77.6\ degrees\ Celcious$$

The average temperature of water is (298+350.6)/2= 324.3 K= 51.6 ^oC

The heat capacity of water at 51.6 ^oC is 4181J/kg. K

2. The mean temperature

$$\Delta T_{lm} = \frac{(T_1 - t_2) - (T_2 - t_1)}{\ln\left(\frac{T_1 - t_2}{T_2 - t_1}\right)} = [(950 - 77.6) - (650 - 25)]/\ln\left(\frac{(950 - 77.6)}{(650 - 25)}\right) = 741.8^oC$$

$$R = \frac{(T_{hin} - T_{hout})}{(t_{cout} - t_{cin})} = \frac{950 - 650}{77.6 - 25} = 5.40$$

$$P = \frac{(t_{cout} - t_{cin})}{(T_{hin} - t_{cin})} = \frac{77.6 - 25}{950 - 25} = 0.06$$

Since R>1, P becomes (5.40*0.06) =0.324 and R=1/5.40=0.185

From Figure 4-17, F_t =1

$\Delta T_m = F_t\Delta T_{lm} = 1.0 \times 741.8$=741.8$^oC$

Given that the overall coefficient to be 34W/m^2 ^{o}C (Lienhard & Leinhard, 2006)

Therefore,

3. Area of heat transfer

$Q = UA\Delta T_m$=22 000 000W

$A = \frac{Q}{U\Delta T_m} = \frac{22\ 000\ 000}{34 \times 741.8} = \mathbf{872.3 m^2}$

5 Chapter five

5. Conclusions and Recommendations

It has been found out from the research that carbonation, sulphation as well as calcination reactions are temperature dependent. As temperature increases, the rate of carbonation decreases while the rate of sulphation increases. Carbonation is an exothermic reaction and increasing the temperature of the system will favor the reverse reaction thus lowering the rate of carbonation. It is therefore necessary to have a low temperature that allows little sulphation, as sulphation reduces the amount of active calcium carbonate for carbonation, and at the same time the temperature should not be too low to suppress the carbonation reaction. Temperatures below 500^{o}C are too low to drive the carbonation reaction (Lu, et al., 2008). For temperatures below 600 ^{o}C, the decrease in amount of carbonate formed (carbonation) is less than it is after 600 ^{o}C. The optimal temperature for carbonation would be 600^{o}C for it is high enough to drive the carbonation reaction and not too high to accelerate the sulphation reaction.

Rate of carbonation increases as carbon dioxide concentration in flue gas increases. This is because carbonation is directly proportional to amount of carbon dioxide in the flue gas stream.

Increase in the sorbent to carbon dioxide flow ratio lead to an increase in both carbonation and sulphation, as more reactant will be available for reaction with the flue gas stream. High sorbent to carbon dioxide flow ratios also lead to a more concentrated stream of carbon dioxide being removed from the calciner as more carbon dioxide would have been absorbed in the carbonator.

A temperature increase in the calciner leads to an increase in rate of calcination. If temperatures become too high (above 900^{o}C for calcium oxide), sintering occurs at an elevated pace (Grasa, et al., 2008). This means that although the rate of calcination increases with an increase in temperature, temperatures above 900 ^{o}C should be avoided.

Increase in carbon dioxide partial pressure in the calciner causes a decrease in calcination reaction. A low carbon dioxide partial pressure is recommended for an increase in calcination.

The amount of active calcium oxide particles decreases as the number of carbonation-calcination cycles increase. There is a sharp decrease in the first 10 cycles and after about 100 cycles; the active calcium particles remain constant. It is recommended that the number of carbonation-calcination not exceed 20 after which most (more than 75 %) of the sorbent will be inactive.

Neglecting the effect of sulphation in the design of the coupled fluidized bed system leads to overestimation of the active fraction of calcium oxide particles that will react with carbon dioxide in the flue gas. Lower amount of carbon dioxide will be absorbed than estimated.

Energy adsorbed and released by calcination and carbonation respectively decreases as the number of carbonation-calcination cycles increase due to the decrease in carbonation and calcination reactions as number of cycles increase.

The model reveals conditions on which carbon dioxide capture is effective and not effective. A 200 kW (power consumption) pilot plant was built in IFK, University of Stuttgart, (Hawthorne, et al., 2011) . The pilot plant had a carbonator operating at 600-700 ^{o}C and calciner operating at 850-950 ^{o}C. The pilot plant was able to recover 90% of the carbon dioxide in the flue gas. The model presented in this research was able to recover 83 % of the carbon dioxide from flue gas at sorbent to carbon dioxide flow ratio of 20. Carbon dioxide recovery increases as the sorbent to carbon dioxide flow ration increase (100% recovery at a sorbent to carbon dioxide ratio of 13333), making the model presented in this research applicable in predicting the performance of the coupled system.

Further work need to be carried out to investigate sorbent reactivation after carbonation-calcination deactivation using partial hydration system. This would have to be done by employing a hydrating unit separate to the calcium looping system.

Bibliography

Abanades, J. & Alvarez, D., 2003. Conversion Limits in the Reaction of CO2 with Lime. *Energy & Fuels,* Volume 17, pp. 308-315.

Abanades, J., Anthony, E., Lu, D. & Salvador, C., 2004. Capture of CO2 from Combustion Gases in a Fluidised Bed of CaO. *AIChE,* 50(7), pp. 1614-1622.

Alonso, M., Rodriguez, M., Grasa, G. & Abanades, J., 2009. Modelling of a fluidised bed carbonator reactor to capture CO2 from a combustion flue gas. *Chemical Engineering Science,* Volume 64, pp. 883-891.

Alonso, M. et al., 2010. Carbon dioxide capture from combustion flue gases with calcium oxide chemical loop: Experimental results and process development. *International Journal of Greenhouse Gas Control,* 4(2), pp. 167-173.

Alonso, M., Rodriguez, N., Grasa, G. & Abanades, J., 2009. Modelling of a fluidised bed carbonator reactor to capture CO2 from a combustion flue gas. *Chemical Engineering Science,* Volume 64, pp. 883-891.

Alonso, M., Rodriguz, N., Grasa, G. & Abanades, J., 2009. Modelling of a fluidized bed carbonator reactor to capture CO2 from combustion flue gas. *Chemical Engineering Science,* Volume 64, pp. 883-891.

Bhatia, S. & Perlmutter, D., 1981. A Random Pore Model for Fluid-Solid Reactions. *AIChe Journal,* 27(2), pp. 247-254.

Bhatia, S. & Permutter, D., 1983. Effect of the Product Layer on the Kinetics of the CO2-Lime Reaction. *AIChE Journal,* 29(1), pp. 79-86.

Charitos, A. et al., 2011. Experimental validation of the calcium looping CO2 capture process with two circulating fluidized bed carbonator reactors. *Ind. Eng. Chem. Res,* Volume 50, pp. 9685-9695.

Cordero, J. & Alonso, M., 2015. Modelling of the kinetics of sulphation of CaO particles under CaL reactor conditions. *Fuel,* Volume 150, pp. 501-511.

Coulson, J. & Richardson, J., 1999. *Coulson & Richardson's Chemical Engineering. Fluid Flow, Heat Transfer and Mass Transfer.* 6th ed. Oxford: Butterworth Heinemann.

Curran, G., Fink, C. & Gorin, E., 1967. CO2 acceptor gasification process. Studies of acceptor properties. *Advanced in Chemistry Series,* Volume 69, pp. 141-161.

Dean, C. et al., 2011. The calcium looping cycle for carbon dioxide capture from power generation, cement manufacture and hydrogen production. *Chemical Engineering Research and Design,* 89(6), pp. 836-855.

De-Souza Santos, M., 2010. *Solid fuels combustion and gasification.* 1 ed. New York: CRC Press.

F.Garcia-Labiano, et al., 2002. Calcination of calcium-based sorbents at pressure in a broad range of CO2 concentrations. *Chemical Engineering Science,* Volume 57, pp. 2381-2392.

Fransson, E. & Detert, M., 2014. *Process Integration of CO2 capture by means of calcium looping technology: Masters thesis in Sustainable Energy Systems programme.* Sweden: Department of Heat and Power Technology CHALMERS UNIVERSITY OF TECHNOLOGY.

Garcia-Labiano, F. et al., 2002. Calcination of calcium-based sorbents at pressure in a broad range of CO2 concentrations. *Chemical Engineering Science,* Volume 57, pp. 2381-2392.

Global CCS Institute, 2012. *The Global Status of CCS.* [Online]
Available at: http://www.globalccsinstitute.com/publications/global-status-ccs-2012/online/48321
[Accessed 10 November 2016].

Global CCS Institute, 2014. *Understanding CCS. How CCS works-capture.* [Online]
Available at: http://www.globalccinstitute.com/understanding-ccs/how-ccs-works-capture
[Accessed 30 January 2018].

Grasa, G., Abanaded, J., Alonso, M. & Gonzalez, B., 2008. Reactivity of highly cycled particles of CaO in carbonation/calcination loop. *Chemical Engineering Journal,* Volume 137, pp. 561-567.

Hawthorne, C. et al., 2008. *Design of a dual fluidised bed system for the post-combustion removal of CO2 using CaO.* Hamburg, Germany, TuTech Innovation Gmbh.

Hawthorne, C. et al., 2011. CO2 Capture with CaO in a 200KWth Dual Fluidized Bed Pilot Plant. *Energy Procedia,* Volume 4, pp. 441-448.

Hawthorne, C. et al., 2011. CO2 Capture with CaO in a 200kWth Dual Fluidized Bed pilot Plant. *Energy Procedia,* Volume 4, pp. 441-448.

I.Martinez, et al., 2013. Modelling the continuous calcination of CaCO3 in a Ca-looping system. *Chemical Engineering Journal,* Volume 215-216, pp. 174-181.

I.Martinez, G.Grasa, R.Murillo & B.Arias, J., 2013. Modelling the continuos calcination of CaCO3 in a Ca-looping system. *Chemical Engineering Journal,* Volume 215-216, pp. 174-184.

Ihde, J., 1989. Le Chatelier and chemical equilibrium. *Journal of Chemical Education,* 66(3), p. 238.

IPCC, 2007. *Climate change 2007 Mitigation of climate change; Contribution of Working Group III to the Fourth Assessment Report of the Intergovernmental Panel on Climate Change,* United Kingdom and New York: Cambridge Universuty Press.

J.M.Cordero & M.Alonso, 2015. Modelling of the kinetics of sulphation of CaO particles under CaL reactor conditions. *Fuel,* Volume 150, pp. 501-511.

J.Ylatalo, et al., 2012. 1-Dimensional modelling and simulation of calcium looping process. *International Journal of Greenhouse Gas Control,* Volume 9, pp. 130-135.

J.Ylatalo, et al., 2012. 1-Dimensional modelling and simulation of the calcium looping process. *International Journal of Greenhouse Gas Control,* Volume 9, pp. 130-135.

J.Yltalo, et al., 2012. 1-Dimensional modelling and simulation of calcium looping process. *International Journal of Greenhouse Gas Control,* Volume 9, pp. 130-135.

Khinast, J., Krammer, G., Brunner, C. & Staudinger, G., 1996. Decomposition of limestone: The influence of CO2 and particle size on the reaction rate. *Chemical Engineering Science,* 51(4), pp. 623-634.

Kunii, D. & Levenspiel, O., 1991. *Fluidisation Engineering.* 2nd ed. London: Buttworth-Heinemann.

Levenspiel, O., 1999. *Chemical reaction Engineering.* 3rd ed. New York: John Wiley & Sons.

Levenspiel, O., 1999. *Chemical reaction Engineering.* 3rd ed. New York: John Wiley & Sons.

Lienhard, J. I. & Leinhard, J. V., 2006. *A Heat Transfer Textwork.* 3rd ed. USA: Phlogiston Press.

Lu, D., Hughes, R. & Anthony, E., 2008. Ca-based sorbent looping combustion for CO2 capture in pilot-scale dual fluidised beds. *Fuel Processing Technology,* Volume 89, pp. 1386-1395.

Manovic, V. & Anthony, E., 2010. Competition of Sulphattion and Carbonation Reactions during Looping Cycles for CO2 Capture by CaO-Based Sorbents. *J. Phys. Chem,* 114(11), pp. 3997-4002.

Martunus, et al., 2012. Improved carbon dioxide capture using metal reinforced hydrotalcite under wet conditions. *International Journal of Greenhouse Gas Control,* Volume 7, pp. 127-136.

N.Rodriguez, M.Alonso & J.C.Abanades, 2011. Experimental Investigation of a Circulating Fluidized-bed Reacror to Capture CO2 with CaO. *AIChE,* 57(5), pp. 1356-1366.

Ortiz, C. et al., 2015. A new model of the carbonator reactor in the Calcium Looping technology for post-combustion. *Fuel,* Volume 160, pp. 328-338.

Perry, R. H. & Green, D. W., 2008. *Perry's Chemical Engineer's Handbook.* 8th ed. New York: McGraw-Hill.

Romano, M., 2009. Coal-fired plant with calcium oxide carbonation for post-combustion CO2 capture. *Energy Procedia,* Volume 1, pp. 1099-1106.

Romano, M., 2012. Modelling the carbonator of a Ca-looping process for CO2 capture from power plant flue gas. *Chemical Engineering Science,* Volume 69, pp. 257-269.

Romano, M. et al., 2013. Process simulation of Ca-looping processes; review and guidelines. *Energy Procedia,* Volume 37, pp. 142-150.

S.K.Bhatia & D.D.Perlmutter, 1981. A Random Pore Model for Fluid-Solid Reactions. *AIChE Journal,* 27(2), pp. 247-254.

Sevilla, M. & Fuertes, A., 2012. CO2 adsorption by activated carbons. *Journal of Colloid and Interface Science,* Volume 366, pp. 147-154.

Shimizu, T. et al., 1999. A twin fluidised-bed reactor for removal of CO2 from combustion systems. *Trans IChemE,* 77(Part A), pp. 62-68.

Shimizu, T. et al., 1999. A twin fluid-bed reactor for removal of CO2 from combustion processes. *Trans IChemE,* 77(Part A), pp. 62-68.

Silcox, D., Kramlich, J. & Pershing, D., 1989. A Mathematical Model for the Flash Calcination of Dispersed CaCO3 and Ca(OH)2 Particles. *Ind. Eng. Chem. Res,* Volume 28, pp. 155-160.

Sivalingam, S., 2013. *CO2 separation by calcium looping from full and partial fuel oxidation.* Germany: Technical University of Munich.

Spliethoff, H., 2010. *Power Generation from Solid Fuels.* 1st ed. s.l.:Springer-Verlag Berlin Heidelberg.

Stanmore, B. & Gilot, P., 2005. Review-calcination and carbonation of limestone during thermal cycling for CO2 sequestration. *Fuel Processing Technology,* Volume 86, pp. 1707-1743.

Thiruvenkatachari, R., Su, S., An, H. & Yu, X., 2009. Post combustion CO2 capture by carbon fibre monolithic adsorbents. *Progress in Energy and Combustion Science,* Volume 35, pp. 438-455.

United Nations, 2015. *Millenium Development Goals Report.* New York: United Nations.

Ylatalo, J., 2013. *Model Based Analysis of the Post-combustion Calcium Looping Process for Carbon dioxide Capture.* Finland: s.n.

Ylatalo, J. et al., 2012. 1-Dimensional modelling and simulation of the calcium looping process. *International Journal of Greenhouse Gas Control,* Volume 9, pp. 130-135.

Ylatto, J., Ritvanen, J., Tynjala, T. & Hyppanen, T., 2014. Model based scale-up study of the calium looping process. *Fuel,* pp. 329-337.

Yltalo, J., 2013. *Model Based Analysis of the Post-combustion Calcium Looping Process for Carbon dioxide Capture.* Finland: s.n.

Appendix A: MATLAB Codes

Carbonator Mass Balances

Calcium Oxide

```
syms s m t min Win Wi m1 m1(t) Save r1(t) fa fm fw Fo Fr A E R Tcarb Cco2e T
A B k Xr Xave kcarb C Min N CCO2 xso2 xo2 rcarb
Win=0.95; Min=Fo+Fr;Wcao=0.95*(Fo+Fr);
eqn1=(Min*Win)
k=0.52;
Xr=0.075;
for N=0:100
    Wi=Xr+(1/(k*N+(1/(1-Xr))))
end
eqn2=(0.95*Min*(1-Wi))
z=(Wcao/(Fr))
fa=1-exp(-t/z)
B=1.462*10^11; C=19130;
kcarb=5.95*10^-10
CCO2e=(B/(Tcarb+273))*exp(-C/(Tcarb+273))
Xave=Wi; Pcao=3320; VMcaco3=36.9* 10^-3; emax=50*10^-9; PMcao=56;
Save=((Xave*Pcao*VMcaco3)/(PMcao*emax))
rcarb=m*(fa)*kcarb*Save*(CCO2-CCO2e)
R=8.314; Xcao=0.95;
k=4.9*10^3*((-3.843*(Tcarb+273))+5640)*exp(-8810/(Tcarb+273))
rsulf=(m)*k*Xcao*xso2*xo2
eqn3=eqn1-eqn2-rcarb-rsulf
m1(t)=eqn3 % mass in sutract mass out equals consumption
eqn4=eqn1-eqn2-rcarb
m1=dsolve('Dm1=eqn3', 'm1(0)==0')
% Fo is mass flow of spend sorbent=mass of fresh sorbent added
% t is time
% z is residence time of solids in the carbonator
% Fr is the mass flow of sorbent after reaction with carbon dioxide in
% carbonator
% Wi is conversion degree of the element
% T is temperature
% Min is mass flow of solids in to the reactor
% Win is conversion degree of incoming solids
% m is mass of solid
% CCO2e is equilibrium concentration of carbon dioxide
% CCO2 is carbon dioxide concentration
% R is ideal gas constant
% B and C are constants
% kcarb is the constant for carbonation
%rcarb is the rate of carbonation
% fa is fraction of active calcium particles
% m1 is mass flow of calcium oxide in carbonator
```

Calcium carbonate

```
syms m t min Wcao Win Wi m2(t) Cco2e kcarb Min CCO2 rcarb Tcarb Fo Fr
Min=0;Wcao=0.95*(Fo+Fr);
eqn1=0;
z=(Wcao/(Fr))
fa=1-exp(-t/z)
B=1.462*10^11; C=19130;
kcarb=5.95*10^-10
CCO2e=(B/(Tcarb+273))*exp(-C/(Tcarb+273))
k=0.52;
Xr=0.075;
for N=0:100
    Wi=Xr+(1/(k*N+(1/(1-Xr))))
end
Xave=Wi; Pcao=3320; VMcaco3=36.9* 10^-3; emax=50*10^-9; PMcao=56;PMcaco3=100
Save=((Xave*Pcao*VMcaco3)/(PMcao*emax))
rcarb=m*(fa)*Save*kcarb*(CCO2-CCO2e)
rcaco3=rcarb*PMcaco3/PMcao
eqn3=eqn1+rcaco3
syms m(t) s
Dm2=diff(m2);
m2(t)=eqn3
m2=dsolve('Dm2=eqn3', 'm2(0)==0')
% mass out is equal to generation
%Fo is mass flow of spend sorbent=mass of fresh sorbent added
% t is time
% z is residence time of solids in the carbonator
% Fr is the mass flow of sorbent after reaction with carbon dioxide in
% carbonator
% fa is active fraction of calcium particles
% Wi is conversion degree of the element
% T is temperature
% Min is mass flow of solids in to the reactor
% Win is conversion degree of incoming solids
% m is mass of solid
% CCO2e is equilibrium concentration of carbon dioxide
% CCO2 is carbon dioxide concentration
% R is ideal gas constant
% B and C are constants
% kcarb is the constant for carbonation
%rcarb is the rate of carbonation
% m2 is mass flow of calcium carbonate in carbonator
```

Calcium sulphate

```
syms m t s Min Win Wi m3(t) Mout xso2 xo2 Tcarb Xcao
Min=0; a=0; b=0; c=1; d=2;
eqn1=symsum(Min*Win/10, Win, a, b);
eqn2=symsum(Min*Wi/100,Wi, c, d);
Xcao=0.95;PMcaso4=136; PMcao=56;
k=4.9*10^3*((-3.843*(Tcarb+273))+5640)*exp(-8810/(Tcarb+273))
```

```
rsulf=(m)*k*Xcao*xso2*xo2
rcaso4=rsulf*PMcaso4/PMcao
eqn3=(eqn1-eqn2+rcaso4)
m3(t)=eqn3
m3=dsolve('Dm3=eqn3', 'm3(0)==0')% mass out is equal to generation
% Wi is conversion degree of the element
% T is temperature
% Min is mass flow of solids in to the reactor
% Win is conversion degree of incoming solids
% m is mass of solid
% A, B, C and D are constants
%rsulf is the rate of sulfation
% xso2 and xo2 are partial fraction of sulphur dioxide and oxygen
% respectively
% m3 is mass flow of calcium sulphate in carbonator
```

Carbon dioxide

```
syms m t min Win r3(t) Wi ms fm fw fa Fo Fr R Tcarb w3(t) w3 mg min mout
Cco2e T A B k Xr Xave kcarb C Min N CCO2 a b c d rcarb
min=0.216*mg;
eqn1=min
Wcao=0.95*(Fo+Fr);
z=(Wcao/(Fr))
fa=1-exp(-t/z)
B=1.462*10^11; C=19130;
kcarb=5.95*10^-10
CCO2e=(B/(Tcarb+273))*exp(-C/(Tcarb+273))
k=0.52;
Xr=0.075;
for N=0:100
    Wi=Xr+(1/(k*N+(1/(1-Xr))))
end
Xave=Wi; Pcao=3320; VMcaco3=36.9* 10^-3; emax=50*10^-9; PMcao=56;
Save=((Xave*Pcao*VMcaco3)/(PMcao*emax))
rcarb=m*Save*(fa)*kcarb*(CCO2-CCO2e)
MCO2=44; MCaO=56;
rCO2=-rcarb*(MCO2/MCaO)
eqn3=eqn1+rCO2
w3(t)=(1/mg)*(eqn3)% mass fraction of carbon dioxide in exit stream equals
CO2 in subtract carbon dioxide adsorbed by calcium oxide
wCO2(t)=((1/mg)*(eqn1-(mg*w3(t))))/t
wCO2=dsolve('DwCO2=eqn3', 'wCO2(0)==0')
% Fo is mass flow of spend sorbent=mass of fresh sorbent added
% t is time
% z is residence time of solids in the carbonator
% Fr is the mass flow of sorbent after reaction with carbon dioxide in
% carbonator
% Wi is conversion degree of the element
% T is temperature
% Min is mass flow of solids in to the reactor
% Win is conversion degree of incoming solids
```

```
% m is mass of solid
% CCO2e is equilibrium concentration of carbon dioxide
% CCO2 is carbon dioxide concentration
% R is ideal gas constant
% B and C are constants
% fa is active fraction of calcium particles
% kcarb is the constant for carbonation
%rcarb is the rate of carbonation
% M is mass of gas
% MCO2 and MCaO are molar masses of carbon dioxide and calcium oxide
% wCO2 is mass fraction of carbon dioxide in carbonator exit gas stream
```

Oxygen

```
yms m t r2(t)  Win Wi ms fa w2(t) mg min mout T CCO2e Tcarb kcarb C Min CCO2
rO2 Fo Fr xo2
min=xo2*mg;
eqn1=min
k=4.9*10^3*((-3.843*(Tcarb+273))+5640)*exp(-8810/(Tcarb+273))
rsulf=m*k*Xcao*xso2*xo2
MSO2=64; MCaSO4=136;MCaO=56; MO2=32; MCaO=56;
rO2=-rsulf*(MO2/MCaO)
eqn3=eqn1+ rO2
w2(t)=(1/mg)*(eqn3)% mass fraction of oxygen in exit stream equals O2 in
subtract O2 reacted divide by total amount of gas in the reactor
wO2(t)=((1/mg)*(eqn1-(mg*w2(t))))/t
wO2=dsolve('DwO2=eqn3', 'wO2(0)==0')
% Fo is mass flow of spend sorbent=mass of fresh sorbent added
% t is time
% Fr is the mass flow of sorbent after reaction with carbon dioxide in
% carbonator
% Wi is conversion degree of the element
% T is temperature
% Min is mass flow of solids in to the reactor
% Win is conversion degree of incoming solids
% A, B, C and k are constants
% Xr is residual conversion
% M is mass of gas
% MO2 and MCaO are molar masses of oxygen and calcium oxide
% rcarb is rate of carbonation
% wO2 is mass fraction of oxygen in carbonator exit gas stream
```

Sulphur dioxide

```
syms m t min mout Win Wi ms  w1(t) fw Fo Fr Mso2(t) Tcarb  xso2 xo2 mg
min=xso2*mg;Xcao=0.95
eqn1=min
k=4.9*10^3*((-3.843*(Tcarb+273))+5640)*exp(-8810/(Tcarb+273))
rsulf=(m)*k*Xcao*xso2*xo2
MSO2=64; MCaSO4=136;MCaO=56
rSO2=-rsulf*(MSO2/MCaO)
eqn3=eqn1+ rSO2
```

```
w1(t)=(1/mg)*(eqn3)% mass out equals mass in subtract consumption
wso2(t)=((1/mg)*(eqn1-(mg*w1(t))))/t
wso2=dsolve('Dwso2=eqn3', 'wso2(0)==0')
% Fo is mass flow of spend sorbent=mass of fresh sorbent added
% t is time
% Fr is the mass flow of sorbent after reaction with carbon dioxide in
% carbonator
% Wi is conversion degree of the element
% T is temperature
% Min is mass flow of solids in to the reactor
% mg is total mass flow of gas
% Xcao, xso2 and xo2 are molar fractions of calcium oxide, sulphur dioxide
and oxygen
% R is the ideal gas constant
% ws02 is mass fraction of Sulphur dioxide in carbonator exit gas stream
```

Calciner Mass Balances

Calcium oxide

```
syms m1calc(t) s m t min Win Wi ms fm fw Fo Fr Tcarb Tcalc PCO2e Tcalc A B
xso2 xo2 k Xr Xave mCaO mCaCO3 MCaCO3 kcalc C Min N PCO2 a b c d rcalc pCaO
pCaCO3
k=0.52;
Xr=0.075;
for N=0:100
    Wi=Xr+(1/(k*N+(1/(1-Xr))))
end
Min=(1-Wi)*Fr;
eqn1=Min
eqn2=Fo
PMCaCO3=100;pCaCO3=2800; PMcao=56
A=0.00122*10^-5;E=29; R=8.134;B=4.317*10^12; C=20474;
kcalc=A*exp(-4026/(Tcalc+273))
PCO2e=B*exp(-C/(Tcalc+273))
Xave=Wi; Pcao=3320; VMcaco3=36.9* 10^-3; emax=50*10^-9; PMcao=56;
Save=((Xave*Pcao*VMcaco3)/(PMcao*emax))
rcalc=m*Wi*(Save)*(PMCaCO3/pCaCO3)*(kcalc)*(1-(PCO2/PCO2e))
rcao=rcalc*PMcao/PMCaCO3
eqn3=(eqn1-eqn2+rcao)
ode=diff(m1calc,t)==eqn3;
cond=m1calc(0)==Min;
m1calc(t)=dsolve(ode,cond)
m1calc(t)=eqn3 % mass flow out equals generation
m1calc=dsolve('Dm1calc=eqn3', 'm1calc(0)==0')
%Fo is mass flow of spend sorbent=mass of fresh sorbent added
% t is time
% Fr is the mass flow of sorbent after reaction with carbon dioxide in
% carbonator
% Wi is conversion degree of the element
% T is temperature
% Min is mass flow of solids in to the reactor
% Win is conversion degree of incoming solids
% m is mass of solid
% PCO2e is equilibrium pressure of carbon dioxide
% PCO2 is carbon dioxide pressure
% R is ideal gas constant
```

```
% fm, fw, A, B and k are constants
% Xr is residual conversion
% Xave is fraction of active calcium particles
% kcalc is the constant for calcination
%rcalc is the rate of calcination
% pCaO and pCaCO3 are densities of calcium oxide and calcium carbonate
repectvely
% MCaO and MCaCO3 are molar masses of calcium oxide and calcium carbonate
% respectively
% Save is the average reaction surface area
% m1calc is mass flow calcium oxide in calciner
```

Calcium carbonate

```
syms m2calc(t) m t min Win Wi fm fw Fo Fr Tcarb PCO2e Tcalc A B kcalc Min
PCO2 rcalc pCaO pCaCO3
k=0.52;
Xr=0.075;
for N=0:100
    Wi=Xr+(1/(k*N+(1/(1-Xr))))
end
Min=Fo+(Wi*Fr);
eqn1=(Min)
eqn2=0;
fm=0.77;
fw=0.17;
W=0.8;
PMCaCO3=100, pCaCO3=2800;PMcao=56
A=0.00122*10^-5;E=29;B=4.317*10^12; C=20474;
kcalc=A*exp(-4026/(Tcalc+273))
PCO2e=B*exp(-C/(Tcalc+273))
Xave=Wi; Pcao=3320; VMcaco3=36.9* 10^-3; emax=50*10^-9; PMcao=56;
Save=((Xave*Pcao*VMcaco3)/(PMcao*emax))
rcalc=m*W*(Save)*(PMCaCO3/pCaCO3)*(kcalc)*(1-(PCO2/PCO2e))
eqn3=(eqn1-eqn2-rcalc)
m2calc(t)=eqn3 % mass flow in subtract mass flow out equals rate of
consumption
m2calc=dsolve('Dm2calc=eqn3', 'm2calc(0)==0')
% Fo is mass flow of spend sorbent=mass of fresh sorbent added
% t is time
% Fr is the mass flow of sorbent after reaction with carbon dioxide in
% carbonator
% Wi is conversion degree of the element
% T is temperature
% Min is mass flow of solids in to the reactor
% Win is conversion degree of incoming solids
% m is mass of solid
% PCO2e is equilibrium pressure of carbon dioxide
% PCO2 is carbon dioxide pressure
% R is ideal gas constant
% fm, fw, A, B and k are constants
% Xr is residual conversion
% Xave is the active fraction of calcium particles
% kcalc is the constant for calcination
%rcalc is the rate of calcination
```

```
% pCaO and pCaCO3 are densities of calcium oxide and calcium carbonate
repectvely
% MCaO and MCaCO3 are molar masses of calcium oxide and calcium carbonate
% respectively
% Save is reaction surface area
% m2calc is mass flow of calcium carbonate in calciner
```

Carbon dioxide

```
syms m t Min Win Wi w3calc(t) T PCO2e Tcalc  kcalc C W  PCO2 mCaO mCaCO3
rcalc pCaO pCaCO3
mg=0.05
Min=0.0005*mg
eqn1=Min
fm=0.77;
fw=0.17;
PMCaCO3=100,pCaCO3=2800;
W=(mCaCO3/(mCaO+mCaCO3));
W=0.8;
k=0.52;
Xr=0.075;
for N=0:100
    Wi=Xr+(1/(k*N+(1/(1-Xr))))
end
Xave=Wi; Pcao=3320; VMcaco3=36.9* 10^-3; emax=50*10^-9; PMcao=56;
Save=((Xave*Pcao*VMcaco3)/(PMcao*emax))
A=0.00122*10^-5;E=29;B=4.317*10^12; C=20474;
kcalc=A*exp(-4026/(Tcalc+273))
PCO2e=B*exp(-C/(Tcalc+273))
rcalc=m*W*(Save)*(PMCaCO3/pCaCO3)*kcalc*(1-(PCO2/PCO2e))
MCO2=44; MCaCO3=100;
rCO2=rcalc*(MCO2/MCaCO3)
eqn3=(1/(mg+rCO2))*(eqn1+rCO2)
w3calc(t)=eqn3 % mass flow out equals generation
wco2(t)=((1/(mg+rCO2))*(-eqn1+((mg+rCO2)*eqn3)))/t
w3calc=dsolve('Dw3calc=eqn3', 'w3calc(0)==0')
% t is time
% T is temperature
% Min is mass flow of solids in to the reactor
% m is mass of solid
% PCO2e is equilibrium pressure of carbon dioxide
% PCO2 is carbon dioxide pressure
% R is ideal gas constant
% A and B and are constants
% kcalc is the constant for calcination
%rcalc is the rate of calcination
% pCaO and pCaCO3 are densities of calcium oxide and calcium carbonate
repectvely
% MCaO and MCaCO3 are molar masses of calcium oxide and calcium carbonate
% respectively
% Save is the average reaction surface area
% w3calc is mass fraction of carbon dioxide in exit gas stream
```

Energy Balances

Carbonator

```
syms qcao Fo Fr Cpcao Cpcaco3 Cpcaso4 hn2 ho2 hco2 hair wCO2(t) x T wO2(t)
Qsulp Qcarb Qcalc mg mgout Ps A Tx rcarb rsulph rcalc yco2in yo2in yn2in
yco2out yo2out yn2out m m1 m2 m3
qcao=0.95*(Fo+Fr);T=923;
Cpcao=(4.184*(10+(0.0048*T)-(108000*(T.^-2))))/56
Cpcaco3= (4.184*(19.68+(0.01189*T)-((307600/(T.^2)))))/100
Cpcaso4= (4.184*(18.52+(0.02197*T)-((156800/(T.^2)))))/136
hn2in=10.763; ho2in=10.809; hco2in=12.148; hairin=298.18;
hn2i=27.532; ho2i=28.616; hco2i=38.467; x=100;
dT=((1223-x)-(923-298))/(log((1223-x)/(923-298)))
Qcarb=-1.78*10^6; Qcalc=1.78*10^6; Qsulph=-8.966*10^6;
Tntd=298;Tsin=1223-Tntd; Ti=923-Tntd;yo2in=0.05; yco2in=0.15;
yn2in=0.7998;Ps=1800;
dTimscp=(Cpcao*qcao*(Tsin))-
((Ti)*((Cpcao*m1)+(Cpcaco3*m2)+(Cpcaso4*m3)))+mg*((yco2in*hco2in)+(yo2in*ho2i
n)+(yn2in*hn2in))-mgout*((yco2out*hco2i)+(yo2out*ho2i)+(yn2out*hn2i))-
mg*((wO2(t)*ho2i)+(wCO2(t)*hco2i))+((rcarb*Qcarb)+(rsulph*Qsulph))
```

Calciner

```
syms qcao m Fo Fr Cpcao Cpcaco3 Cpcaso4 hn2 ho2 hco2 hair wCO2(t) T wO2(t)
Qsulp Qcarb Qcalc mg mgout Ps A Tx rcarb rsulph rcalc yco2in yo2in yn2in
yco2out yo2out yn2out wN2(t) rCO2 m1calc m2calc
k=0.52;
Xr=0.075;
for N=0
    Wi=Xr+(1/(k*N+(1/(1-Xr))))
end
mcaoin=0;mcaco3in=0.95*Wi*(Fo+Fr)*100/56;qcao=0.95*Wi*(Fo+Fr);
qcaco3=0;qcaso4=m3;T=1223;mg=0.05;
Cpcao=(4.184*(10+(0.0048*T)-(108000*(T.^-2))))/56;
Cpcaco3=(4.184*(19.68+(0.01189*T)-((307600*(T.^-2)))))/100;
Cpcaso4=(4.184*(18.52+(0.02197*T)-((156800*(T.^-2)))))/136;
hn2in=27.532; ho2in=28.616; hco2in=38.467;
hn2i=30.784; ho2i=39.162; hco2i=54.977;
Qcalc=1.78*10^6;
Tntd=298; Tsin=923-Tntd; Ti=1223-Tntd;yo2in=0.2195; yco2in=0.00035;
yn2in=0.7900;yco2out=0.733; yo2out=0.056; yn2out=0.211;
dTimscp=(Cpcao*mcaoin*(Tsin))+(Cpcaco3*mcaco3in*(Tsin))+(Cpcaso4*qcaso4*(Tsin
))-(Cpcao*qcao*Ti)-
(Cpcaso4*qcaso4*Ti)+mg*((yco2in*hco2in)+(yo2in*ho2in)+(yn2in*hn2in))-
((mg+rCO2)*((yco2out*hco2i)+(yo2out*ho2i)+(yn2out*hn2i)))-
mg*((wO2(t)*ho2i)+(wCO2(t)*hco2i)+(wN2(t)*hn2i))+(rcalc*Qcalc)
```

Appendix B: Simulated Experiments Results

NB// Appendix B is on a disk